Max Sorantin, BSc

Theoretical investigations of vibronic effects on the steady state current through a molecular ring structure

MASTER THESIS

For obtaining the academic degree
Diplom-Ingenieur

Master Programme of
Technical Physics

Graz University of Technology

Supervisor:

Univ.-Prof. Dipl.-Phys. Dr.rer.nat. Wolfgang von der Linden

Institute of Theoretical and Computational Physics
Graz University of Technology

Graz, March 2014

Deutsche Fassung:
Beschluss der Curricula-Kommission für Bachelor-, Master- und Diplomstudien vom 10.11.2008
Genehmigung des Senates am 1.12.2008

EIDESSTATTLICHE ERKLÄRUNG

Ich erkläre an Eides statt, dass ich die vorliegende Arbeit selbstständig verfasst, andere als die angegebenen Quellen/Hilfsmittel nicht benutzt, und die den benutzten Quellen wörtlich und inhaltlich entnommenen Stellen als solche kenntlich gemacht habe.

Graz, am …… ……..
(Unterschrift)

Englische Fassung:

STATUTORY DECLARATION

I declare that I have authored this thesis independently, that I have not used other than the declared sources / resources, and that I have explicitly marked all material which has been quoted either literally or by content from the used sources.

…… ……..
date (signature)

Abstract

We study vibrational effects on the steady state current through a molecular ring structure. In contrast to the, in the context of molecular junctions with electron-phonon (e-ph) coupling, widely studied Anderson-Holstein model where the ion motion couples to the electronic onsite energies, we use the Su-Schriefer-Heeger (SSH) type of electron-phonon interatcion, which describes how the electronic hoppings are altered when the molecule vibrates, to model a system with an extended molecule as central region. We continue the work by Michael Knap et al [PhysRevB.88.054301] where the e-ph interaction was confined to the molecule and hence the important effect of vibrations altering the electronic molecule-lead coupling was not taken into account. To include the latter effect into the model the interacting region is extended to inhabit the first lead sites. To study the system at strong electron-phonon interaction we extend the linear SSH model to its exponential generalisation. We solve the system by applying steady state Cluster Perturbation Theory (ssCPT), a systematically improvable approximation to study molecular junctions out of equilibrium where correlation effects of the molecule are treated non perturbatively, in conjunction with Exact Diagonalization Techniques. We show results for the Anderson-Holstein model in the CPT approximation and find good agreement with data found in the literature in the parameter regime where the temperature is much smaller than the molecule lead coupling from weak to strong e-ph interaction. Furthermore, we present electronic properties for the isolated molecular ring in equilibrium as well as for the non-equilibrium situation where it is coupled to non-interacting leads. From weak to strong e-ph coupling the current voltage characteristics can be qualitatively predicted from the equilibrium Density Of States of the central region. For intermediate e-ph coupling where the linear SSH model is applicable the steady state current obtained from ssCPT matches well to a calculation where the e-ph coupling is treated in the Born-Oppenheimer approximation indicating that ion dynamics play an inferior role for this parameters. In this regime the altered equilibrium geometry leads to enhanced/suppressed molecule lead coupling explaining the likewise behaviour of the current. The Born-Oppenheimer approximation starts to disagree with the CPT results for parameters where the linear SSH model breaks down. For strong e-ph coupling the I/V curves can not be interpreted by the geometry change anymore and many-body correlation effects like the Franck-Condon blockade take over.

Kurzfassung

Es wurde der Einfluss von Vibrationen auf den stationären Strom durch eine Molekulare Ring Struktur untersucht. Im Gegensatz zu dem, im Zusammenhang von kontaktierten Molekülen mit Elektron-Phonon (e-ph) Wechselwirkung, umfassend untersuchten Anderson-Holstein Model, bei dem die Ionenbewegung an die elektronische Onsite-Energie koppelt, verwenden wir den Su-Schrieffer-Heeger (SSH) Typ von e-ph Wechselwirkung, der beschreibt wie das elektronische Hüpfen durch die Ionendynamik beeinflusst wird, um ein System mit einem ausgedehnten Molekül zu modellieren. Wir führen die Untersuchungen von Michael Knap et al [PhysRevB.88.054301] weiter, bei der die SSH Wechselwirkung auf das zentrale Molekül beschränkt war und daher der wichtige Effekt der Veränderung des elektronischen Hüpfens von Molekül zu Kontakt durch die Ionenbewegung nicht berücksichtigt wurde. Um diesen Effekt in das Model zu integrieren weiten wir den e-ph korrelierten Bereich auf die ersten Plätze der Kontakte aus. Um das System auch für starke e-ph Wechselwirkung untersuchen zu können generalisieren wir das lineare SSH Model zu seiner exponentiellen Verallgemeinerung. Wir berechnen Observablen wie den stationären Strom über die Einteilchen Greensfunction des vollen Systems welche wir durch Anwendung von stationärer Cluster Perturbation Theory in Verbindung mit Exakten Diagonalisierungs Techniken auf unser System erhalten. Wir präsentieren Ergebnisse für das Anderson-Holstein Model und zeigen, dass die CPT-Daten für schwache bis starke e-ph Wechselwirkung gut mit Resultaten aus der Literatur, im Parameterbereich in dem die Temperatur gegenüber der Molekül-Kontakt Kopplung klein ist, übereinstimmen. Weiters präsentieren wir elektronische Gleichgewichtseigenschaften des isolierten molekularen Ringes sowie Ergebnisse für den stationären Strom im Fall des kontaktierten Moleküls im Nichtgleichgewicht. Von schwacher zu starker e-ph Wechselwirkung lässt sich die Strom-Spannungs-Kennlinie qualitativ durch die elektronische Zustandsdichte des zentralen Moleküls im Gleichgewicht vorhersagen. Für mittlere e-ph Kopplung, bei der das lineare SSH Model noch gültig ist, lassen sich die CPT-Resultate gut durch eine Rechnung, in der die e-ph Wechselwirkung in der Born-Oppenheimer Näherung berücksichtigt wird, annähern. Dies deutet darauf hin, dass in diesem Parameterbereich die Ionendynamik eine untergeordnete Rolle spielt. In selbigem Parameterbereich führt die geänderte Gleichgewichtslage der Ionen zu einer verstärkten bzw. unterdrückten Molekül-Kontakt-Kopplung die das entsprechende Verhalten in den Strom-Spannungs-Kennlinien erklärt. Die Born-Oppenheimer Näherung beginnt von den CPT-Resultaten abzuweichen sobald das lineare SSH Model zusammenbricht. Für starke e-ph Wechselwirkung kann das Verhalten des Stromes als Funktion der Biasspannung nicht mehr allein durch die geänderte Gleichgewichtsgeometrie erklärt werden sondern es müssen Vielteilcheneffekte wie die Franck-Condon Blockade berücksichtigt werden.

Acknowledgments

Many thanks to:
Wolfgang von der Linden and Enrico Arrigoni for their kind supervision during the work on my master thesis.
Michael Knap for his notes, his assistance and introduction to some of the needed numerics in the early stages of my work.
Christoph Heil, Martin Nuss, Antonio Dorda, Markus Eichhorn and the whole many-body physics group at TU-Graz for fruitful discussions and the supply with program codes.
Dmitry Ryndyk for taking the time to provide me with tips and useful literature during his short stay in Graz.
My family for their sincere support throughout my studies.

Contents

Introduction

Over the last decades, the interplay of ion motions and electrons was the key to some of the most striking and technically important phenomena in solid state physics. The BCS theory of conventional superconductivity [2] was able to explain the vanishing electric resistivity at low temperatures for certain metals with the help of a positive interaction between electrons mediated through lattice vibrations/phonons. Other effects include the colossol magneto resistance [23] technically used in magnetic harddrives, thermoelectricity [9] and piezo electric crystals which paved the way for mechanical precision in the nanometer regime. A relatively new and growing field in solid state physics is molecular electronics [27]. Its aim is to build electronic devices, such as transistors, out of (organic) molecules without the help of metallic semiconductors. If possible this technology brings advantages, like reducing the costs and biological footprints of electronics, to the table [33]. In this context the non-equilibrium properties, such as the current voltage characteristics, of an organic molecule attached to two metallic leads have become a subject of great interest. In this systems the e-ph coupling can give rise to nonlinear effects such as bistability, negative differential conductance and hysteric behaviour [5, 19, 11, 12, 13, 15, 29, 4]. Experimentally this setups can be investigated by (resonant) inelastig electron tunneling spectroscopy [31]. With this technique experimentalists where able to faithfully verify signatures of e-ph correlation in the transport properties of such systems [8, 34, 26, 7, 32, 16, 30].
The most common theoretical description of these experiments is within the framework of nonequilibrium Greensfunctions (NEGF) evaluated in the Local Density Approximation (LDA) [10]. The LDA-NEGF approach has the advantage of being ab initio but does not inlcude correlation effects beyond mean field. Theoretical investigations of electron-phonon (el-ph) interactions in these setups are mainly done by studying the Anderson-Holstein model (a single electronic level with a local phonon mode coupled to two non-interacting tight-binding chains). Although, this model inherits basic effects, such as the Franck-Condon blockade or the step like behaviour of the I/V curves, it is not a suitable model to describe an extended molecule coupled to leads. Especially the altering of the electronic coupling to the leads due to the vibrations of the molecule is not captured in the Anderson-Holstein model. In 2012 Michael Knapp et al [17] started to theoretically study a benzene ring attached to two leads. To include correlations between non-local vibronic modes with electrons into the model the e-ph interaction on the molecule was modeled by the linear Su-Schriefer-Heeger type of interaction. They studied the influence of the breathing mode of free benzene, which allows an analytical solution of the central region, on the electronic properties. Since they considered the modes of free benzene, the effect of the altered coupling to the leads was not taken into account.
In this work we will continue the study of a six site ring attached to two leads when imposing a SSH type of e-ph interaction in the central region and the first lead site. By calculating the vibronic modes of a contacted ring we are able to incorporate the interplay between the vibrations of the molecule and the electronic coupling to the leads into the model. Furthermore, we extend

the linear SSH model to its exponential form to study the system in the regime of strong e-ph interaction.
This work is structured into four main parts. Chapter one covers some needed theoretical basics. Chapter two is concerned with testing our method against the literature by applying it to the Anderson-Holstein model. Chapter three presents and discusses results of the electronic properties for a contacted molecular ring in and out of equilibrium while the last chapter is denoted to summary, conclusion and outlook.

Chapter 1

Basics

In this chapter we want to review some of the needed basics. Sec.(1.2.1) gives an overview of the theoretical treatment of the electron phonon coupling and its formulation in second quantisation. Sec.(1.3) revises how to extract the vibronic eigenmodes of a classical system consisting of pointmasses and springs. At last, sec.(1.4) discusses the Lang-Firsov transformation and its application in the Holstein and SSH model.

1.1 Steady state CPT

We give a short introduction to the steady state Cluster Perturbation Theory (CPT) formalism used to obtain non-equilibrium quantities. Details and further improvements of the method can be found in [18, 25, 24]. First, we outline how to obtain the CPT approximation to the full steady state single particle greensfunction $\tilde{G}$. Than we will consider the example of an interacting electron region coupled to two noninteracting leads and derive the formula of the steady state current.

1.1.1 The CPT approximation to the single particle Greensfunction

In CPT the system of interest is divided into clusters with the only restriction that one has to be able to solve each individual cluster without interaction bewteen the clusters. With the greensfunctions of the isolated clusters (here denoted with a lowercase g) at hand CPT tells us how to obtain an approximation for the greensfunction(s) of the system when the interaction between the clusters is switched on (denoted with an uppercase G). Note that in the present work we will only consider time-translation invariant (hence steady state) systems and thus it is always possible to fourier transform the greensfunctions into frequency/energy space.

CPT in equilibrium

In equilibrium there are two (single particle) greensfuntions namely the advanced and retarded greensfunction which are just the complex conjugate of each other and therefore carry the same information. Within CPT the greensfunction of the coupled clusters G is given in terms of the greensfunctions of the isolated clusters g by

$$G^{-1} = g^{-1} - T \tag{1.1}$$

where T is a matrix holding the intra cluster hoppings and g is the blockdiagonal matrix made of the isolated greensfunctions. Note that G is a matrix in orbital and, if one studies magnetic effects, spin space. With an approximation to the greensfunction at hand one can continue to calculate obersvables of interest which require only single particle greensfunctions such as the DOS.

Steady state CPT in non equilibrium

In non equlibrium time has to be viewed along the Keldysh contour leading to four possibilities of greensfunctions instead of two. Like the retarded and advanced greensfunction above these four greensfunctions are not independent allowing a formalism which is only concerned with the retarded, advanced and the so called Keldysh greensfunction which for an isolated cluster in equlibrium may be obtained as

$$g^k = (g^r - g^a)(1 - 2f(E)) \tag{1.2}$$

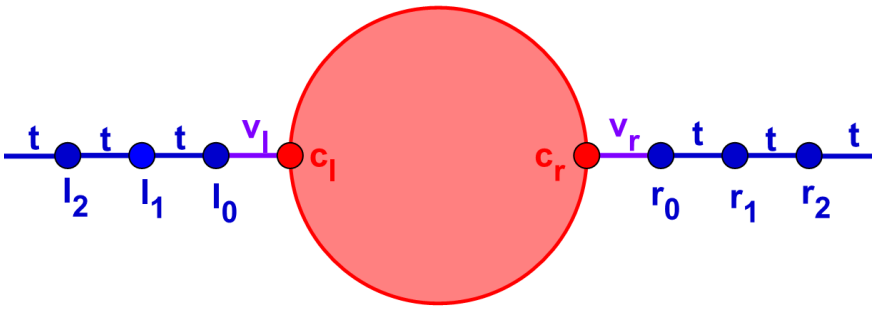

Figure 1.1: A sketch of an interacting electron region (red) coupled to two semi-infinite leads (blue).

where $f(E)$ is the Fermi-Dirac distribution function. These three greensfunctions (which may be matrices them selves) are now embedded in a two by two matrix which is called Kyldysh space (it corresponds to the four different time argument possibilities on the Keldysh contour), as

$$\tilde{G} = \begin{pmatrix} G^r & G^k \\ 0 & G^a \end{pmatrix} \tag{1.3}$$

Note that the occupation or different chemical potentials of the isolated custers enter only in the Keldysh component of the greensfunction $\tilde{G}$. Similar to the furmula in equlibrium the full greensfunction withing CPT is

$$\tilde{G} = \begin{pmatrix} G^r & G^k \\ 0 & G^a \end{pmatrix} = \left[\begin{pmatrix} g^r & g^k \\ 0 & g^a \end{pmatrix}^{-1} - \begin{pmatrix} T & 0 \\ 0 & T \end{pmatrix} \right]^{-1} \tag{1.4}$$

The desired steady state greensfunction is then obtained by picking out the corresponding entries from the final matrix.

1.1.2 Steady state Current through an interacting electron region

We start with a, for simplicity spinless, model for an interacting electron region coupled to two non-interacting leads sketched in fig.(1.1). The hamiltonian can be written as

$$\begin{aligned} \hat{H} =& H_{leads} + H_{center} + H_{coupling} = \sum_{\alpha=\{l,r\};i=0}^{\infty} \varepsilon_{\alpha_i} \hat{n}_{\alpha_i} - t(f^\dagger_{\alpha_i} f_{\alpha_{i+1}} + f^\dagger_{\alpha_{i+1}} f_{\alpha_i}) \\ &+ H_{center}(\{c^\dagger, c\}) + \sum_{\alpha=\{l,r\}} v_\alpha (f^\dagger_{\alpha_0} c_\alpha + c^\dagger_\alpha f_{\alpha_0}) \end{aligned} \tag{1.5}$$

The starting point to derive an expression for the steady state current is the continuity equation

$$\frac{\mathrm{d}\hat{\rho}_i}{\mathrm{d}t} = I_{i-1,i} - I_{i,i+1} \text{ with } \hat{\rho}_i = e c^\dagger_i c_i \tag{1.6}$$

where we define e positively and the current beeing positive from left to right. In the steady state the current is of course the same everywhere, with the exceptions of vortices in the central region, and we can choose to evaluate it anywhere. A logical choice would be the current from the last site of the left lead f_{l_0} and the corresponding coupled site of the central region c_l. The continuity equation for ρ_{l_0}

$$\frac{\mathrm{d}\hat{\rho}_{l_0}}{\mathrm{d}t} = I_{l_1,l_0} - I_{l_0,c_l} \tag{1.7}$$

together with the equation of motion for an operator in the Heisenberg picture

$$\frac{\mathrm{d}\hat{\rho}_{l_0}}{\mathrm{d}t} = \frac{i}{\hbar}[\hat{H}, \hat{\rho}_{l_0}] \tag{1.8}$$

leads to

$$I_{l_1,l_0} - I_{l_0,c_l} = \frac{i}{\hbar}[\hat{H}, \hat{\rho}_{l_0}] \tag{1.9}$$

Evaluating the commutator and arranging the terms conveniently, yields

$$I_{l_1,l_0} - I_{l_0,c_l} = \frac{ie}{\hbar}t(f^\dagger_{l_1}f_{l_0} - f^\dagger_{l_0}f_{l_1}) - \frac{ie}{\hbar}v_l(f^\dagger_{l_0}c_l - c^\dagger_l f_{l_0}) \tag{1.10}$$

This allows us to identify the operator for the current from the left lead to the central region. Taking the average with respect to the steady state, we arrive at

$$I^{ss}_{l_0,c_l} = \langle I_{l_0,c_l}\rangle = \frac{ie}{\hbar}v_l(\langle f^\dagger_{l_0}c_l\rangle - \langle c^\dagger_l f_{l_0}\rangle) \tag{1.11}$$

Due to the electrons carrying negative charge the average of the hopping from the center to the left, which is the negative direction of the current, leads to positive and the hopping from the left lead to the center negative contributions to the current. To make the connection between eq.(1.11) and the Keldysh greensfunctions we make use of the definition of the lesser greensfunction

$$G^<_{c_i,c_j}(t,t') = i\langle c^\dagger_i(t')c_j(t)\rangle \tag{1.12}$$

which in the (time translation invariant) steady state is only a function of the time difference $G(t,t') = G(t-t')$ and can be written in terms of its Fourier transform

$$G^<_{c_i,c_j}(t,t') = G^<_{c_i,c_j}(t-t') = \int_{-\infty}^{\infty}\frac{dE}{2\pi}e^{\frac{i}{\hbar}E(t-t')}G^<_{c_i,c_j}(E) \tag{1.13}$$

and for equal times

$$G^<_{c_i,c_j}(t,t) = G^<_{c_i,c_j} = \int_{-\infty}^{\infty}\frac{dE}{2\pi}G^<_{c_i,c_j}(E) \tag{1.14}$$

where we suppress the time argument since in the steady state the greensfunction is time independent. With the lesser greensfunction for equal times we can rewrite the current as

$$I^{ss}_{l_0,c_l} = \frac{e}{\hbar}v_l\int_{-\infty}^{\infty}\frac{dE}{2\pi}\left(G^<_{f_{l_0},c_l}(E) - G^<_{c_l,f_{l_0}}(E)\right) \tag{1.15}$$

To make use of the CPT formula eq.(1.4) we rewrite the last expression in terms of the Keldysh greensfunction $G^k(E)$. From the relations

$$G^a - G^r = G^< - G^> \text{ and } G^k = G^< + G^> \tag{1.16}$$

we get

$$G^k(E) = 2G^<(E) - (G^a(E) - G^r(E)) = 2G^<(E) - 2\pi A(E) \tag{1.17}$$

where $A(E)$ is the spectralfunction $A(E) = -\frac{1}{\pi}\Im(G^r(E))$ with the normalisation property

$$\int_{-\infty}^{\infty} dE A(E) = 1 \tag{1.18}$$

Hence,

$$G^< = \int_{-\infty}^{\infty} dE \frac{1}{2}\Big(G^k(E) + A(E)\Big) = \frac{1}{2}\int_{-\infty}^{\infty} dE G^k(E) + \pi \tag{1.19}$$

This allows us to rewrite the expression for the current, eq.(1.15), and obtain

$$\boxed{I^{ss}_{l_0,c_l} = \frac{ev_l}{2\hbar}\int_{-\infty}^{\infty}\frac{dE}{2\pi}\Big(G^k_{f_{l_0},c_l}(E) - G^k_{c_l,f_{l_0}}(E)\Big)} \tag{1.20}$$

a formula for the steady state current in terms of the Keldysh greensfunction. Note that eq.(1.20) is exact for the true greensfunction. The approximation enters in the calculation of the greensfunction by CPT.

Connection to Meier-Wingreen/Landauer-Büttinger type of formulas [22]

Often times formulas for the current are written as

$$I_{l,r} = \frac{e}{\hbar}\int\frac{dE}{2\pi}[f(E-\mu_r) - f(E-\mu_l)]\mathcal{T}(E) \tag{1.21}$$

where $\mathcal{T}(E)$ is a suitable transmission function. Interestingly the formula for the current within CPT can be casted into a Landuaer-Büttinger type of formula [6] which was initionally derived for non-interacting systems. Its transmission function is given by

$$\mathcal{T}(E) = \mathcal{T}^{CPT}(E) = tr(G^r_{cc}\Gamma_l G^a_{cc}\Gamma_r) \text{ with } \Gamma_\alpha = 2\Im(T_{ca}g^a_{\alpha\alpha}T_{ac}) \tag{1.22}$$

where T_{ca} is the matrix holding the couplings from the central region to lead α, $g^a_{\alpha\alpha}$ is the advanced greensfunction of the left lead at the last site and $G^{r/a}_{cc}$ is the greensfunction of the central region coupled to the leads. Therefore, whithin the CPT approximation the Landauer-Büttinger formula is still formally correct. Note that G_{cc} and Γ_α are matrices in the sites of the central region and the products have to be performed as matrix multiplications. Having different formulas for the current may be useful since for different systems and parameters one formula may be numerically more suitable than others.

1.2 Electron phonon coupling

In this section we derive the Holstein and SSH model as linear approxiamtions to the e-ph coupling term and translate the models to second quantisation. We discuss the validity of the models, sec.(1.2.2), and extend the linear SSH model to an exponential form in sec.(1.2.3). Note that, although this notation will be used later in this work, we do not denote operators by $\hat{O}$ in this section as we think there is little chance for misunderstandings.

1.2.1 Electron phonon coupling in second quantisation

We consider a many body hamiltonian of N_I ions and N_e electrons with no e-e interaction.

$$\begin{aligned} H &= H_{e,kin} + H_{I,kin} + H_{II} + H_{eI} \\ &= \sum_i \frac{\mathbf{p}_i^2}{2m_e} + \sum_J \frac{\mathbf{p}_J^2}{2M_J} + V_{II}(\{\mathbf{R}\}) + \sum_{iJ} v_{eI}(\mathbf{r}_i - \mathbf{R}_J) \end{aligned} \tag{1.23}$$

Where $V_{II}(\{\mathbf{R}\})$ is the coulomb potential for the ion geometry, $v_{eI}(\mathbf{r}_i - \mathbf{R}_J)$ is the coulomb interaction between ion J and electron i and we denoted the ensemble of the ion position vectors $(\mathbf{R}_1, ..., \mathbf{R}_N)$ in shorthand notation by $\{\mathbf{R}\}$. As is common, we expand the potentials V_{II} and v_{eI} up to leading order around the equilibrium postions of the ions $\mathbf{R}_I^0$ given by the condition $\nabla V_{II}(\{\mathbf{R}^0\}) = 0$. Introducing the deviations from equilibrium $\mathbf{X}_I$ as new dynamic variables, leaves us with

$$\begin{aligned} \mathbf{R}_I &= \mathbf{R}_I^0 + \mathbf{X}_I \\ V_{II}(\{\mathbf{R}^0 + \mathbf{X}\}) &= V_{II}(\{\mathbf{R}^0\}) + \frac{1}{2}\sum_{I \geq J} \mathbf{X}_I^\top \tilde{K}_{IJ} \mathbf{X}_J = V_{II}^0 + V_{II,harmonic} \\ (\tilde{K}_{IJ})_{\alpha\beta} &= \left.\frac{\partial^2 V_{II}(\{\mathbf{R}^0 + \mathbf{X}\})}{\partial X_{I\alpha} \partial X_{J\beta}}\right|_{\{\mathbf{X}=0\}} \text{ where } \alpha, \beta = 1, 2, 3 \\ v_{eI}(\mathbf{r}_i - \mathbf{R}_J^0 - \mathbf{X}_J) &= v_{eI}(\mathbf{r}_i - \mathbf{R}_J^0) - \nabla_{X_J} v_{eI}(\mathbf{r}_i - \mathbf{R}_J^0 + \mathbf{X}_J)|_{\mathbf{X}_J=0} \mathbf{X}_j \end{aligned} \tag{1.24}$$

Where $X_{I\alpha}$ is the α coordinate of ion I. We ignore the constant V_{II}^0 and split the hamiltonian into three parts, namely

$$H_e = \sum_i \frac{\mathbf{p}_i^2}{2m_e} + \sum_J v_{eI}(\mathbf{r}_i - \mathbf{R}_J^0) \text{ the electronic part,} \tag{1.25}$$

$$H_I = \sum_J \frac{\mathbf{p}_J^2}{2M_J} + \frac{1}{2}\sum_{I \geq J} \mathbf{X}_I^\top \tilde{K}_{IJ} \mathbf{X}_J \text{ the ionic part,} \tag{1.26}$$

$$H_{eI} = -\sum_{iJ} \nabla_{x_j} v_{eI}(\mathbf{r}_i - \mathbf{R}_J^0 + \mathbf{X}_J)\,|_{\mathbf{X}_J=0}\, \mathbf{X}_J \text{ and the coupling.} \tag{1.27}$$

By Second quantisation of the electronic Hamiltonian eq.(1.25) with respect to some basis $|\psi_i\rangle$, we obtain

$$H_e^{sq} = \sum_{ij} t_{ij} c_i^\dagger c_j \text{ with } t_{ij} = \langle\psi_i|\frac{\mathbf{p}^2}{2m_e} + \sum_J v_{eI}(\mathbf{r} - \mathbf{R}_J^0)|\psi_j\rangle \tag{1.28}$$

a non-interacting Hamiltonian of fermions. Next, we bring our attantion to the ionic part and construct the $3N_I$ dimensional vector $\mathcal{X}^\top = (\mathbf{X}_1^\top, ..., \mathbf{X}_N^\top)$ containing all deviations from equilibrium. This allows us to rewrite eq.(1.26) as

$$H_I = \frac{1}{2}\mathcal{X}^\top M\mathcal{X} + \frac{1}{2}\mathcal{X}^\top \bar{K}\mathcal{X} \tag{1.29}$$

with a suitable matrix $\bar{K} \in (\mathbb{R}^{3N_I} \times \mathbb{R}^{3N_I})$ and the diagonal mass matrix M. To decouple the system of coupled harmonic oscillators eq.(1.29), we first change variables once more by absorbing M into the definition of a new vector $\bar{\mathcal{X}} \equiv \sqrt{M}\mathcal{X}$, resulting in

$$H_I = \frac{1}{2}\dot{\bar{\mathcal{X}}}^2 + \frac{1}{2}\bar{\mathcal{X}}^\top K\bar{\mathcal{X}} \text{ with } K = \sqrt{M}^\top \bar{K}\sqrt{M} \tag{1.30}$$

Expanding the new deviation vector $\bar{\mathcal{X}}$ in eigenvectors of K and changing dynamic variables to the expansion coefficients η_μ, we get

$$\bar{\mathcal{X}} = \sum_\mu \eta_\mu \mathcal{U}^\mu;\ \dot{\bar{\mathcal{X}}} = \sum_\mu \dot{\eta}_\mu \mathcal{U}^\mu \tag{1.31}$$

$$\begin{aligned} H_I &= \frac{1}{2}\dot{\bar{\mathcal{X}}}^2 + \frac{1}{2}\bar{\mathcal{X}}^\top K\bar{\mathcal{X}} = \frac{1}{2}\sum_{\mu\nu}\eta_\mu\eta_\nu\mathcal{U}^\mu\mathcal{U}^\nu + \frac{1}{2}\sum_{\mu\nu}\eta_\mu\eta_\nu\mathcal{U}^\mu K\mathcal{U}^\nu \\ &= \sum_\mu \frac{1}{2}\dot{\eta}_\mu^2 + \frac{1}{2}\omega_\mu^2\eta_\mu^2 \end{aligned} \tag{1.32}$$

Where we used the eigenvalue equation $\mathcal{U}^\mu\tilde{K} = \omega_\mu^2\mathcal{U}^\mu$ and the orthonormality of the eigenvectors $\mathcal{U}^\mu\mathcal{U}^\nu = \delta_{\mu,\nu}$. Note that we use supperscripts $\mathcal{U}^\mu$ only for convenience later on. Eq.(1.32) is the hamiltonian of uncoupled harmonic oscillators, thus using the relation,

$$b_\mu^\dagger = \frac{1}{2\hbar\omega_\mu}(\omega_\mu\eta_\mu - i\dot{\eta}_\mu) \tag{1.33}$$

and because we need it later, we also state its inverse,

$$\eta_\mu = \sqrt{\frac{\hbar}{2\omega_\mu}}(b_\mu^\dagger + b_\mu) \text{ and } \dot{\eta}_\mu = i\sqrt{\frac{\hbar\omega_\mu}{2}}(b_\mu^\dagger + b_\mu) \tag{1.34}$$

we obtain the second quantisation of the ionic part

$$H_I^{sq} = \sum_\mu \hbar\omega_\mu(b_\mu^\dagger b_\mu + \frac{1}{2}) \tag{1.35}$$

The excitations/quasiparticles corresponding to the bosonic creation/annihilation operators b are called phonons or vibrons depending on literature. Up to this

point we have translated the ionic and electronic part of our hamiltonian and we are left with the part we are interested in, namely the electron-phonon coupling eq.(1.27). We expand the scalar product in eq.(1.27), resulting in

$$H_{eI} = -\sum_{J\alpha i} \left.\frac{\partial v_{eI}(\mathbf{r}_i - \mathbf{R}_J^0 - \mathbf{X}_J)}{\partial X_{J\alpha}}\right|_{X_{J\alpha}=0} X_{J\alpha} \equiv -\sum_{J\alpha}\sum_i T^{J\alpha}(\mathbf{r_i}) X_{J\alpha} \quad (1.36)$$

The operator $\sum_i T^{J\alpha}(\mathbf{r}_i)$ is an electronic single particle operator, thus its second quantisation with respect to the same basis as in eq.(1.28) reads

$$T^{J\alpha} = \sum_{ij} T_{ij}^{J\alpha} c_i^\dagger c_j \text{ with } T_{ij}^{J\alpha} = \langle\psi_i| \left.\frac{\partial v_{eI}(\mathbf{r} - \mathbf{R}_J^0 - \mathbf{X}_J)}{\partial X_{J\alpha}}\right|_{X_{J\alpha}=0} |\psi_j\rangle \quad (1.37)$$

This leaves us with the task of transforming the coordinate $X_{J\alpha}$ into second quantisation. First, we note that

$$X_{J\alpha} = \mathcal{X}_{\widetilde{J\alpha}} = \frac{1}{\sqrt{M_J}} \bar{\mathcal{X}}_{\widetilde{J\alpha}} \text{ with } \widetilde{J\alpha} \equiv 3(J-1) + \alpha \quad (1.38)$$

and using eq.(1.31) together with eq.(1.34), we arrive at

$$X_{J\alpha} = \frac{1}{\sqrt{M_J}} \bar{\mathcal{X}}_{\widetilde{J\alpha}} = \frac{1}{\sqrt{M_J}} \sum_\mu \eta_\mu \mathcal{U}^\mu_{\widetilde{J\alpha}} = \sum_\mu \sqrt{\frac{\hbar}{2M_J\omega_\mu}} \mathcal{U}^\mu_{\widetilde{J\alpha}} (b_\mu^\dagger + b_\mu) \quad (1.39)$$

Combining eq.(1.37) with eq.(1.39), we finish with the second quantisation of the coupling term eq.(1.27)

$$H_{eI}^{sq} = -\sum_{\mu ij} G_{ij}^\mu c_i^\dagger c_j (b_\mu^\dagger + b_\mu) \quad (1.40)$$

where the coupling matrix G for the mode μ is given by

$$G_{ij}^\mu = \sum_{J\alpha} \sqrt{\frac{\hbar}{2M_J\omega_\mu}} \mathcal{U}^\mu_{\widetilde{J\alpha}} T_{ij}^{J\alpha} \quad (1.41)$$

By combining the three parts, eq.(1.28), eq.(1.35) and eq.(1.40), we obtain

$$\boxed{H = \sum_{ij} t_{ij} c_i^\dagger c_j + \sum_\mu \hbar\omega_\mu (b_\mu^\dagger b_\mu + \frac{1}{2}) - \sum_{\mu ij} G_{ij}^\mu c_i^\dagger c_j (b_\mu^\dagger + b_\mu)} \quad (1.42)$$

the total hamiltonian with linear electron phonon coupling.

1.2.2 Holstein type and Su-Schriefer-Heeger type of interaction

In the literature the electron phonon coupling is divided into the Holstein type and Su-Schriefer-Heeger, from now on we will use the abberivation SSH, type of interaction. As we will see later on, the two types are merely different parts of the linear interaction, eq.(1.40), derived above. At first we will give a more illustrative derivation of the electron phonon coupling which seperates naturally in the two interaction types.

Alternative derivation: We want to think of the system as a molecule where the ions have some equilibrium positions and can move along one specific mode. Hence, the ion motion can be expressed in the form

$$\{\mathbf{R}\} = \{\mathbf{R}_0\} + \eta_\mu \{\mathbf{X}_\mu\} \tag{1.43}$$

where curly brackets indicate the whole ensemble of ions. The motion is quasi one dimensional as the only free parameter in eq.(1.43) is the expansion coefficient η_μ which is the stretching amplitude of the mode. The starting point of the derivation is a hamiltonian of electrons and a single phonon mode μ in second quantisation.

$$\begin{aligned} H &= \sum_{ij} h^e_{ij} c_i^\dagger c_j + \hbar\omega_\mu (b_\mu^\dagger b_\mu + \frac{1}{2}) \\ &= -\sum_{i \neq j} t_{ij} c_i^\dagger c_j + \sum_i \epsilon_i n_i + \hbar\omega_\mu (b_\mu^\dagger b_\mu + \frac{1}{2}) \end{aligned} \tag{1.44}$$

As it is common, we devided the electronic hamiltonian in its diagonal, also called onsite energy, and offdiagonal part, also called hopping. The interpretation of ϵ_i is simply the energy that one has to pay to put an electron in the orbital c_i. It originates from the fact that orbitals with lower energy are allready filled and can be thought of as an potential. The parameter t_{ij} is obtained as the overlap integral of two different wavefunctions and therefore is proportianal to the propability that an electron in orbital c_j hopps into an orbital c_i. This part can be thought of as the kinetic energy part of the hamiltonian, hence the artifical minus sign. We will ignore the phonon part for now and concentrate on the electronic one. Lets say the electronic part describes electrons moving in the potential of a fixed but arbitrary ion geometry $\{\mathbf{R}\}$. Thus, the parameters t_{ij} and ϵ_i in eq.(1.44) are functions of the ion geometry $\{\mathbf{R}\}$. Keeping in mind that we constrained the ion motion along one specific mode eq.(1.43) and abusing notation, we write

$$t_{ij} = t_{ij}(\{\mathbf{R}\}) = t^\mu_{ij}(\{\mathbf{R}_0\} + \eta_\mu\{\mathbf{X}_\mu\}) = t^\mu_{ij}(\eta_\mu) \tag{1.45}$$

$$\epsilon_i = \epsilon_i(\{\mathbf{R}\}) = \epsilon^\mu_i(\{\mathbf{R}_0\} + \eta_\mu\{\mathbf{X}_\mu\}) = \epsilon^\mu_i(\eta_\mu) \tag{1.46}$$

Note that we used superscripts μ to indicate that these functions will be different for each mode. We drop the index μ for now and will reintroduce them later. The exact functions are unknown and modelling them is a non-trivial task of ab initio calculations. But assuming only that these functions are analytic, we can allways expand them in a taylor series around some η_0

$$t_{ij}(\eta) = t_{ij}(\eta_0) + \left.\frac{\partial t_{ij}(\eta)}{\partial \eta}\right|_{\eta=\eta_0} (\eta - \eta_0) + O((\eta - \eta_0)^2) \tag{1.47}$$

$$\epsilon_i(\eta) = \epsilon_i(\eta_0) + \left.\frac{\partial \epsilon_i(\eta)}{\partial \eta}\right|_{\eta=\eta_0} (\eta - \eta_0) + O((\eta - \eta_0)^2) \tag{1.48}$$

To guarantee that we expand in a small parameter we make the obviouse choice of $\eta_0 = 0$ as this corresponds to the equilibrium positions. Truncating the above

expansions after the linear order yields

$$t_{ij} = t_{ij}^0 - g_{ij}\eta \qquad \epsilon_i = \epsilon_i^0 + \lambda_i \eta \tag{1.49}$$

with the definition of the electron phonon coupling constants

$$g_{ij} \equiv -\left.\frac{\partial t_{ij}(\eta)}{\partial \eta}\right|_{\eta=0} \qquad \lambda_i \equiv \left.\frac{\partial \epsilon_i(\eta)}{\partial \eta}\right|_{\eta=0} \tag{1.50}$$

The artifical minus sign in the definition of g_{ij} is due to the fact that t_{ij} will decrease if η increases (the overlap integral becomes smaller if the atoms are further apart) and guarantees that g_{ij} has positive values. Using this in the hamiltonian eq.(1.44) and the standart relation for the displacement of a harmonic oscillator in second quantisation

$$\eta = \sqrt{\frac{\hbar}{2m\omega}}(b^\dagger + b) \tag{1.51}$$

we obtain

$$\begin{aligned} H =& -\sum_{i\neq j} t_{ij}^0 c_i^\dagger c_j + \sum_i \epsilon_i^0 n_i + \hbar\omega_\mu (b_\mu^\dagger b_\mu + \frac{1}{2}) \\ &+ \sqrt{\frac{\hbar}{2m\omega_\mu}} \sum_{i\neq j} g_{ij}^\mu c_i^\dagger c_j (b_\mu^\dagger + b_\mu) + \sqrt{\frac{\hbar}{2m\omega_\mu}} \sum_i \lambda_i^\mu n_i (b_\mu^\dagger + b_\mu) \\ =& H_0 + H_{SSH} + H_{Holstein} \end{aligned} \tag{1.52}$$

the total hamiltonian for a single mode with the SSH and Holstein interaction. Comparing eq.(1.52) to eq.(1.42), we see that the Holstein interaction is the diagonal part and the SSH type of interaction is the offdiagonal part. One could also say that the Holstein interaction couples to the electronic onsite energies and the SSH type alters the electronic hoppings.

Validity of the SSH and Holstein model

In both derivations discussed above the electron phonon coupling is expressed in terms of a taylor series and truncated after the linear term which leads to the SSH and Holstein type of electron phonon interaction. Now we turn to the examination of this approxiamtion. As the starting point of our investigation we return to eq.(1.47) and eq.(1.48). Unfortunately we do not know the functions $t_{ij}(\eta)$ and $\epsilon_i(\eta)$ so we can not make use of formulas for the kth remainder of a taylor series as they require the $(k+1)$th derivative. Though, we know that we are only interested in a small region around the equilibrium because we know from experiments that the deviation from equilibrium is small compared to the equilibrium distances, which in our case translates to $\eta \ll 1$. Like any taylor series expanded in a small parameter it is only sensible to truncate after the linear order if the linear term is already small compared to the equilibrium contribution. This leads to the the following conditions for validity of the SSH and Holstein model

$$\left|\frac{g_{ij}\eta}{t_{ij}^0}\right| \ll 1 \text{ for the SSH interaction and equivalentely} \tag{1.53}$$

$$\left|\frac{\lambda_i\eta}{\epsilon_i^0}\right| \ll 1 \text{ for the Holstein interaction} \tag{1.54}$$

For the following considerations we want to think of an electronic basis which is localized around the position of the ions. The electronic onsite energies ϵ_i typically do not change significantely as η is varied (or in other words as the geometry is altered) because ϵ_i depends only on the wave function localized at site i. Thus, the electron phonon coupling constant λ_i in eq.(1.50) is small in most cases leading to the fact that the Holstein model is usually valid. However, the same can not be said about the electron phonon coupling in the SSH model as g_{ij} in eq.(1.50) depends on two different wave functions localized at different sites i and j respectively. Thus, $t_{ij}(\eta)$ can change considerably as we vary the ion geometry and hence the validity of the SSH model is situational. To this end we note that the requirements for the SSH model are definitely violated if $\left|\frac{g_{ij}\eta}{t_{ij}^0}\right| > 1$ because then $t_{ij} = t_{ij}^0 - g_{ij}\eta < 0$ which is unphysical as these parameters are defined strictly positive. Thus, for given bare hoppings t_{ij}^0 and onsite energies ϵ_i^0 we can calculate an upper bound for g_{ij} if we search for the root of $f(\eta) = t_{ij}^0 - g_{ij}\langle\eta\rangle$. Here, $\langle\eta\rangle \equiv \langle\psi_0|\eta|\psi_0\rangle$ is evaluated in the ground state of the system, which is the reason why all the system parameters enter in the evaluation of $f(\eta)$.

1.2.3 Beyond the SSH model

As mentioned above the linear approximation for the electronic hopping, eq.(1.49), leading to the SSH model can be unjustified and even unphysical. The simple answer to the question of what to do if the linear approximation is wrong is of course that we do not truncate the taylor expansion, eq.(1.47), after the linear order but rather keep more terms. The downside of this simple solution is that for every order of the taylor expansion that we keep, we need to determine another constant namely $g_{ij}^{(n)} \equiv \frac{\partial^n t_{ij}(\eta)}{\partial\eta^n}$. Getting those additional parameters is rather problematic as they need to be determined either by ab initio calculations or by fitting the model to some experimental data. In both cases it is difficult enough to get the paramater for the linear order and introducing further parameters into the model will just lead to a bad statistik in the case of fitting to experimental data and larger quantitative disagreement between different ab initio approaches. In addition to the issue of obtaining these additional parameters they would make the model more complicated than it needs to be and therefore it would be an more unlikely description of reallity (occam's razor). For that reason we want another non linear model for the function $t_{ij}(\eta; g_{ij})$ that depends only on the parameter g_{ij} for the cases were g_{ij} is large and the linear SSH model is not applicable anymore. For concreteness we write down

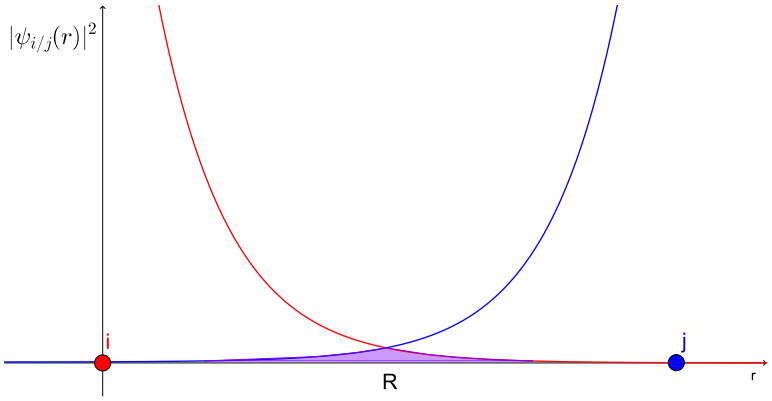

Figure 1.2: Sketch for the wavefunction overlap of atom i and j.

the defining equation for $t_{ij}(\eta)$

$$t_{ij}(\eta) = \langle\psi_i|\hat{H}|\psi_j\rangle = \int_{\mathbb{R}} d\mathbf{r}^3 \psi_i(\mathbf{r};\eta)\hat{H}(\mathbf{r};\eta)\psi_j(\mathbf{r};\eta)$$
$$\simeq \int_{\mathbb{R}} d\mathbf{r}^3 \psi_i(\mathbf{r};\eta)\hat{H}(\mathbf{r})\psi_j(\mathbf{r};\eta) \tag{1.55}$$

Recall that our ion geometry enters through η in this expression. In eq.(1.55) we have omitted the η dependence of $\hat{H}$ because the geometry enters only through the coulomb potential which is small in the region where the wavefunctions overlap and thus its variation can be neglected. To get an idea of what the function $t(\eta)$ should look like, we want to consider the following. Imagine a system of two atoms, atom i and atom j, seperated by a distance R away from each other. The main contributions to the hopping amplitude/overlap integral eq.(1.55) will come from the regions where the wavefunctions centered around the two sites overlap. This region will be far enough away from the center of the atoms that we can assume an exponential decrease and increase of the wavefunctions for site i and j respectively. The situation is sketched in fig.(1.2). The assymptotic form of the wavefunctions motivates the following functional form of the overlap integral

$$t(\eta) = t_0 e^{-\alpha\eta} \tag{1.56}$$

In order for the more general form eq.(1.56) to be a valid candidate for our sought for function $t(\eta)$ it has to agree with the linear SSH model up to linear order. By expanding eq.(1.56) as

$$t(\eta) = t_0(1 - \alpha\eta + \frac{1}{2}\alpha^2\eta^2 + O(\eta^3)) \tag{1.57}$$

and comparing it to the SSH model eq.(1.47), we conclude that eq.(1.56) is a rightful candidate given that $\alpha = \frac{g}{t_0}$. Using the second quantization of η, eq.(1.51), and reintroducing the site indices ij and mode index μ, we finally

obtain what we want to call the electron phonon interaction beyond the SSH model

$$t_{ij}^{sq} = t_{ij}^0 e^{-\sum_\mu \alpha_{ij}^\mu (b_\mu^\dagger + b_\mu)} \text{ with } \alpha_{ij}^\mu = \sqrt{\frac{\hbar}{2m\omega_\mu}} \frac{g_{ij}^\mu}{t_{ij}^0} \tag{1.58}$$

Because it is more illustrative we also state its analogue in first quantization

$$t_{ij}^{fq} = t_{ij}^0 e^{-\frac{g_{ij}}{t_{ij}^0}\Delta_{ij}} \text{ with } \Delta_{ij} = r_{ij}^0 - |\mathbf{r}_i - \mathbf{r}_j| \tag{1.59}$$

and r_{ij}^0 is the equilibrium bond length. Thus, the interpretation of the electron phonon coupling beyond the SSH model is that the electronic hopping from site i to j is exponentially suppressed/enhanced as the atoms move further apart/closer together. Plugging our more general interaction, eq.(1.58), into eq.(1.44) we obtain

$$\begin{aligned} H = &- \sum_{i \neq j} t_{ij}^0 e^{-\sum_\mu \alpha_{ij}^\mu (b_\mu^\dagger + b_\mu)} c_i^\dagger c_j + \sum_i \epsilon_i^0 n_i + \hbar\omega_\mu (b_\mu^\dagger b_\mu + \frac{1}{2}) \\ &+ \sum_\mu \sqrt{\frac{\hbar}{2m\omega_\mu}} \sum_i \lambda_i^\mu n_i (b_\mu^\dagger + b_\mu) \end{aligned} \tag{1.60}$$

and neglecting the Holstein ineraction we arrive at what we want to call the beyond SSH model

$$\boxed{H = - \sum_{i \neq j} t_{ij}^0 e^{-\sum_\mu \alpha_{ij}^\mu (b_\mu^\dagger + b_\mu)} c_i^\dagger c_j + \sum_i \epsilon_i^0 n_i + \hbar\omega_\mu (b_\mu^\dagger b_\mu + \frac{1}{2})} \tag{1.61}$$

This nonlinear form of e-ph interaction is hard to treat analytically but is not a problem for numerical techniques like Exact Diagonalisation. Note that for isolated molecules the Holstein interaction is much weaker than the coupling through the altered hoppings (SSH type) which justifies the approximation from eq.(1.60) to eq.(1.61). However, the Holstein interaction becomes important when modelling a molecule on a substrate where it can be used to describe the interaction between the phonons of the substrate and the molecule. Generally, the Holstein interaction (altering of the onsite energies) is used to model vibronic effects of surroundings on the system of interest which often times acts as a relaxation channel which is able dissipate energy.

1.3 Calculation of modes

In this section we want to derive the vibronic eigenmodes of a system of masses and springs.

1.3.1 General form for a system of masses and springs

We want to calculate the eigenmodes and eigenfrequencies of a classical system of masses and springs. This amounts to considering N masses moving in the potential

$$V(\{\mathbf{R}\}) = \sum_{ij} \frac{k_{ij}}{2}(|\mathbf{R}_i - \mathbf{R}_j| - r_{ij}^0)^2 \tag{1.62}$$

where r_{ij}^0 are the equilibrium distances and $\mathbf{R}_i$ is the position vector of mass i. Some people like to put a factor $\frac{1}{2}$ in front of the sum in eq.(1.62) to account for double counting appearing in the sum but here we want to assume that by common sense each bond ij contributes only once in the potential above. Given the potential, we can write down the lagrangian of our system

$$\mathcal{L}(\{\mathbf{R}(t)\}) = \sum_i \frac{m_i}{2}\dot{\mathbf{R}}_i - \sum_{ij} \frac{k_{ij}}{2}(|\mathbf{R}_i - \mathbf{R}_j| - r_{ij}^0)^2 \tag{1.63}$$

Rewriting the position vectors as deviation from equilibrium $\mathbf{R}_i(t) = \mathbf{R}_i^0 + \mathbf{r}_i(t)$, eq.(1.63) becomes

$$\mathcal{L}(\{\mathbf{r}(t)\}) = \sum_i \frac{m_i}{2}\dot{\mathbf{r}}_i - \sum_{ij} \frac{k_{ij}}{2}(|\mathbf{R}_{ij}^0 + \mathbf{r}_i - \mathbf{r}_j| - r_{ij}^0)^2 \tag{1.64}$$

To extract the modes we need to get the lagrangian/potential into a quadratic/harmonic form. Dispite the fact that we are considering a harmonic potential for each bond, the overall potential in eq.(1.64) is not quadratic in the variables $\mathbf{r}_i$. In order to get an harmonic approximation for the lagrangian we rewrite it once again by introducing the vector of all deviations from equilibrium $\boldsymbol{\xi}^\top = (\mathbf{r}_1^\top, ..., \mathbf{r}_N^\top)$. Doing so, we otbain

$$\mathcal{L}(\boldsymbol{\xi}(t)) = \frac{1}{2}\dot{\boldsymbol{\xi}}^\top M \dot{\boldsymbol{\xi}} - V(\boldsymbol{\xi}) \tag{1.65}$$

Next, we expand the potential up to leading order around the equilibrium positions which amounts to $\xi = 0$.

$$V(\boldsymbol{\xi}) = V(\boldsymbol{\xi} = 0) + \underbrace{\nabla V(\boldsymbol{\xi} = 0)}_{=0}\boldsymbol{\xi} + \frac{1}{2}\boldsymbol{\xi}^\top K \boldsymbol{\xi} \tag{1.66}$$

where the linear order is zero by the definition of the equilibrium position and K is the hessian matrix of the potential $V(\boldsymbol{\xi})$. We neglect the constant $V(\boldsymbol{\xi} = 0)$ and plug the rest of the expansion, eq.(1.66), back into the lagrangian, eq.(1.65).

$$\mathcal{L}(\boldsymbol{\xi}(t)) = \frac{1}{2}\dot{\boldsymbol{\xi}}^\top M \dot{\boldsymbol{\xi}} - \frac{1}{2}\boldsymbol{\xi}^\top K \boldsymbol{\xi} = \frac{1}{2}\sum_i m_i \dot{\xi}_i^2 - \frac{1}{2}\sum_{ij} \xi_i K_{ij} \xi_j \tag{1.67}$$

The equations of motion are given by the Euler-Lagrange equations

$$\frac{\partial \mathcal{L}}{\partial \xi_k} = \frac{\mathrm{d}}{\mathrm{d}t}\frac{\partial \mathcal{L}}{\partial \dot{\xi}_k} \tag{1.68}$$

Respecting that K is symetric we calculate the derivatives

$$\begin{aligned}\frac{\partial \mathcal{L}}{\partial \xi_k} &= -\frac{1}{2}\left(\sum_i j\delta_{ik}K_{ij}\xi_j + \sum_i j\xi_i K_{ij}\delta_{jk}\right) \\ &= -\frac{1}{2}\left(\sum_j K_{kj}\xi_j + \sum_i K_{ik}\xi_i\right) = -\sum_i K_{ki}\xi_i\end{aligned}$$

and

$$\frac{\mathrm{d}}{\mathrm{d}t}\frac{\partial \mathcal{L}}{\partial \dot{\xi}_k} = \frac{1}{2}\frac{\mathrm{d}}{\mathrm{d}t}\sum_i m_i 2\dot{\xi}_i\delta_{ik} = \frac{\mathrm{d}}{\mathrm{d}t}m_k\dot{\xi}_k = m_k\ddot{\xi}_k$$

Plugging these derivatives into eq.(1.68), we get $m_k\ddot{\xi}_k = -\sum_i K_{ki}\xi_i$ which is the kth component of the vector equation

$$M\ddot{\boldsymbol{\xi}}(t) = -K\boldsymbol{\xi}(t) \tag{1.69}$$

By making the harmonic ansatz $\boldsymbol{\xi}(t) = e^{i\omega t}\boldsymbol{\xi}$ we eliminate the time dependence and eq.(1.69) transforms into the generalized eigenvalue equation

$$\boxed{M\boldsymbol{\xi}_\mu = \omega_\mu^2 K\boldsymbol{\xi}_\mu} \tag{1.70}$$

for the mode μ with the eigenvector $\boldsymbol{\xi}_\mu$ and eigenfrequency ω_μ. Thus, after calculating the matrices K and M we can solve for the modes numerically or analytically if the system has enough symetries.

1.3.2 Writing expressions in terms of modes

As we saw in section (1.2) the objects we quantise are the expansion coefficients η_μ in

$$\boldsymbol{\xi}(t) = \sum_\mu \eta_\mu(t)\boldsymbol{\xi}_\mu \tag{1.71}$$

Therefore, we want to be able to write all expressions above in terms of modes and their expansion coefficients. We start with expressing the position vector of mass i $\mathbf{R}_i = \mathbf{R}_i^0 + \mathbf{r}_i$ where $\mathbf{R}_i^0$ is the equilibrium position. By defining a matrix S_i as

$$S_i^{3\times 3N} \equiv (\underbrace{0...0}_{i-1}\,\mathbb{1}_{3\times 3}\,\underbrace{0..0}_{N-i}) \tag{1.72}$$

we can write

$$\mathbf{r}_i = S_i\boldsymbol{\xi} \tag{1.73}$$

where S_i just picks out the deviation vector for the mass i out of a $\boldsymbol{\xi}^\top = (\mathbf{r}_1^\top, ..., \mathbf{r}_N^\top)$. Combining eq.(1.72) with eq.(1.71) we obtain

$$\mathbf{R}_i = \mathbf{R}_i^0 + \mathbf{r}_i = \mathbf{R}_i^0 + \sum_\mu \eta_\mu(t)S_i\boldsymbol{\xi}_\mu = \mathbf{R}_i^0 + \sum_\mu \eta_\mu(t)\mathbf{r}_i^\mu \tag{1.74}$$

with $\mathbf{r}_i^\mu \equiv S_i \boldsymbol{\xi}_\mu$ which defines the direction in which the mass i is moving in the mode μ. Next we bring our attention to the expression

$$\Delta_{ij} \equiv |\mathbf{R}_i - \mathbf{R}_j| - r_{ij}^0 = |\mathbf{R}_{ij}^0 + \mathbf{r}_i - \mathbf{r}_j| - r_{ij}^0 \tag{1.75}$$

which is the change of bondlenght between mass i and j if mass i/j moves away from its equilibrium position according to $\mathbf{r}_{i/j}$. This time rewriting it is not so straight forward as it was in the case above because of the norm and the square root it introduces. By expanding the norm, we get

$$|\mathbf{R}_{ij}^0 + \mathbf{r}_i - \mathbf{r}_j| = \sqrt{\sum_\alpha (R_\alpha^{ij,0} + r_{i\alpha} - r_{j\alpha})^2} \tag{1.76}$$

We are only interested in small deviations from equilibrium (recall expansion up to leading order of the potential eq.(1.66)) thus we want to keep only the leading order of the square root in eq.(1.76) with respect to the deviations $r_\alpha^{i/j}$. We expand the square root in eq.(1.76) around $r_\alpha^{i/j} = 0$

$$|\mathbf{R}_{ij}^0 + \mathbf{r}_i - \mathbf{r}_j| = \underbrace{\sqrt{\sum_\alpha (R_\alpha^{ij,0})^2}}_{r_{ij}^0} + \sum_\beta \left.\frac{\partial \sqrt{}}{\partial r_{i\beta}}\right|_{r=0} r_{i\beta} + \left.\frac{\partial \sqrt{}}{\partial r_{j\beta}}\right|_{r=0} r_{j\beta} \tag{1.77}$$

where $\sqrt{} \equiv \sqrt{\sum_\alpha (R_\alpha^{ij,0} + r_{i\alpha} - r_{j\alpha})^2}$ is used as abbreviation. The derivatives are given by

$$\begin{aligned}
\frac{\partial \sqrt{}}{\partial r_{i\beta}} &= \frac{1}{2\sqrt{}} 2(R_\beta^{ij,0} + r_{i\beta} - r_{j\beta}) \overset{r=0}{=} \frac{1}{r_{ij}^0} R_\beta^{ij,0} \\
\frac{\partial \sqrt{}}{\partial r_{j\beta}} &= \frac{1}{2\sqrt{}} 2(R_\beta^{ij,0} + r_{i\beta} - r_{j\beta})(-1) \overset{r=0}{=} -\frac{1}{r_{ij}^0} R_\beta^{ij,0}
\end{aligned} \tag{1.78}$$

Plugging these derivatives back into eq.(1.77), using eq.(1.75) and writing the sum over β as scalar product, we arrive at

$$|\mathbf{R}_{ij}^0 + \mathbf{r}_i - \mathbf{r}_j| = r_{ij}^0 + \frac{1}{r_{ij}^0} \mathbf{R}_{ij}^0 \mathbf{r}_i - \frac{1}{r_{ij}^0} \mathbf{R}_{ij}^0 \mathbf{r}_j$$

$$|\mathbf{R}_{ij}^0 + \mathbf{r}_i - \mathbf{r}_j| - r_{ij}^0 = \frac{\mathbf{R}_{ij}^0}{r_{ij}^0} (\mathbf{r}_i - \mathbf{r}_j) \tag{1.79}$$

$$\Delta_{ij} = \mathbf{e}_{ij}^0 (\mathbf{r}_i - \mathbf{r}_j) \text{ with } \mathbf{e}_{ij}^0 \equiv \frac{\mathbf{R}_{ij}^0}{r_{ij}^0} \tag{1.80}$$

The rest of the calculation is now straight forward again. We use eq.(1.73) to write everything in terms of $\boldsymbol{\xi}$

$$\Delta_{ij} = \mathbf{e}_{ij}^0 (\mathbf{r}_i - \mathbf{r}_j) = \mathbf{e}_{ij}^0 (S_i \boldsymbol{\xi} - S_j \boldsymbol{\xi}) \tag{1.81}$$

Defining $S_{ij} \equiv S_i - S_j$ and expanding $\boldsymbol{\xi}$ in terms of modes, we find

$$\Delta_{ij} = \mathbf{e}_{ij}^0 S_{ij} \sum_\mu \eta_\mu \boldsymbol{\xi}_\mu = \sum_\mu \mathbf{e}_{ij}^0 S_{ij} \boldsymbol{\xi}_\mu \eta_\mu \tag{1.82}$$

or in short

$$\boxed{\Delta_{ij} = \sum_{\mu} d_{ij}^{\mu} \eta_{\mu} \quad \text{with } d_{ij}^{\mu} \equiv \mathbf{e}_{ij}^{0} S_{ij} \boldsymbol{\xi}_{\mu}} \tag{1.83}$$

Thus, the total difference in the bondlenght Δ_{ij} is the sum of the contributions from every mode. The constants d_{ij}^{μ} describe the change of the bondlenght of the bond ij if the masses move according to mode μ with a stretching amplitude of $\eta_{\mu} = 1$. This also means that if the total sum of the d_{ij} is zero for a paricular mode that the net difference in bondlenght is zero. This just means that some masses move closer together and others further apart leading to a cancelation in the above mentioned sum.

1.4 Lang-Firsov Transformation

In this section, we want to introduce the Lang-Firsov transformation which is widely used in the field of electron phonon coupling to remove the coupling term in the hamiltonian. The operator of the Lang-Firsov transformation can be written in the general form

$$\hat{L} = e^{-i\gamma\hat{T}\hat{p}} \tag{1.84}$$

with a real parameter γ, the phononic momentum operator $\hat{p}$ and an hermitian operator $\hat{T}$ that commutes with $\hat{p}$ (for example a purely electronic operator). Under these assumptions the transformation is unitary since

$$LL^\dagger = e^{\gamma\hat{T}(b^\dagger - b)} e^{\gamma(b^\dagger - b)^\dagger \hat{T}^\dagger} = e^{\gamma\hat{T}(b^\dagger - b)} e^{-\gamma\hat{T}(b^\dagger - b)} = \mathbb{1} \tag{1.85}$$

First we will demonstrate the basic idea of the Lang-Firsov transformation and give some useful formulas. Then we will show how this transformation removes the coupling term in the Holstein and SSH model.

1.4.1 Basic idea of the Lang-Firsov transformation

To demonstrate the basic idea of the transformation and why it removes the electron-phonon coupling, we want to consider an hamiltonian of the form

$$\hat{H} = \hat{H}_e + \hat{H}_p + g\hat{H}_{ep} = \hat{H}_e + \frac{1}{2m}\hat{p}^2 + \frac{m\omega_0^2}{2}\hat{x}^2 + g\hat{T}_e\hat{x} \tag{1.86}$$

where we have assumed an harmonic oscillator for the the phonon part $\hat{H}_p$, a generic form $gT_e\hat{x}$ for the coupling term motivated by sec.(1.2) and $\hat{H}_e$ is the electronic hamiltonian. The basic idea is now to absorb the coupling term proportional to $\hat{x}$ into the $\hat{x}^2$. By completing the square, we get

$$\hat{H} = \hat{H}_e + \frac{1}{2m}\hat{p}^2 + \frac{m\omega_0^2}{2}(\hat{x} + \frac{g}{m\omega_0^2}\hat{T}_e)^2 - \frac{g^2}{2m\omega_0^2}\hat{T}_e^2 \tag{1.87}$$

which is again an harmonic oscillator but $\hat{x}$ is shifted by an amount $\frac{g}{m\omega_0^2}\hat{T}_e$. However, this shift is not constant but inhabits an electronic operator which means that the amplitude of the shift depends on the electronic configuration. We could of course define the operator $\hat{\tilde{x}} = \hat{x} + \frac{g}{m\omega_0^2}\hat{T}_e$ but that would just hide the coupling and not remove it since the new operator $\hat{\tilde{x}}$ would not be purely phononic. Luckily instead of just defining a new operator one can also achieve the desired shift by a suitable transformation which is then called Lang-Firsov transformation. Before we continue, we want to review how one introduces a constant shift $\hat{x} \mapsto \hat{x} + \Delta$ in space.

1.4.2 Generating a shift in space

For the following considerations, we will set $\hbar = 1$. Recall that in quantum mechanics a translation Δ in space is done by applying the operator $e^{-i\Delta\hat{p}}$,

where the momentum operator $\hat{p}$ is referred to as the generating operator of spatial translations. To demonstrate this property, we consider the wavefunction $|\psi_{zero}\rangle$ of an harmonic oscillator centered around $x = 0$ in its groundstate. The subscript *zero* here does not indicate that it is the groundstate but rather that this wavefunction is centered around $x = 0$. Before continuing, we note that

$$e^{-\Delta \frac{\mathrm{d}}{\mathrm{d}x}} f(x) = \sum_{n=0}^{\infty} \frac{(-\Delta)^n}{n!} \frac{\mathrm{d}^n f(x)}{\mathrm{d}x^n} = f(x - \Delta) \tag{1.88}$$

where we expanded the exponential as its taylor series in the first equality and use the definition of a taylor series in the last equality. Using the spacial representation of the momentum operator $\langle x|\hat{p}| = -i\dfrac{\mathrm{d}}{\mathrm{d}x}$ we can apply $e^{-i\Delta\hat{p}}$ to our wavefunction

$$\begin{aligned} e^{-i\Delta\hat{p}}|\psi_{zero}\rangle &= \int dx|x\rangle\langle x|e^{-i\Delta\hat{p}}|\psi_{zero}\rangle = \int dx|x\rangle e^{-\Delta\frac{\mathrm{d}}{\mathrm{d}x}}\psi_{zero}(x) \\ &= \int dx|x\rangle\psi_{zero}(x-\Delta) = \int dx|x\rangle\langle x|\psi_\Delta\rangle = |\psi_\Delta\rangle \end{aligned} \tag{1.89}$$

which results in the same wavefunction centered around $x = \Delta$. This is clear if we look at the expectation value of $\hat{x}$

$$\langle\hat{x}\rangle_{zero} = \langle\psi_{zero}|\hat{x}|\psi_{zero}\rangle = \int dx\psi^*_{zero}(x)x\psi_{zero}(x) = 0 \tag{1.90}$$

which is zero since the wavefunction is symmetric with respect to x. Now we evaluate the same expectation value in the transformed/shifted state $|\psi_\Delta\rangle$

$$\begin{aligned} \langle\hat{x}\rangle_\Delta = \langle\psi_\Delta|\hat{x}|\psi_\Delta\rangle &= \int dx\psi^*_\Delta(x)x\psi_\Delta(x) = \int dx\psi^*_{zero}(x-\Delta)x\psi_{zero}(x-\Delta) \\ &\overset{u=x-\Delta}{=} \int du\psi^*_{zero}(u)(u+\Delta)\psi_{zero}(u) = \Delta \end{aligned} \tag{1.91}$$

As expected we get the value Δ. Until now we have applied the transformation to the states. Equivalently we can apply it to the operators instead.

General formulas for the transformation of operators Before we continue with the special case of the Lang-Firsov transformation we will state some general rules about how operators transform under a specific transformation. The prescription is

$$\hat{\tilde{B}} = \hat{O}^\dagger\hat{B}\hat{O} \tag{1.92}$$

where $\hat{B}$ is an unitary operator, $\hat{O}$ is the operator of the transformation and $\hat{\tilde{B}}$ is the transformed operator. For the transformation of the hermitian conjugate operator $\hat{B}^\dagger$ we get

$$\hat{\tilde{B}}^\dagger = \hat{O}^\dagger\hat{B}^\dagger\hat{O} = (\hat{O}^\dagger\hat{B}\hat{O})^\dagger = \hat{\tilde{B}}^\dagger \tag{1.93}$$

That means it does not matter if one transforms first and then builds the hermitian conjugate or the other way around. The practical consequence is

that if one has transformed an operator, one gets the transformation of its hermitian conjugate for free.
The prescription eq.(1.92) is readily obtained if we rewrite the expression for a matrix element between transformed states $|\tilde{\psi}_{m/n}\rangle = \hat{O}|\psi_{m/n}\rangle$

$$\langle\tilde{\psi}_m|\hat{B}|\tilde{\psi}_n\rangle = \langle\psi_m|\hat{O}^\dagger\hat{B}\hat{O}|\psi_n\rangle = \langle\psi_m|\hat{\tilde{B}}|\psi_n\rangle \tag{1.94}$$

which is the same if we transform the states directly or the operators according to eq.(1.92). Note that in the context of time evolution, which is also a transformation, the freedom to transform either the states or the operators is referred to as the Schrödinger (transformation of the states) or Heisenberg (transformation of the operators) picture, respectively.
In the case that the transformation operator $\hat{O}$ can be written as $\hat{O} = e^{-A}$ with an anti hermitian ($\hat{A}^\dagger = -\hat{A}$)operator $\hat{A}$, eq.(1.92) becomes

$$\hat{\tilde{B}} = (e^{-\hat{A}})^\dagger\hat{B}e^{-\hat{A}} = e^{-\hat{A}^\dagger}\hat{B}e^{-\hat{A}} = e^{\hat{A}}\hat{B}e^{-\hat{A}} \tag{1.95}$$

One way to evaluate the above expression is to make use of the Baker-Hausdorff formula

$$e^{\hat{A}}\hat{B}e^{-\hat{A}} = \sum_n^\infty \frac{1}{n!}[\hat{A},\hat{B}]_n \text{ with } [\hat{A},\hat{B}]_{n+1} = [\hat{A},[\hat{A},\hat{B}]_n] \text{ and } [\hat{A},\hat{B}]_0 \equiv \hat{B} \tag{1.96}$$

We want to mention two special cases.

- First, we assume that $[\hat{A},\hat{B}]_n = 0$ for $n > 1$. In this case the series in the Baker-Hausdorff formula breaks down and we get

$$e^{\hat{A}}\hat{B}e^{-\hat{A}} = \hat{B} + [\hat{A},\hat{B}] \tag{1.97}$$

- Second, we assume that the commutator reproduces $\hat{B}$

$$[\hat{A},\hat{B}] = \hat{C}\hat{B} \text{ and } [\hat{A},\hat{C}] = 0 \tag{1.98}$$

Under these circumstances the n-th commutator is given by

$$[\hat{A},\hat{B}]_n = \hat{C}^n\hat{B} \tag{1.99}$$

proof by induction: The $n = 1$ case is true due to eq.(1.98). The step from $n \to n+1$ is proven by

$$[\hat{A},\hat{B}]_{n+1} = [\hat{A},[\hat{A},\hat{B}]_n] = [\hat{A},\hat{C}^n\hat{B}] = \hat{C}^n[\hat{A},\hat{B}] = \hat{C}^{n+1}\hat{B} \quad \square \tag{1.100}$$

Then the tranformed operator is given by

$$\boxed{e^{\hat{A}}\hat{B}e^{-\hat{A}} = \sum_n^\infty \frac{1}{n!}\hat{C}^n\hat{B} = e^{\hat{C}}\hat{B}} \tag{1.101}$$

This is what some would call the brute force method. A more elegant way of performing the transformation is to introduce a parameter γ and viewing the transformed operator $\hat{\tilde{B}}$ as function of this parameter

$$\hat{\tilde{B}}(\gamma) = e^{\gamma\hat{A}}\hat{B}e^{-\gamma\hat{A}} \tag{1.102}$$

By differentiating this expression with respect to γ, we get

$$\frac{\mathrm{d}\hat{\tilde{B}}(\gamma)}{\mathrm{d}\gamma} = e^{\gamma\hat{A}}\hat{A}\hat{B}e^{-\gamma\hat{O}} - e^{\gamma\hat{A}}\hat{B}\hat{A}e^{-\gamma\hat{A}} = e^{\gamma\hat{A}}[\hat{A},\hat{B}]e^{-\gamma\hat{A}} \tag{1.103}$$

a differential equation for $\hat{\tilde{B}}(\gamma)$. If we assume that $[[\hat{A},\hat{B}],\hat{A}] = 0$ we can further simplify to

$$\frac{\mathrm{d}\hat{\tilde{B}}(\gamma)}{\mathrm{d}\gamma} = [\hat{A},\hat{B}] \tag{1.104}$$

with the solution

$$\boxed{\hat{\tilde{B}}(\gamma) = [\hat{A},\hat{B}]\gamma + \hat{\tilde{B}}(0) = [\hat{A},\hat{B}]\gamma + \hat{B}} \tag{1.105}$$

where we used that, see eq.(1.102), $\hat{\tilde{A}}(0) = \hat{A}$.

Now we turn back to our previous example and apply the transformation $\hat{O} = e^{-i\Delta\hat{p}}$ to the operator $\hat{x}$. Thus, we are interested in

$$\hat{\tilde{x}} = e^{i\Delta\hat{p}}\hat{x}e^{-i\Delta\hat{p}} \tag{1.106}$$

Comparing with the general form eq.(1.95) yields the identifications

$$\hat{A} = i\Delta\hat{p} \text{ and } \hat{B} = \hat{x} \tag{1.107}$$

First we calculate the commutator appearing in both transformation approaches mentioned above, eq.(1.96) and eq.(1.103).

$$[\hat{A},\hat{B}] = [i\Delta\hat{\tilde{p}},\hat{x}] = i\Delta\underbrace{[\hat{p},\hat{x}]}_{-i} = \Delta \tag{1.108}$$

Since this commutator is just a constant we also have $[i\Delta\hat{\tilde{p}},\hat{x}]_{n>1} = 0$. Keeping that in mind, we use eq.(1.108) in the Baker-Hausdorff formula eq.(1.96) and obtain

$$\hat{\tilde{x}} = e^{i\Delta\hat{p}}\hat{x}e^{-i\Delta\hat{p}} = \sum_n^\infty \frac{1}{n!}[i\Delta\hat{p},\hat{x}]_n = \hat{x} + \Delta \tag{1.109}$$

For the differential equation approach, eq.(1.103), we can think of Δ taking the role of γ and therefore needs to be excluded in the identification of $\hat{A}$. With the new identification $\hat{A} = i\hat{p}$ eq.(1.105) yields

$$\hat{\tilde{x}} = [i\hat{p},\hat{x}]\Delta + \hat{x} = \hat{x} + \Delta \tag{1.110}$$

Which is, as it should be, the same as eq.(1.109).

1.4.3 Removing the coupling term

Having learned how to generate a shift of amplitude Δ in space, we can use the Lang-Firsov transformation to remove the coupling term in the hamiltonian eq.(1.86). From eq(1.87) we know that we want to generate the shift

$$\hat{\tilde{x}} = \hat{x} + \frac{g}{m\omega_0^2}\hat{T}_e \Leftrightarrow \hat{x} = \hat{\tilde{x}} - \frac{g}{m\omega_0^2}\hat{T}_e \tag{1.111}$$

Motivated by the considerations above on how to introduce a constant shift in space and ignoring the fact that we know the exact value of the needed shift, we make the ansatz

$$\hat{O} = \hat{L} = e^{-i\gamma\hat{T}_e\hat{p}} \tag{1.112}$$

with a real and to be determined parameter γ which will shift the harmonic oscillator by an amount $\gamma\hat{T}_e$. To show also how the transformation is done if one uses the ladder operators $\hat{b}$ and $\hat{b}^\dagger$, we write the phonon operators $\hat{x}$ and $\hat{p}$ in terms of ladder operators

$$\hat{x} = \sqrt{\frac{1}{2m\omega_0}}(\hat{b}^\dagger + \hat{b}) \text{ and } \hat{p} = i\sqrt{\frac{m\omega_0}{2}}(\hat{b}^\dagger - \hat{b}) \tag{1.113}$$

From now on we will omit the hat for b and $b^\dagger$ since the risk of confusion is minimal. With this relations, our hamiltonian eq.(1.86) becomes

$$\hat{H} = \hat{H}_e + \omega_0(b^\dagger b + \frac{1}{2}) + \underbrace{g\sqrt{\frac{1}{2m\omega_0}}}_{\equiv\bar{g}}\hat{T}_e(b^\dagger + b) \tag{1.114}$$

and our ansatz eq.(1.112) is modified to

$$\hat{L} = e^{-i\gamma\hat{T}_e\hat{p}} = e^{\bar{\gamma}\hat{T}_e(b^\dagger - b)} \tag{1.115}$$

where we absorbed the constants into the definition of $\bar{\gamma} = \gamma\sqrt{\frac{m\omega_0}{2}}$. Next we calculate how the ladder operators transform. We start with

$$\tilde{b} = e^{-\bar{\gamma}\hat{T}_e(b^\dagger - b)} b e^{\bar{\gamma}\hat{T}_e(b^\dagger - b)} \tag{1.116}$$

Analogous to the procedure of transforming $\hat{x}$, eq.(1.107) and below, we begin by identifying the operators $\hat{A}$ and $\hat{B}$ to make use of the formulas in paragraph (1.4.2).

$$\hat{A} = -\hat{T}_e(b^\dagger - b) \text{ and } \hat{B} = b \tag{1.117}$$

Again we calculate the needed commutators

$$\begin{aligned} [A, B] &= [-\hat{T}_e(b^\dagger - b), b] = -\hat{T}_e \underbrace{[b^\dagger, b]}_{-1} = \hat{T}_e \\ [A, [A, B]] &= [\hat{T}_e(b^\dagger - b), [-\hat{T}_e(b^\dagger - b), b]] = -[\hat{T}_e(b^\dagger - b), \hat{T}_e] = 0 \end{aligned} \tag{1.118}$$

where we used the assumption that $\hat{T}_e$ is an electronic operator and commutes with the bosonic ones. This time we use eq.(1.105) instead of the Baker-Hasudorff formula, which is the reason why we excluded $\bar{\gamma}$ from the definition of $\hat{A}$, and end up with

$$\tilde{b} = [-\hat{T}_e(b^\dagger - b), b]\bar{\gamma} + b = b + \bar{\gamma}\hat{T}_e \tag{1.119}$$

Because of eq.(1.93) we get the transformation of $b^\dagger$ as the hermitian conjugate of $\tilde{b}$, which reads explicitly

$$\tilde{b}^\dagger = b^\dagger + \bar{\gamma}\hat{T}_e \tag{1.120}$$

With this relations, the hamiltonian eq.(1.114) transforms into

$$\begin{aligned}
\hat{\tilde{H}} &= \hat{L}^\dagger \hat{H} \hat{L} = \hat{L}^\dagger \hat{H}_e \hat{L} + \omega_0(\hat{L}^\dagger b^\dagger b \hat{L} + \frac{1}{2}) + \bar{g}\hat{L}^\dagger \hat{T}_e(b^\dagger + b)\hat{L} \\
&= \hat{\tilde{H}}_e + \omega_0(\hat{L}^\dagger b^\dagger \underbrace{\hat{L}\hat{L}^\dagger}_{\mathbb{1}} b\hat{L} + \frac{1}{2}) + \bar{g}\hat{T}_e\hat{L}^\dagger(b^\dagger + b)\hat{L} \\
&= \hat{\tilde{H}}_e + \omega_0(\tilde{b}^\dagger\tilde{b} + \frac{1}{2}) + 2\bar{g}\hat{T}_e(\tilde{b}^\dagger + \tilde{b})
\end{aligned} \tag{1.121}$$

where we used in the second equality that $\hat{T}_e$ commutes with the Lang-Firsov operator $\hat{L}^\dagger$ because the latter one only consists of $\hat{T}_e$ itself and the bosonic operators. With eq.(1.119) and eq.(1.120), we rewrite the hamiltonian further

$$\begin{aligned}
\hat{\tilde{H}} &= \hat{\tilde{H}}_e + \omega((b^\dagger + \bar{\gamma}\hat{T}_e)(b + \bar{\gamma}\hat{T}_e) + \frac{1}{2}) + \bar{g}\hat{T}_e(b^\dagger + \bar{\gamma}\hat{T}_e + b + \bar{\gamma}\hat{T}_e) \\
&= \hat{\tilde{H}}_e + \omega_0(b^\dagger b + \frac{1}{2}) + \omega_0\bar{\gamma}\hat{T}_e(b^\dagger + b) + \omega_0\bar{\gamma}^2\hat{T}_e^2 + \bar{g}\hat{T}_e(b^\dagger + b) + 2\bar{g}\bar{\gamma}\hat{T}_e^2
\end{aligned} \tag{1.122}$$

To remove the coupling term (to make the two terms proportional to $\hat{T}_e(b^\dagger + b)$ cancel), we demand that

$$\begin{aligned}
\omega_0\bar{\gamma} &\stackrel{!}{=} -\bar{g} = -g\sqrt{\frac{1}{2m\omega_0}} \\
\bar{\gamma} &= -g\sqrt{\frac{1}{2m\omega_0^3}}
\end{aligned} \tag{1.123}$$

or writing this relation in terms of the physical shift γ

$$\begin{aligned}
\gamma = \bar{\gamma}\sqrt{\frac{m\omega_0}{2}} &\stackrel{!}{=} -g\sqrt{\frac{1}{2m\omega_0^3}} \\
\gamma &= -\frac{g}{m\omega_0^2}
\end{aligned} \tag{1.124}$$

By plugging this result back into eq.(1.112)

$$\hat{L} = e^{-i(-\frac{g}{m\omega_0^2}\hat{T}_e)\hat{p}} \tag{1.125}$$

we see that the needed shift $-\frac{g}{m\omega_0^2}\hat{T}_e$ coincides with the suspected one in eq.(1.111). With the proper choice for $\bar{\gamma}$ the transformed hamiltonian takes the final form

$$\boxed{\hat{\tilde{H}} = \hat{\tilde{H}}_e + \omega_0(b^\dagger b + \frac{1}{2}) - \frac{\bar{g}^2}{\omega_0}\hat{T}_e^2} \tag{1.126}$$

In this form it seems like that we have gotten rid of the coupling all together and just had to pay the price of an extra term proportional to $\hat{T}_e^2$. But we have yet to specify the electronic hamiltonian $\hat{H}_e$ and as we will see beneath that is where the coupling has hidden itself in eq.(1.126).

1.4.4 Lang-Firsov Transformation in the Hubbard Holstein model

We continue by applying the Lang-Firsov transformation discussed above to concrete hamiltonians with electron phonon coupling. In sec.(1.2), we saw that we can devide the e-ph coupling into two parts, namely the Holstein and SSH type of interaction. First, we will illustrate in which form the e-ph coupling enters in the hamiltonian after the Lang-Firsov transformation, despite the removed coupling term, using the single mode Hubbard-Holstein model as an example. Then we continue by stating the result for the case of multiple modes.

Lang-Firsov Transformation in the Single mode Hubbard-Holstein model

The hamiltonian for the single mode Hubbard-Holstein model (using $\hbar = 1$) reads

$$\begin{aligned}\hat{H} =& \hat{H}_e + \hat{H}_{ph} + \hat{H}_{e-ph} = -\sum_{ij\sigma} t_{ij} c_{i\sigma}^\dagger c_{j\sigma} + \sum_{i\sigma} \varepsilon_{i\sigma} n_{i\sigma} + U\sum_i n_{i\uparrow} n_{i\downarrow} \\ &+ \omega_0(b^\dagger b + \frac{1}{2}) + \sum_{i\sigma} \underbrace{\sqrt{\frac{1}{2m\omega_0}}\lambda_i}_{\equiv \bar{\lambda}_i}(b^\dagger + b) n_{i\sigma}\end{aligned} \tag{1.127}$$

It consists of an electronic hamilton $\hat{H}_e$ with Hubbard like electron-electron interaction, the hamiltonian of an harmonic oscillator $\hat{H}_{ph}$ and the coupling term $\hat{H}_{e-ph}$. To remove the coupling term we need to introduce a shift proportianal to the operator $\sum_{i\sigma} \bar{\lambda}_i n_{i\sigma}$, which leads to the ansatz for the Lang-Firsov operator

$$\hat{L} = e^{\gamma \sum_{i\sigma} \bar{\lambda}_i n_{i\sigma}(b^\dagger - b)} \tag{1.128}$$

Comparing with eq.(1.115) we identify $\hat{T}_e = \sum_{i\sigma} \bar{\lambda}_i n_{i\sigma}$. We allready derived in eq.(1.126) the transformed hamilton operator, where only the electronic part of hamiltonian $\hat{H}_e$ was not explicitely transformed. For the single mode Hubbard-Holstein model this part is given by

$$\hat{H}_e = -\sum_{ij\sigma} t_{ij} c_{i\sigma}^\dagger c_{j\sigma} + \sum_{i\sigma} \varepsilon_{i\sigma} n_{i\sigma} + U\sum_i n_{i\uparrow} n_{i\downarrow} \tag{1.129}$$

Since $n_{i\sigma} = c^\dagger_{i\sigma} c_{i\sigma}$, its building blocks are only two operators, namely $c^\dagger_{i\sigma}$ and $c_{i\sigma}$. Because they are the hermitian conjugate of each other we only need to transform one of them and obtain the other by eq.(1.93). We choose to transform $c_{j\sigma}$

$$\tilde{c}_{j\sigma} = e^{-\gamma \sum_{i\sigma} \bar{\lambda}_i n_{i\sigma}(b^\dagger - b)} c_{j\sigma'} e^{\gamma \sum_{i\sigma} \bar{\lambda}_i n_{i\sigma}(b^\dagger - b)} \tag{1.130}$$

As in the previous cases we calculate the needed commutator

$$\left[-\gamma \sum_{i\sigma} \bar{\lambda}_i n_{i\sigma}(b^\dagger - b), c_{j\sigma'} \right] = -\gamma \sum_{i\sigma} \bar{\lambda}_i (b^\dagger - b) \underbrace{[n_{i\sigma}, c_{j\sigma'}]}_{-\delta_{ij}\delta_{\sigma\sigma'} c_{j\sigma'}} = \gamma \bar{\lambda}_j (b^\dagger - b) c_{j\sigma'} \tag{1.131}$$

It reproduces the operator $c_{j\sigma'}$ that we want to transform. We already derived this case which resulted in eq.(1.101) and therefore we arrive at

$$\tilde{c}_{i\sigma} = c_{i\sigma} e^{\gamma \bar{\lambda}_i (b^\dagger - b)} \text{ with its hermitian conjugate } \tilde{c}^\dagger_{i\sigma} = c^\dagger_{i\sigma} e^{-\gamma \bar{\lambda}_i (b^\dagger - b)} \tag{1.132}$$

Before we transform the whole hamiltonian eq.(1.127) note that the density operators $n_{i\sigma}$ are invariant under the Lang-Firsov transformation because they commute with $\hat{L}$. With the choice of $\gamma = -\frac{1}{\omega_0}$ the coupling term cancels and we obtain the transformed hamiltonian

$$\boxed{\begin{aligned} \hat{\tilde{H}} = &- \sum_{ij\sigma} t_{ij} c^\dagger_{i\sigma} c_{j\sigma} e^{\frac{1}{\omega_0}(\bar{\lambda}_i - \bar{\lambda}_j)(b^\dagger - b)} + \sum_{i\sigma} \varepsilon_{i\sigma} n_{i\sigma} + U \sum_i n_{i\uparrow} n_{i\downarrow} \\ &+ \omega_0 (b^\dagger b + \frac{1}{2}) - \frac{1}{\omega_0} \left(\sum_{i\sigma} \bar{\lambda}_i n_{i\sigma} \right)^2 \end{aligned}} \tag{1.133}$$

From the last equation we see that the e-ph coupling now enters in the hopping term in contrast to the hamiltonian before the Lang-Firsov transformation where it was an extra term. The last term introduces all sorts of negative density-density interactions.This and the considerations beneath are the reason why this term is generally called a negative U-term.

Special case of a single site system

Imagine if there was no hopping term in the original hamiltonian to begin with, than the Lang-Firsov transformation does not only remove the coupling term but exactly removes the e-ph coupling all together. This condition is fulfilled if the system in question consists only of a single site, because then the electron has no where to hop. In the following we will consider this special case. The original hamiltonian eq.(1.114) and the transformed one eq.(1.133) simplify to

$$\hat{H} = \sum_\sigma \varepsilon_\sigma n_\sigma + U n_\uparrow n_\downarrow + \omega_0 (b^\dagger b + \frac{1}{2}) + \sum_\sigma \bar{\lambda} n_\sigma (b^\dagger + b) \tag{1.134}$$

and

$$\hat{\tilde{H}} = \sum_\sigma \varepsilon_\sigma n_\sigma + U n_\uparrow n_\downarrow + \omega_0 (b^\dagger b + \frac{1}{2}) - \frac{1}{\omega_0} \left(\sum_\sigma \bar{\lambda} n_\sigma \right)^2 \tag{1.135}$$

respectively. Indeed the e-ph coupling has vanished from the hamiltonian and the only collateral side effect of the transformation is the arising of additional last term. Eq.(1.135) can be further simplified by rewriting the last term as

$$-\frac{1}{\omega_0}\left(\sum_\sigma \bar{\lambda} n_\sigma\right)^2 = -\frac{\bar{\lambda}^2}{\omega_0}(n_\uparrow + n_\downarrow)^2 = -\frac{\bar{\lambda}^2}{\omega_0}(\underbrace{n_\uparrow^2}_{n_\uparrow} + 2n_\uparrow n_\downarrow + \underbrace{n_\downarrow^2}_{n_\downarrow})$$
$$= \sum_\sigma \left(-\frac{\bar{\lambda}^2}{\omega_0}\right) n_\sigma - \frac{2\bar{\lambda}^2}{\omega_0} n_\uparrow n_\downarrow \tag{1.136}$$

With that, eq.(1.135) becomes

$$\boxed{\begin{aligned}\hat{\tilde{H}} &= \sum_\sigma \left(\varepsilon_\sigma - \frac{\bar{\lambda}^2}{\omega_0}\right) n_\sigma + \left(U - \frac{2\bar{\lambda}^2}{\omega_0}\right) n_\uparrow n_\downarrow + \omega_0(b^\dagger b + \frac{1}{2}) \\ &= \sum_\sigma \tilde{\varepsilon}_\sigma n_\sigma + \tilde{U} n_\uparrow n_\downarrow + \omega_0(b^\dagger b + \frac{1}{2})\end{aligned}}$$

This is exactly the same as the starting hamiltonian eq.(1.134) but with renormalized parameters

$$\tilde{\varepsilon}_\sigma = \varepsilon_\sigma - \frac{\bar{\lambda}^2}{\omega_0} \text{ and } \tilde{U} = U - \frac{2\bar{\lambda}^2}{\omega_0} \tag{1.137}$$

Due to its property to negatively renormalize U the additionally arising term is called a negative U-term. Note that for small U the renormalized value $\tilde{U}$ can become negative. This leads to effectively negative e-e interactions in such systems.

Hubbard-Holstein model with multiple modes

Before we close the discussion about the Lang-Firsov transformation in the Hubbard-Holstein model, we want to state the result of the transformed hamiltonian in the case of multiple modes. The hamiltonian then reads,

$$\hat{H} = -\sum_{ij\sigma} t_{ij} c_{i\sigma}^\dagger c_{j\sigma} + \sum_{i\sigma} \varepsilon_{i\sigma} n_{i\sigma} + U \sum_i n_{i\uparrow} n_{i\downarrow}$$
$$+ \sum_\mu \omega_\mu (b_\mu^\dagger b_\mu + \frac{1}{2}) + \sum_{i\sigma\mu} \underbrace{\sqrt{\frac{1}{2m\omega_\mu}} \lambda_i}_{\equiv \bar{\lambda}_i^\mu} (b_\mu^\dagger + b_\mu) n_{i\sigma} \tag{1.138}$$

Respecting all modes in the ansatz for the Lang-Firsov transformation yields

$$\hat{L} = e^{\sum_\mu \gamma_\mu \sum_{i\sigma} \bar{\lambda}_i^\mu n_{i\sigma} (b_\mu^\dagger - b_\mu)} \tag{1.139}$$

An analog calculation as in the single mode case, with the choice of $\gamma_\mu = -\frac{1}{\omega_\mu}$, transforms eq.(1.138) into

$$\boxed{\begin{aligned}\hat{\tilde{H}} = &-\sum_{ij\sigma} t_{ij} c^\dagger_{i\sigma} c_{j\sigma} e^{\sum_\mu \frac{1}{\omega_\mu}(\bar{\lambda}^\mu_i - \bar{\lambda}^\mu_j)(b^\dagger_\mu - b_\mu)} + \sum_{i\sigma} \varepsilon_{i\sigma} n_{i\sigma} + U \sum_i n_{i\uparrow} n_{i\downarrow} \\ &+ \sum_\mu \omega_\mu (b^\dagger_\mu b_\mu + \frac{1}{2}) - \sum_\mu \frac{1}{\omega_\mu} \left(\sum_{i\sigma} \bar{\lambda}^\mu_i n_{i\sigma} \right)^2 \end{aligned}} \tag{1.140}$$

1.4.5 Lang-Firsov transformation in the SSH model

At last, we demonstrate how to apply the Lang-Firsov transformation to the SSH model.

Lang-Firsov transformation in the single mode SSH model

Above, we showed how to remove the e-ph coupling term in the Hubbard-Holstein model using the Lang-Fisrsov transformation. Now, we turn to doing so for the SSH model where the e-ph interaction alters the electronic hopping amplitudes t_{ij} instead of the onsite energies ε_i. The single mode SSH model is readily obtained from eq.(1.52) if we disregard the Holstein interaction, leading to (again we use $\hbar = 1$)

$$\hat{H} = -\sum_{\substack{i\neq j \\ \sigma}} t_{ij} c^\dagger_{i\sigma} c_{j\sigma} + \sum_{i\sigma} \varepsilon_i n_{i\sigma} + \omega_0 (b^\dagger b + \frac{1}{2}) \tag{1.141}$$

$$+ \sum_{\substack{ij \\ \sigma}} \bar{g}_{ij} c^\dagger_{i\sigma} c_{j\sigma} (b^\dagger + b) \tag{1.142}$$

where we defined $\bar{g}_{ij} = \sqrt{\frac{1}{2m\omega_0}} g_{ij} \delta_{i\neq j}$ which allows us to extend the sum over all combination of indices ij.

The naive unsuitable ansatz of the Lang-Firsov transformation

Following the recipe from the last section we would make the ansatz for the Lang-Firsov transformation

$$\hat{L} = e^{\gamma \sum_{\substack{ij \\ \sigma}} \bar{g}_{ij} c^\dagger_{i\sigma} c_{j\sigma} (b^\dagger - b)} \tag{1.143}$$

The transformation of the phononic operators is straight forward and yields

$$\tilde{b} = b + \gamma \sum_{\substack{ij \\ \sigma}} \bar{g}_{ij} c^\dagger_{i\sigma} c_{j\sigma} \tag{1.144}$$

With $\gamma = \frac{1}{\omega_0}$ the coupling term would cancel, but if we try to transform an electronic operator $c_{j_0\sigma}$, or the whole electronic part for that mather, we run

into troubles. What is troublesome, is that the needed commutators neither reproduce $c_{j_0\sigma}$, nor terminate naturally. To demonstrate this, we calculate

$$
\begin{aligned}
&[-\gamma \sum_{\substack{ij\\ \sigma'}} \bar{g}_{ij} c^\dagger_{i\sigma'} c_{j\sigma'}(b^\dagger - b), c_{j_0\sigma}] = -\gamma \sum_{\substack{ij\\ \sigma'}} \bar{g}_{ij}(b^\dagger - b) \underbrace{[c^\dagger_{i\sigma'} c_{j\sigma'}, c_{j_0\sigma}]}_{-\delta_{\sigma\sigma'}\delta_{ij_0} c_{j\sigma}} \\
&= \gamma \sum_j \bar{g}_{j_0 j} c_{j\sigma}(b^\dagger - b)
\end{aligned}
$$

and

$$
\begin{aligned}
&[-\gamma \sum_{\substack{ij_2\\ \sigma'}} \bar{g}_{ij_2} c^\dagger_{i\sigma'} c_{j_2\sigma'}(b^\dagger - b), c_{j_0\sigma}]_2 \\
&= [-\gamma \sum_{\substack{ij_2\\ \sigma'}} \bar{g}_{ij_2} c^\dagger_{i\sigma'} c_{j_2\sigma'}(b^\dagger - b), \gamma \sum_{j_1} \bar{g}_{j_0 j_1} c_{j_1\sigma}(b^\dagger - b)] \\
&= -\gamma^2 (b^\dagger - b)^2 \sum_{\substack{ij_2\\ \sigma' j_1}} \bar{g}_{j_0 j_1} \bar{g}_{ij_2} \underbrace{[c^\dagger_{i\sigma'} c_{j_2\sigma'}, c_{j_1\sigma}]}_{-\delta_{\sigma\sigma'}\delta_{ij_1} c_{j_2\sigma}} \\
&= \gamma^2 (b^\dagger - b)^2 \sum_{j_1 j_2} \bar{g}_{j_0 j_1} \bar{g}_{j_1 j_2} c_{j_2\sigma} \qquad (1.145)
\end{aligned}
$$

We see that the operator $c_{j_0\sigma}$ is not reproduced but for every step from n to $n+1$ a new sum of the form $\sum_{j_n+1} \bar{g}_{j_n j_{n+1}}$ and a factor of $\gamma(b^\dagger - b)$ is added. This consideration leads to the generalization

$$
\begin{aligned}
&[-\gamma \sum_{\substack{ij\\ \sigma'}} \bar{g}_{ij} c^\dagger_{i\sigma'} c_{j\sigma'}(b^\dagger - b), c_{j_0\sigma}]_n \\
&= \gamma^n (b^\dagger - b)^n \sum_{j_1 j_2 \dots j_n} \bar{g}_{j_0 j_1} \bar{g}_{j_1 j_2} \cdots \bar{g}_{j_{n-1} j_n} c_{j_n\sigma} \qquad (1.146)
\end{aligned}
$$

proof by induction of eq.(1.146): The base case is given by eq.(1.145). The inductive step from $n \mapsto n+1$ is prooven by

$$
\begin{aligned}
[\ ,\ ]_{n+1} =& [-\gamma \sum_{\substack{ij_{n+1}\\ \sigma'}} \bar{g}_{ij_{n+1}} c^\dagger_{i\sigma'} c_{j_{n+1}\sigma'}(b^\dagger - b), [-\gamma \sum_{\substack{ij_{n+1}\\ \sigma'}} \bar{g}_{ij} c^\dagger_{i\sigma'} c_{j\sigma'}(b^\dagger - b), c_{j_0\sigma}]_n] \\
=& -\gamma(b^\dagger - b)\gamma^n (b^\dagger - b)^n \sum_{\substack{ij_{n+1}\\ \sigma'}} \bar{g}_{ij_{n+1}} \sum_{j_1 j_2 \dots j_n} \bar{g}_{j_0 j_1} \bar{g}_{j_1 j_2} \cdots \bar{g}_{j_{n-1} j_n} \underbrace{[c^\dagger_{i\sigma'} c_{j_{n+1}\sigma'}, c_{j_n\sigma}]}_{-\delta_{\sigma\sigma'}\delta_{ij_n} c_{j_{n+1}\sigma}} \\
=& \gamma^{n+1}(b^\dagger - b)^{n+1} \sum_{j_1 j_2 \dots j_{n+1}} \bar{g}_{j_0 j_1} \bar{g}_{j_1 j_2} \cdots \bar{g}_{j_n j_{n+1}} c_{j_{n+1}\sigma} \ \square \qquad (1.147)
\end{aligned}
$$

If we plug the generalisation eq.(1.146) into the Baker-Hausdorff formula, we obtain

$$
\boxed{\tilde{c}_{j_0\sigma} = \sum_{n=0}^{\infty} \frac{\gamma^n (b^\dagger - b)^n}{n!} \left(\sum_{j_1 j_2 \dots j_n} \bar{g}_{j_0 j_1} \bar{g}_{j_1 j_2} \cdots \bar{g}_{j_{n-1} j_n} c_{j_n\sigma} \right)^n} \qquad (1.148)
$$

which does not allow an analytical simplification due to the sums. For that reason, it is not possible to perform the summation in eq.(1.148) up to infinity leading to the fact that this transformation can not be done exactly. Even if one introduces a cut off for the maximal occupation number of the phonons n_{max}, which is a common thing to do in numerical approaches, the summation can not be performed consistently. In this context consistently would mean that, given a phonon cut off n_{max}, all terms with $n > n_{max}$ are zero. This is not the case here since

$$(b^\dagger - b)^n |n_{max}\rangle \hat{=} \sum_{l+m=n} \alpha_{lm} (b^\dagger)^l b^m |n_{max}\rangle \neq 0 \tag{1.149}$$

even for $n > n_{max}$. Of course, if one chooses the cut off high enough that the $\frac{\gamma^n}{n!}$ dominates it can be a viable approximation but typically this cut off is too large to treat numerically.

Diagonalizing the coupling term to apply the Lang-Firsov transformation

So far, we have shown that the naive ansatz for the Lang-Firsov transformation, eq(1.143), does not work in the case of a SSH type of interaction. The problem is that it is not possible to perform the transformation for the fermionic operators $c_{i\sigma}$ if we put a hopping term $\sum_{ij\sigma} t_{ij} c^\dagger_{i\sigma} c_{j\sigma}$ into the ansatz for the Lang-Firsov transformation. Recall, that we did not find this issue in the case of the Holstein interaction where the fermionic operators entered in the ansatz for the Lang-Firsov transformation, eq.(1.128), only as densities n_i. This suggests that we have to rewrite the coupling term

$$\hat{H}_{e-ph} = \sum_{ij\sigma} \bar{g}_{ij} c^\dagger_{i\sigma} c_{j\sigma} (b^\dagger + b) = (b^\dagger + b) \sum_\sigma \mathbf{c}^\dagger_\sigma G \mathbf{c}_\sigma \tag{1.150}$$

in a way that it only inhabits densities anymore. In eq.(1.150) we defined the vector $\mathbf{c} = (c_1, c_2, \ldots, c_N)$ and the matrix $(G)_{ij} = \bar{g}_{ij}$. To rewrite the coupling in term of densities we make use of the spectral representation of $G = U^\dagger \Lambda U$ and write

$$\hat{H}_{e-ph} = (b^\dagger + b) \sum_\sigma \mathbf{c}^\dagger_\sigma U^\dagger \Lambda U \mathbf{c}_\sigma = (b^\dagger + b) \sum_\sigma \mathbf{d}^\dagger_\sigma \Lambda \mathbf{d}_\sigma = (b^\dagger + b) \sum_{i\sigma} \lambda_i n_i \tag{1.151}$$

where we transformed from the $\mathbf{c}$ to the $\mathbf{d}$ particles/orbitals by defining

$$\mathbf{d}_\sigma = U \mathbf{c}_\sigma \tag{1.152}$$

With eq.(1.151) we have achieved the goal of rewriting the coupling hamiltonian, eq.(1.150), in terms of densities. Therefore, one has to diagonalize the electronic part of the e-ph coupling first before one can apply the Lang-Firsov transformation. We start by transforming the whole hamiltonian, eq.(1.142),

from the **c** to the **d** particles.

$$\begin{aligned}\hat{H} =& -\sum_{\substack{i\neq j\\ \sigma}} t_{ij} c_{i\sigma}^\dagger c_{j\sigma} + \sum_{i\sigma} \varepsilon_i n_{i\sigma} + \omega_0(b^\dagger b + \frac{1}{2}) \\ &+ \sum_{\substack{ij\\ \sigma}} \bar{g}_{ij} c_{i\sigma}^\dagger c_{j\sigma}(b^\dagger + b) \\ =& \sum_\sigma \mathbf{c}_\sigma^\dagger H_0 \mathbf{c}_\sigma + \omega_0(b^\dagger b + \frac{1}{2}) + \sum_\sigma \mathbf{c}_\sigma^\dagger G \mathbf{c}_\sigma (b^\dagger + b) \end{aligned} \tag{1.153}$$

where we defined the matrix $(H_0)_{ij} = -\delta_{i\neq j} t_{ij} + \delta_{ij}\varepsilon_i$. By inserting the identity $U^\dagger U$ in suitable places in eq.(1.153), we obtain the hamiltonian in terms of **d** particles

$$\begin{aligned}\hat{H} =& \sum_\sigma \mathbf{c}_\sigma^\dagger \underbrace{U^\dagger U}_{\mathbb{1}} H_0 U^\dagger \underbrace{U \mathbf{c}_\sigma}_{\mathbf{d}_\sigma} + \omega_0(b^\dagger b + \frac{1}{2}) + \sum_\sigma \mathbf{c}_\sigma^\dagger U^\dagger U G U^\dagger U \mathbf{c}_\sigma (b^\dagger + b) \\ =& \sum_\sigma \mathbf{d}_\sigma^\dagger \tilde{H}_0 \mathbf{d}_\sigma + \omega_0(b^\dagger b + \frac{1}{2}) + \sum_\sigma \mathbf{d}_\sigma^\dagger \Lambda \mathbf{d}_\sigma (b^\dagger + b) \\ =& \sum_{ij\sigma} (\tilde{H}_0)_{ij} d_{i\sigma}^\dagger d_{j\sigma} + \omega_0(b^\dagger b + \frac{1}{2}) + \sum_{i\sigma} \lambda_i n_{i\sigma}(b^\dagger + b) \end{aligned} \tag{1.154}$$

with the transformed matrix $\tilde{H}_0 = U H_0 U^\dagger$ and the eigenvalues λ_i of G. We remove the coupling term by applying the Lang-Firsov transformation

$$\hat{L} = e^{\gamma \sum_{i\sigma} \lambda_i n_{i\sigma}(b^\dagger - b)} \tag{1.155}$$

with $\gamma = -\frac{1}{\omega_0}$ to the hamiltonian eq.(1.154) and obtain

$$\boxed{\begin{aligned}\hat{\tilde{H}} =& \sum_{ij\sigma} (\tilde{H}_0)_{ij} d_{i\sigma}^\dagger d_{j\sigma} e^{\frac{1}{\omega_0}(\lambda_i - \lambda_j)(b^\dagger - b)} \\ &+ \omega_0(b^\dagger b + \frac{1}{2}) - \frac{1}{\omega_0}\left(\sum_{i\sigma} \lambda_i n_{i\sigma}\right)^2 \end{aligned}} \tag{1.156}$$

the transformed single mode SSH hamiltonian.

Lang-Firsov transformation in the multiple mode SSH model

Recall that we had to diagonalize the coupling term in eq.(1.153) to be able to remove the coupling term. In the case of multiple modes this is generally not possible since the coupling matrices G^μ for different modes usually do not commute and therefore can not be diagonalized all at ones. Thus, in contrast to the Hubbard-Holstein model, the Lang-Firsov transformation can not be applied to the SSH model in the case of multiple modes.

1.4.6 Calculation of phonon matrix elements appearing after the Lang-Firsov transformation

In all hamiltonians above where we applied the Lang-Firsov transformation a characteristic phonon operator of the form $e^{-\gamma(a^\dagger - a)}$ occurred. For further treatments of this hamiltonians it is useful to calculate its matrix elements. Therefore, we are interested in the matrixelement

$$\langle m|e^{-\gamma(a^\dagger - a)}|n\rangle \tag{1.157}$$

Since $[[a, a^\dagger], a^{(\dagger)}] = 0$, we can use the Baker-Hausdorf formula $e^{A+B} = e^A e^B e^{-[A,B]/2}$ with $A = -\gamma a^\dagger$ and $B = \gamma a$. Using the commutator $[A, B] = -\gamma^2[a^\dagger, a] = \gamma^2$, leads to

$$\langle m|e^{-\gamma(a^\dagger - a)}|n\rangle = e^{-\frac{\gamma^2}{2}}\langle m|e^{-\gamma a^\dagger}e^{\gamma a}|n\rangle$$

Calculation of $e^{\gamma a}|n\rangle$:

$$e^{\gamma a}|n\rangle = \sum_{\nu=0}^{\infty}\frac{\gamma^\nu}{\nu!}a^\nu|n\rangle = \sum_{\nu=0}^{n}\frac{\gamma^\nu}{\nu!}\sqrt{\frac{n!}{(n-\nu)!}}|n-\nu\rangle$$

A similar calculation for $\langle m|e^{-\gamma a^\dagger}$ and we get

$$\begin{aligned}\langle m|e^{-\gamma(a^\dagger - a)}|n\rangle =& e^{-\frac{\gamma^2}{2}}\sum_{\mu=0}^{m}\sum_{\nu=0}^{n}\frac{(-\gamma)^\mu\gamma^\nu}{\mu!\nu!}\frac{\sqrt{n!}\sqrt{m!}}{\sqrt{(m-\mu)!}\sqrt{(n-\nu)!}}\langle m-\mu|n-\nu\rangle \\ =& e^{-\frac{\gamma^2}{2}}\sum_{\mu=0}^{m}\sum_{\nu=0}^{n}\frac{(-\gamma)^\mu\gamma^\nu}{\mu!\nu!}\frac{\sqrt{n!}\sqrt{m!}}{\sqrt{(m-\mu)!}\sqrt{(n-\nu)!}}\delta_{m-\mu,n-\nu}\end{aligned}$$

For $m \geq n$ the sums are restricted by n and we eliminate μ with $\delta_{\mu=m-n+\nu}$

$$\begin{aligned}\langle m|e^{-\gamma(a^\dagger - a)}|n\rangle =& e^{-\frac{\gamma^2}{2}}\sqrt{n!}\sqrt{m!}\sum_{\nu=0}^{n}\frac{(-1)^{m-n+\nu}\gamma^{m-n+2\nu}}{(m-n+\nu)!\nu!\sqrt{m-(m-n+\nu)!(n-\nu)!}} \\ =& \boxed{e^{-\frac{\gamma^2}{2}}\sqrt{n!}\sqrt{m!}(-\gamma)^{m-n}\sum_{\nu=0}^{n}\frac{(-1)^\nu\gamma^{2\nu}}{(m-n+\nu)!\nu!(n-\nu)!}}\end{aligned} \tag{1.158}$$

For $n \geq m$ the sums are restricted by m and we eliminate ν with $\delta_{\nu=n-m+\mu}$

$$\boxed{\langle m|e^{-\gamma(a^\dagger - a)}|n\rangle = e^{-\frac{\gamma^2}{2}}\sqrt{n!}\sqrt{m!}\gamma^{n-m}\sum_{\mu=0}^{m}\frac{(-1)^\mu\gamma^{2\mu}}{(n-m+\mu)!\mu!(m-\mu)!}} \tag{1.159}$$

For $n = m$ both expressions eq.(1.158) and eq.(1.159) lead to

$$\langle n|e^{-\gamma(a^\dagger - a)}|n\rangle = e^{-\frac{\gamma^2}{2}}n!\sum_{\mu=0}^{n}\frac{(-1)^\mu\gamma^{2\mu}}{(\mu!)^2(n-\mu)!} \tag{1.160}$$

And because we need it later we also state the special case

$$\boxed{\begin{aligned}\langle 0|e^{-\gamma(a^\dagger - a)}|n\rangle &= e^{-\frac{\gamma^2}{2}}\frac{\gamma^n}{\sqrt{n!}} \\ |\langle 0|e^{-\gamma(a^\dagger - a)}|n\rangle|^2 &= e^{\gamma^2}\frac{\gamma^{2n}}{n!}\end{aligned}} \tag{1.161}$$

The above derivation did not make use of the particular sign constellation of a and $a^\dagger$ in eq.(1.157). Therefore an analog calculation yields

$$\langle n|e^{\gamma(a^\dagger + a)}|m\rangle = e^{\frac{\gamma^2}{2}}\sqrt{n!m!}\gamma^{n+m}\sum_{l=0}^{min(n,m)}\frac{\gamma^{-2l}}{l!(n-l)!(m-l)!} \tag{1.162}$$

which is the matrix element appearing when treating the beyond SSH model, see sec.(1.2.3).

1.4.7 Greensfunctions and unitary transformations

In this work we solve for properties of our models, for example the steady state current, using greensfunctions. Be it the retarded, advanced or keldysch greensfunction in time or energy/frequency, all of them are defined as expectation values of some operators with respect to some state or ensemble of states for finite temperature. We now want to show that all of this greensfunctions are invariant under a unitary transformation that was applied to the hamiltonian. Denoting the transformation operator by $\hat{L}$ and using the Schrödinger equation as a starting point we write

$$\begin{aligned}\hat{H}|\psi\rangle &= E|\psi\rangle \quad /\hat{L}^\dagger \text{ from left} \\ \hat{L}^\dagger\hat{H}\hat{L}\hat{L}^\dagger|\psi\rangle &= E\hat{L}^\dagger|\psi\rangle \qquad (1.163) \\ \hat{\tilde{H}}|\tilde{\psi}\rangle &= E|\tilde{\psi}\rangle \qquad (1.164)\end{aligned}$$

From that we see that the transformed hamiltonian has the same eigenvalues as the original one and its eigenvectors are given by $|\tilde{\psi}\rangle = \hat{L}^\dagger|\psi\rangle$. To show that any expectation value is invariant under a unitary transformation, we consider an arbitrary expectation value of the form

$$\langle\psi|\hat{A}_1\hat{A}_2\ldots\hat{A}_n|\psi\rangle \tag{1.165}$$

Rewriting it as

$$\langle\psi|\hat{L}\hat{L}^\dagger\hat{A}_1\hat{L}\hat{L}^\dagger\hat{A}_2\hat{L}\hat{L}^\dagger\ldots\hat{L}\hat{L}^\dagger\hat{A}_n\hat{L}\hat{L}^\dagger|\psi\rangle = \langle\tilde{\psi}|\hat{\tilde{A}}_1\hat{\tilde{A}}_2\ldots\hat{\tilde{A}}_n|\tilde{\psi}\rangle \tag{1.166}$$

we see that it is the same as if we replace every quantity appearing in its definition by the transformed one. As a consequence of the greensfunctions being invariant we know that any formalism/approximation that is formulated in terms of only greensfunctions, as for example CPT, can be straightforwardly applied taking the transformed hamiltonian as a starting point.

Chapter 2

Anderson-Holstein model

We apply the CPT formalism to the widely studied Anderson-Holstein and Anderson-Hubbard-Holstein model. First, we introduce the model and derive the single particle greensfunction of the quantum dot. Second, we present some results for weak to strong e-ph coupling and compare them to data found in the literature.

2.1 Anderson-Holstein model

The simplest model to study vibrational effects on the transport properties of an interacting electron region coupled to leads is the so called Anderson-Holstein model. For simplicity we consider spinless fermions. The Hamiltonian

$$\begin{aligned}\hat{H}_{AH} =&\hat{H}_{leads} + \hat{H}_{dot} + \hat{H}_{coupling} \\ =& -\sum_{ij} t_{ij} f_{li}^\dagger f_{lj} + \sum_i (\varepsilon_{li} - \mu_l) n_{li} - \sum_{ij} t_{ij} f_{ri}^\dagger f_{rj} + \sum_i (\varepsilon_{ri} - \mu_r) n_{ri} \\ &+ (\varepsilon_d - \mu) c^\dagger c + \omega_0 b^\dagger b + \lambda (b^\dagger + b) c^\dagger c \\ &+ v_l (f_{l1}^\dagger c + c^\dagger f_{l1}) + v_r (f_{r1}^\dagger c + c^\dagger f_{r1}) \end{aligned} \tag{2.1}$$

consists of three parts. The first one describes the left l and right r leads which are modeled as non interacting tight binding chains with electronic creation/annihilation operators $f_{l/ri}$. The second hamiltonian represents a single electronic level (often referred to as quantum dot) coupled to a local phonon mode with the Holstein interaction. Note that in the literature the coupling term is some times written as $\omega_0 g(b^\dagger + b)$ introducing a dimensionless coupling constant $g = \frac{\lambda}{\omega_0}$. The last term couples the central region (here the quantum dot) to the leads by allowing for hopping from and to the dot from the first left and right lead sites, respectively.

2.1.1 Greensfunction of the central region

As outlined in sec.(1.1) the main ingredient for the steady state CPT formalism is the greensfunction of the central region. The simplest sensible way to devide the system into clusters is by cutting it between the dot and the first site of the right/left lead. In this way we obtain three clusters, the quantum dot as the central cluster and the right/left lead as the other two. We will refer to this case as $N_c = 1$ since the central region is chosen to consist of a single site. For $N_c = 1$ the central region allows an analytical solution. Our starting point is the Lehmann representation of the greensfunctions

$$\begin{aligned} g^{r/a}(E) =& \sum_\alpha \frac{\langle\psi_0|c|\alpha\rangle\langle\alpha|c^\dagger|\psi_0\rangle}{E - (E_\alpha - E_0) \pm i0^+} + \sum_\beta \frac{\langle\psi_0|c^\dagger|\beta\rangle\langle\beta|c|\psi_0\rangle}{E + (E_\beta - E_0) \pm i0^+} \\ =& \sum_\alpha \frac{|\langle\psi_0|c|\alpha\rangle|^2}{E - (E_\alpha - E_0) \pm i0^+} + \sum_\beta \frac{|\langle\psi_0|c^\dagger|\beta\rangle|^2}{E + (E_\beta - E_0) \pm i0^+} \end{aligned} \tag{2.2}$$

This allows us to obtain the greensfunction if we have solved our system for the its eigenstates $|\alpha\rangle$ and corresponding eigenvalues E_α. To do so we remove the coupling term by applying the Lang-Firsov transformation

$$\hat{L} = e^{-\frac{\lambda}{\omega_0} c^\dagger c (b^\dagger + b)} \tag{2.3}$$

to our hamiltonian eq.(2.1). The hamiltonians of the leads remain unchanged because the fermionic lead operators f commute with the Lang-Firsov operator and with the results from sec.(1.4.4), we obtain the transformed hamilton

operator

$$\begin{aligned}\hat{\tilde{H}}_{AH} =&\hat{L}^\dagger \hat{H}_{AH}\hat{L} = \hat{L}^\dagger \hat{H}_{leads}\hat{L} + \hat{L}^\dagger \hat{H}_{dot}\hat{L} + \hat{L}^\dagger \hat{H}_{coupling}\hat{L} \\ =& -\sum_{ij} t_{ij} f_{li}^\dagger f_{lj} + \sum_i (\varepsilon_{li} - \mu_l) n_{li} - \sum_{ij} t_{ij} f_{ri}^\dagger f_{rj} + \sum_i (\varepsilon_{ri} - \mu_r) n_{ri} \\ &+ (\varepsilon_d - \frac{\lambda^2}{\omega_0} - \mu) c^\dagger c + \omega_0 b^\dagger b + v_l (f_{l1}^\dagger c e^{-\frac{\lambda}{\omega_0}(b^\dagger - b)} + c^\dagger e^{\frac{\lambda}{\omega_0}(b^\dagger - b)} f_{l1}) \\ &+ v_r (f_{r1}^\dagger c e^{-\frac{\lambda}{\omega_0}(b^\dagger - b)} + c^\dagger e^{\frac{\lambda}{\omega_0}(b^\dagger - b)} f_{r1}) \end{aligned} \tag{2.4}$$

In particular the transformed dot hamiltonian

$$\hat{\tilde{H}}_{dot} = (\varepsilon_d - \frac{\lambda^2}{\omega_0} - \mu) c^\dagger c + \omega_0 b^\dagger b \tag{2.5}$$

is now decoupled and the eigenvectors are therefore merely a tensor product of an electronic and a phonon state. Since the quantum dot has only a single electronic level and we consider the case of no spin the possible electronic states are the occupied level $|n_e = 1\rangle = c^\dagger |0\rangle_e$ and unoccupied/vacuum level $|n_e = 0\rangle_e = |0\rangle_e$. The phonon states are of course given by the eigenstates of the harmonic oscillator $|n_p\rangle = (b^\dagger)^{n_p}|0\rangle_p$ and thus we can write down the eigensystem of eq.(2.5) as

$$|\tilde{\psi}\rangle = |n_e\rangle \otimes |n_p\rangle \quad \tilde{E}_i = (\varepsilon_d - \frac{\lambda^2}{\omega_0} - \mu)\delta_{n_e,1} + n_p \omega_0 \tag{2.6}$$

The groundstate is the phonon vacuum, as the phonon part gives only positive contributions to the energy, and depending on $\varepsilon_d - \frac{\lambda^2}{\omega_0} - \mu > / < 0$ the electronic vacuum or the occupied dot state. In short

$$|\tilde{\psi}_0\rangle = \begin{cases} |0\rangle_e |0\rangle_p & \varepsilon_d - \frac{\lambda^2}{\omega_0} - \mu > 0 \\ |1\rangle_e |0\rangle_p & \varepsilon_d - \frac{\lambda^2}{\omega_0} - \mu < 0 \end{cases} \tag{2.7}$$

Note that this is the groundstate of the transformed hamiltonian, the original groundstate is related to the transformed one, see eq.(1.164), by

$$|\psi_0\rangle = \hat{L}|\tilde{\psi}\rangle = e^{-\frac{\lambda}{\omega_0} c^\dagger c (b^\dagger - b)} |\tilde{\psi}\rangle = \sum_{n=0}^{\infty} \frac{(-\frac{\lambda}{\omega_0})^n}{n!} (c^\dagger c)^n (b^\dagger - b)^n |\tilde{\psi}\rangle \tag{2.8}$$

which for $\varepsilon_d - \frac{\lambda^2}{\omega_0} - \mu < 0$ evaluates to

$$\begin{aligned} |\psi_0\rangle =& \sum_{n=0}^{\infty} \frac{(-\frac{\lambda}{\omega_0})^n}{n!} \underbrace{(c^\dagger c)^n |1\rangle_e}_{|1\rangle_e} (b^\dagger - b)^n |0\rangle_p = |1\rangle_e \sum_{n=0}^{\infty} \frac{(-\frac{\lambda}{\omega_0})^n}{n!} (b^\dagger - b)^n |0\rangle_p \\ =& |1\rangle_e e^{-\frac{\lambda}{\omega_0}(b^\dagger - b)} |0\rangle_p = |1\rangle_e \sum_{n=0}^{\infty} |n\rangle_{pp}\langle n| e^{-\frac{\lambda}{\omega_0}(b^\dagger - b)} |0\rangle_p \\ =& \boxed{|1\rangle_e e^{-\frac{\lambda^2}{2\omega_0^2}} \sum_{n=0}^{\infty} \frac{\left(-\frac{\lambda}{\omega_0}\right)^n}{\sqrt{n!}} |n\rangle_p} \end{aligned} \tag{2.9}$$

where we have inserted the identity for the phonons $\mathbb{1} = \sum_{n=0}^{\infty} |n\rangle_{pp}\langle n|$ and used eq.(1.158) to express the matrix element $\langle n|e^{-\frac{\lambda}{\omega_0}(b^\dagger - b)}|0\rangle$. From eq.(2.9) we see that the original groundstate is a superposition of all phonon states with the amplitude given by the above matrix element. This is of course just a consequence of the oscillator being shifted by the Lang-Firsov transformation and thus one needs infinitely many states of the original oszillator to represent the groundstate of the shifted one as discussed in sec.(1.4).
However, to obtain the greensfunction, eq.(2.2), we do not need the original groundstate, as was shown in sec.(1.4.7) we get the same greensfunction if we calculate it with all transformed quantities. With the transformed operators, see eq.(1.132),

$$\tilde{c} = \hat{L}^\dagger c \hat{L} = c e^{-\frac{\lambda}{\omega_0}(b^\dagger - b)} \text{ and } \tilde{c}^\dagger = c^\dagger e^{\frac{\lambda}{\omega_0}(b^\dagger - b)} \tag{2.10}$$

eq.(2.2) becomes

$$\begin{aligned} g^{r/a}(E) =& \sum_\alpha \frac{|\langle\psi_0|\hat{L}^\dagger \hat{L} c \hat{L}^\dagger \hat{L}|\alpha\rangle|^2}{E - (E_\alpha - E_0) \pm i0^+} + \sum_\beta \frac{|\langle\psi_0|\hat{L}^\dagger \hat{L} c^\dagger \hat{L}^\dagger \hat{L}|\beta\rangle|^2}{E + (E_\beta - E_0) \pm i0^+} \\ =& \sum_{\tilde{\alpha}} \frac{|\langle\tilde{\psi}_0|c e^{-\frac{\lambda}{\omega_0}(b^\dagger - b)}|\tilde{\alpha}\rangle|^2}{E - (E_{\tilde{\alpha}} - E_0) \pm i0^+} + \sum_{\tilde{\beta}} \frac{|\langle\tilde{\psi}_0|c^\dagger e^{\frac{\lambda}{\omega_0}(b^\dagger - b)}|\tilde{\beta}\rangle|^2}{E + (E_{\tilde{\beta}} - E_0) \pm i0^+} \end{aligned} \tag{2.11}$$

First, we consider the case that $\varepsilon_d - \frac{\lambda^2}{\omega_0} - \mu < 0$ with the groundstate $|\tilde{\psi}_0\rangle = |1\rangle_e|0\rangle_p$ and groundstate energy $E_0 = \varepsilon_d - \frac{\lambda^2}{\omega_0} - \mu$. There are no states $|\tilde{\alpha}\rangle$ with one electron more than in the groudstate and the states with one electron less are $|\tilde{\beta}\rangle = |0\rangle_e|n\rangle_p$. Since the electron part of the greensfunction is zero this leaves us with only the hole part given by

$$\begin{aligned} g^{r/a}(E) =& \sum_{\tilde{\beta}} \frac{|_p\langle 0|_e\langle 1|c^\dagger e^{\frac{\lambda}{\omega_0}(b^\dagger - b)}|\tilde{\beta}\rangle|^2}{E + (E_{\tilde{\beta}} - (\varepsilon_d - \frac{\lambda^2}{\omega_0} - \mu)) \pm i0^+} \\ =& \sum_{n=0}^{\infty} \frac{|_p\langle 0|e^{\frac{\lambda}{\omega_0}(b^\dagger - b)}|n\rangle_p|^2 |_e\langle 1|c^\dagger|0\rangle_e|^2}{E + (\omega_0 n - (\varepsilon_d - \frac{\lambda^2}{\omega_0} - \mu)) \pm i0^+} \\ =& \boxed{e^{-(\frac{\lambda}{\omega_0})^2} \sum_{n=0}^{\infty} \frac{(\frac{\lambda}{\omega_0})^{2n}}{n!} \frac{1}{E - (\varepsilon_d - \frac{\lambda^2}{\omega_0} - \mu - \omega_0 n) \pm i0^+}} \end{aligned} \tag{2.12}$$

In the other case where $\varepsilon_d - \frac{\lambda^2}{\omega_0} - \mu > 0$ the groundstate is the vacuum state and therefore the hole part of the greensfunction vanishes. An analog calculation as above then yields

$$\boxed{g^{r/a}(E) = e^{-(\frac{\lambda}{\omega_0})^2} \sum_{n=0}^{\infty} \frac{(\frac{\lambda}{\omega_0})^{2n}}{n!} \frac{1}{E - (\varepsilon_d - \frac{\lambda^2}{\omega_0} - \mu + \omega_0 n) \pm i0^+}} \tag{2.13}$$

2.1.2 Franck-Condon blockade

The Franck-Condon blockade [20] is the effect that the low bias steady state current through a system with e-ph coupling gets suppressed as the coupling increases. It looks like the Coulomb blockade but unlike the Coulomb blockade it can not be lifted by tuning the gate voltage. From eq.(2.13) and eq.(2.12), we see that we have single particle excitations to the right/left of $\varepsilon_d - \frac{\lambda^2}{\omega_0} - \mu$ for the electron/hole case with a spacing given by the phonon energy ω_0 and an amplitude given by the squared matrix element $|\langle n|e^{-\frac{\lambda}{\omega_0}(b^\dagger - b)}|0\rangle|^2$. These are the states an additional electron can use to hop on and off of the central region. From fig.(2.1) we see that the important excitations get shifted to higher values of n for increasing effective interaction $\frac{\lambda}{\omega_0}$. This shifting translates to a shift of the electronic states to higher energies given by $\Delta E = \hbar\omega_0$. Thus, as the e-ph coupling is increased the states get shifted to higher energies rendering the current at low bias suppressed since the states in the fermi window of the leads lose their spectral weight to higher energy states. The behaviour of the matrix element in fig.(2.1) and therefore the Franck-Condon blockade can also be understood in the simple picture of the shifted harmonic oscillators. Recall that the shift generated by the Lang-Firsov transformation depends, for the Holstein model, on the electronic density n_{dot} or more generally on the electronic configuration of the central region. Therefore, the shift of the oscillator is different for the electronic groundstate and the excited state with one electron more. For small e-ph coupling this difference in the shifts is small and thus the overlap with the phonon groundstate is bigger for the low lying phonon excitations. If the e-ph coupling is large the shift is more severe and the overlap with the low lying states is exponentially suppressed leading to the behaviour described above. The explanation in terms of shifted oscillators is, of course, the reason for the name Franck-Condon blockade.

2.1.3 The Anderson-Hubbard-Holstein model

The Anderson-Hubbard-Holstein model is the generalisation of the Anderson-Holstein model with spin and Hubbard U. The hamiltonian of the central region for this model reads

$$\hat{H}_{dot} = \omega_0 b^\dagger b + \sum_\sigma (\varepsilon_d - \mu) c_\sigma^\dagger c_\sigma + \lambda(b^\dagger + b) c_\sigma^\dagger c_\sigma + \frac{U}{2} c_\sigma^\dagger c_\sigma c_{\sigma'}^\dagger c_{\sigma'} \tag{2.14}$$

As shown in sec.(1.4.4) the e-ph coupling term can again be removed by the Lang-Firsov transformation leading to a hamiltonian with renormalised parameters that is already diagonal. Thus, after choosing the correct groundstate out of the four possibilities, which depends on the interplay of ε, λ and U, the greensfunctions are straight forwardly calculated in analog to the derivation above.

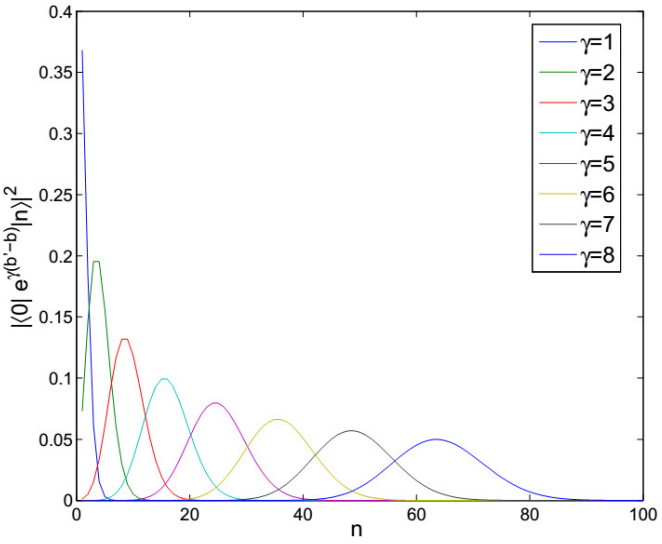

Figure 2.1: The phonon matrix element $|\langle n|e^{-\gamma(b^\dagger - b)}|0\rangle|^2$ for different γ. It follows an poisson distribution

2.2 Comparison with the literature

2.2.1 Weak e-ph coupling regime

We test our method for the weak e-ph coupling regime by comparing with results obtained by Koch et al [21] who investigated the system with perturbation theory in the e-ph coupling. Note that the paper does not give an explicit value for the coupling strength to the leads v but uses a single parameter $\Gamma(\omega) := 2\pi|v|^2\rho(\omega)$ to describe the leads. Furthermore, the perturbation theory result is obtained for the wideband limit where $\Gamma(\omega) = \Gamma^0$ is energy independent. To reproduce the same situation in our formalism we fix $t_{leads} = 40[eV]$, which leads to a very flat DOS of the leads in the bias region, and determine the coupling v so that $\Gamma^0 = \Gamma(\omega = 0) = \frac{2|v|^2}{t_{leads}}$. For the evaluation of the current we set the small imaginary quantity $0^+ = 0$. Fig.(2.2)-(2.4) show results for the $N_c = 1$ case which are already in satisfying agreement with the figures from the paper. The best agreement is met for small Γ^0, fig.(2.2), which means small dot lead coupling. This is to be expected since CPT is a perturbation theory in the intra cluster hoppings.

Next, we compare with data from Hützen et al [14] who used a technique called Iterative summation of path integrals (ISPI for short) to calculate steady state I/V curves. The group themselves compared their results to perturbation theory and rate equation approaches. Fig.(2.5) shows our results for different sizes of the central region N_c and the corresponding figure from the paper. The agreement with the results of the paper is not as good as for the comparison with Koch et al but we see an improvement with increasing size of the central region N_c. For consecutive N_c the data in fig.(2.5) jumps between two solutions which converge only slowly into each other. Fig.(2.6) shows the current voltage

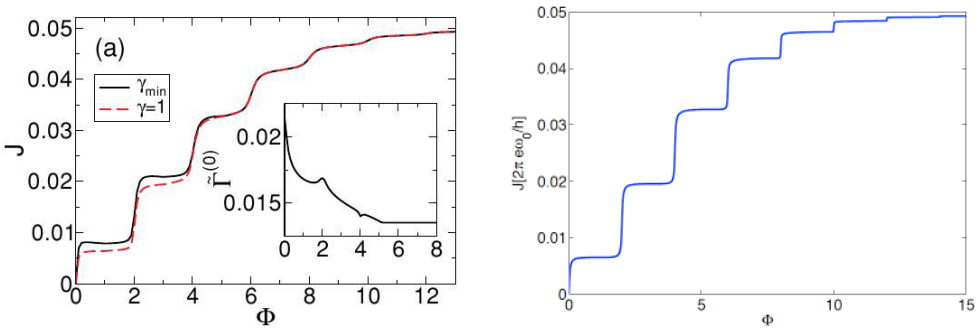

Figure 2.2: Left, fig.(5a) from the paper Koch et al [21]. Right, our plot with the corresponding parameters: $T = 0.01$, $t_{leads} = 40$, $\Gamma^0 = 0.1$, $\varepsilon_d - \mu_c = 2$, $\omega_0 = 1$, $v = 1.4142$, $g = 1.4142$. Note the difference in the y-axis.

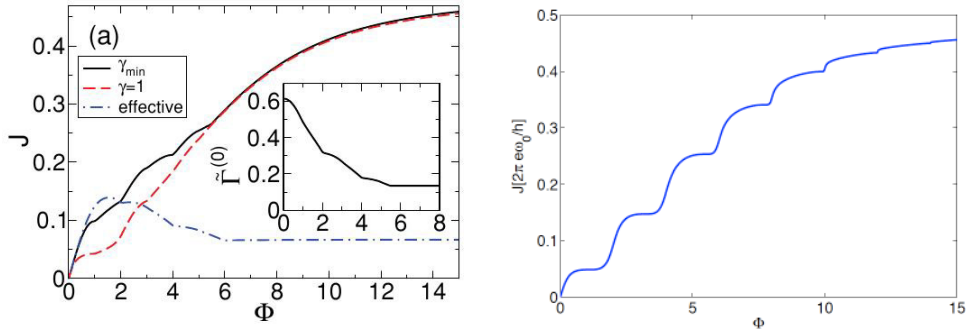

Figure 2.3: Left, fig.(6a) from the paper Koch et al [21]. Right, our plot with the corresponding parameters: $T = 0.01$, $t_{leads} = 40$, $\Gamma^0 = 1$, $\varepsilon_d - \mu_c = 2$, $\omega_0 = 1$, $v = 4.4721$, $g = 1.4142$. Note the difference in the y-axis.

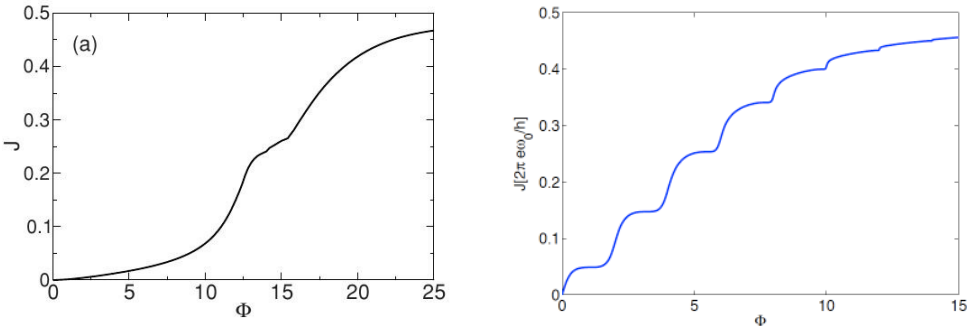

Figure 2.4: Left, fig.(7a) from the paper Koch et al [21]. Right, our plot with the corresponding parameters: $T = 0.01$, $t_{leads} = 40$, $\Gamma^0 = 1$, $\varepsilon_d - \mu_c = 8$, $\omega_0 = 1$, $v = 4.4721$, $g = 1.4142$.

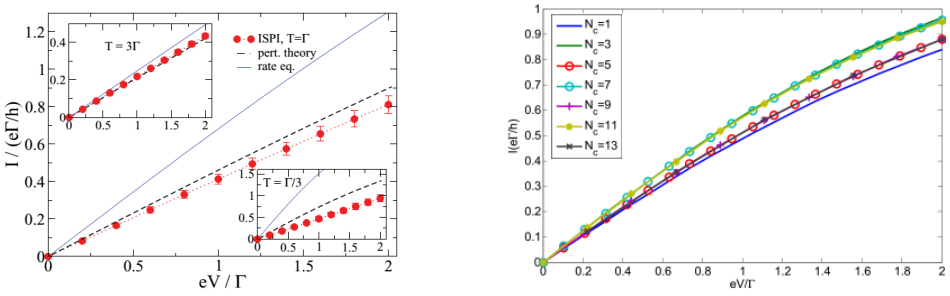

Figure 2.5: Left, fig.1 from the paper Hützen et al [14]. Right, our plot which corresponds to the lower inlet with the parameters: $T = \frac{\Gamma}{3}$, $t_{leads} = 40$, $\Gamma = 1$, $\varepsilon_d - \mu_c = 0$, $\omega_0 = \Gamma$, $g = 0.5\Gamma$.

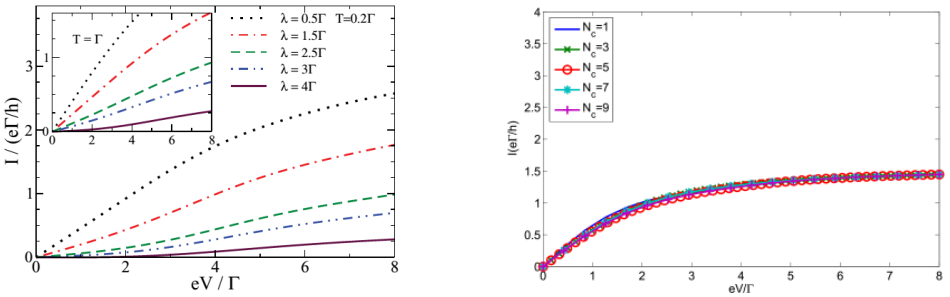

Figure 2.6: Left, fig.1 from the paper Hützen et al [14]. Right, our plot which corresponds to the black doted line in the left figure. Parameters: $T = 0.2\Gamma$, $t_{leads} = 40$, $\Gamma = 1$, $\varepsilon_d - \mu_c = 0$, $\omega_0 = 2\Gamma$, $g = 0.5\Gamma$.

characteristic for weaker dot lead coupling and a higher energy mode. We see that the CPT data is clearly converged in this case, which is again to be expected due to the small Γ, but does not agree with the result from the paper suggesting that ISPI overestimates the current in this case.

2.2.2 Intermediate e-ph coupling

For intermediate e-ph coupling we check against a different observable, namely the electronic conductance. In the paper from Ren et al [28] the group calculates the electronic and thermal conductance by linear response for a range of e-ph couplings. We use the formulas from the paper and replace the full greensfunction by the greensfunction obtained by CPT with $N_c = 1$. The color plots in fig.(2.7) show excellent quantitative and qualitative agreement with the literature.

2.2.3 Strong e-ph coupling and Franck-Condon blockade

Finally, we match our CPT approach against known results in the strong coupling regime. We compare with Koch and Oppen [19] who studied the Anderson-Hubbard-Holstein model by means of rate equations. Looking at fig.(2.8) we see very good agreement with the data from the paper.

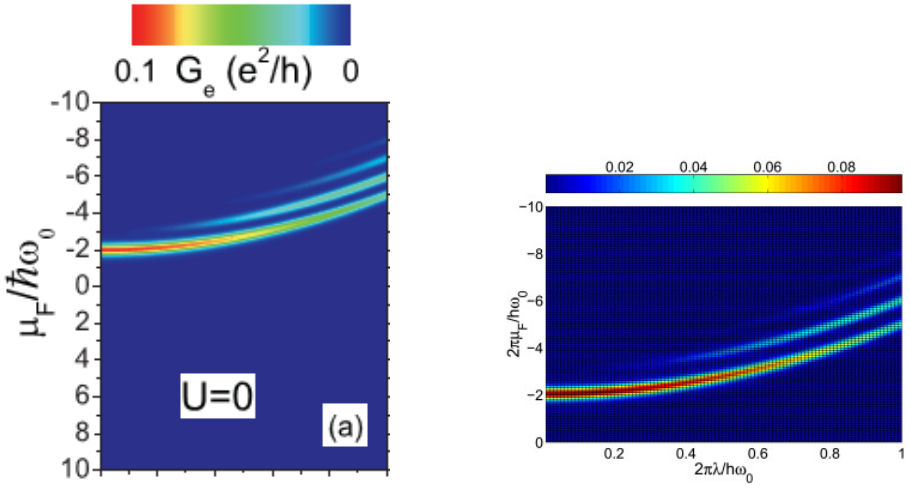

Figure 2.7: Left, fig.1a from the paper Ren et al [28]. Right, our plot. Parameters: $T = 0.2\Gamma$, $t_{leads} = 40$, $\Gamma = 1$, $\varepsilon_d - \mu_c = 0$, $\omega_0 = 2\Gamma$, $g = 0.5\Gamma$. Note the different y-axis.

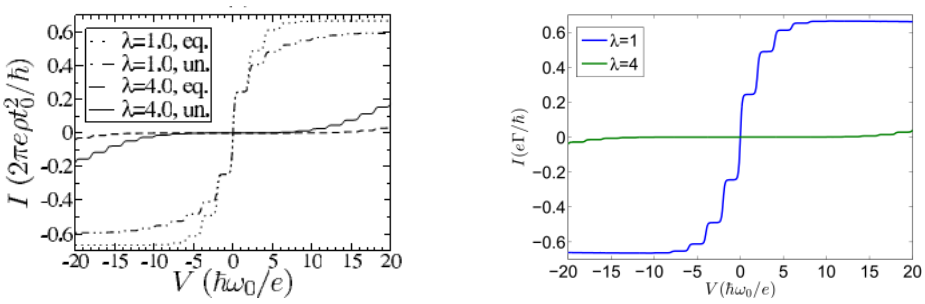

Figure 2.8: Left, fig.1a from the paper Koch and Oppen [19]. Right, our plot which corresponds to the curves labeled equilibrated (eq.). Parameters: $kT = 0.05$, $t_{leads} = 40$, $\varepsilon_d = 0$,$\omega_0 = 1$, $\Gamma^0 = 0.005$, $U = 100$ $N_c = 1$.

Chapter 3

Su-Schrieffer-Heeger model for a molecular ring

We apply our method to a molecular ring with SSH type of e-ph interaction coupled to non-interacting leads. The first section in this chapter is denoted to the vibrational modes of a contacted ring. Then we study the effects of the SSH interaction on the electronic properties of the ring in equilibrium. Finally, we present and discuss the non-equilibrium situation of the contacted ring on the basis of the current voltage characteristics.

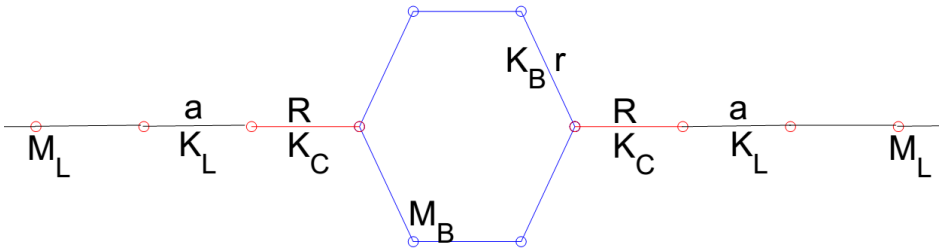

Figure 3.1: A sketch of the benzene lead system

Table 3.1: Parameters for the calculation of the modes

Parameter	Symbol	Value
bond length benzene	r	$1.39[A]$
bond length coupling	R	$1.39[A]$
bond length leads	R_L	$3.92[A]$
benzene Masses	M_B	$13[u]$
lead Masses	M_L	$200[u]$
spring constant benzene	K_B	$21[eV/A]$
spring constant coupling	K_C	$11.5[eV/A]$
spring constant leads	K_L	$10^7[eV/A]$

3.1 Calculation of modes for a contacted ring

3.1.1 System and parameters

We extract the classical vibrational modes of a benzene molecule attached to two metallic leads by modeling it as a system of masses and springs. In principle there are three different geometries in which the six site ring can be contacted. The latter are called para, ortho and meta configuration which refer to two, one and zero benzene sites between the connection points. Fig.(3.1) contains a sketch of the system in para configuration and the parameters are given in table(3.1).

The parameters for benzene are taken from [17] and the parameters of the leads are chosen to model (to some extend) a platinum lead while the coupling parameters are tuned in a way that the lowest energy mode corresponds to the value reported in [16]. Please note that we are not trying to model any specific experiment by choosing the parameter in this way but rather do so to obtain realistic modes.

3.1.2 Results for the modes

We are only interested in modes which involve motions of the benzene sites. These modes show no dependence on the number of lead sites nor the lattice spacing (bond length) a and can be thought of as decoupled from the specific parameters of the leads. Using the formalism outlined in sec.(1.3) and the

Table 3.2: Stretching amplitudes of the modes for free benzene and their sum. Labeling of the sites counterclockwise starting from the right.

	Breathing mode (1)	mode 2	mode 3	mode 4
d_{12}	-0.408248	0.139212	0.693268	0.518532
d_{23}	-0.408248	0.669993	0.226073	0.391382
d_{34}	-0.408248	0.530781	-0.467195	-0.909914
d_{45}	-0.408248	-0.139212	-0.693268	0.518532
d_{56}	-0.408248	-0.669993	-0.226073	0.391382
d_{61}	-0.408248	-0.530781	0.467195	-0.909914
$\sum d$	-2.4495	0	0	0
	mode 5	Pi-mode (6)		
d_{12}	0.751304	0.707107		
d_{23}	-0.824714	-0.707107		
d_{34}	0.073410	0.707107		
d_{45}	0.751304	-0.707107		
d_{56}	-0.824714	0.707107		
d_{61}	0.073410	-0.707107		
$\sum d$	0	0		

above parameters we obtain the modes shown in fig.(3.2) with their properties assembled in table(3.3). Comparing with the modes of free benzene, fig.(3.3), we recognise that the lowest energy mode of free benzene, which is referred to as the breathing mode, does not remain at lowest energy but rather appears slightly changed as mode three in the spectrum of the contacted system. Noteworthy is also the highest energy mode in the isolated case, which we will call Pi-mode, which survives the process of contacting the ring and remains unaltered in energy and geometry at the top of the spectrum. Another mode that the para configuration and free benzene have in common is the second degenerate mode of free benzene which reappears as mode six in the para spectrum. Because it is a degenerate mode in free benzene one may not recognise the equality by looking at the pictures.

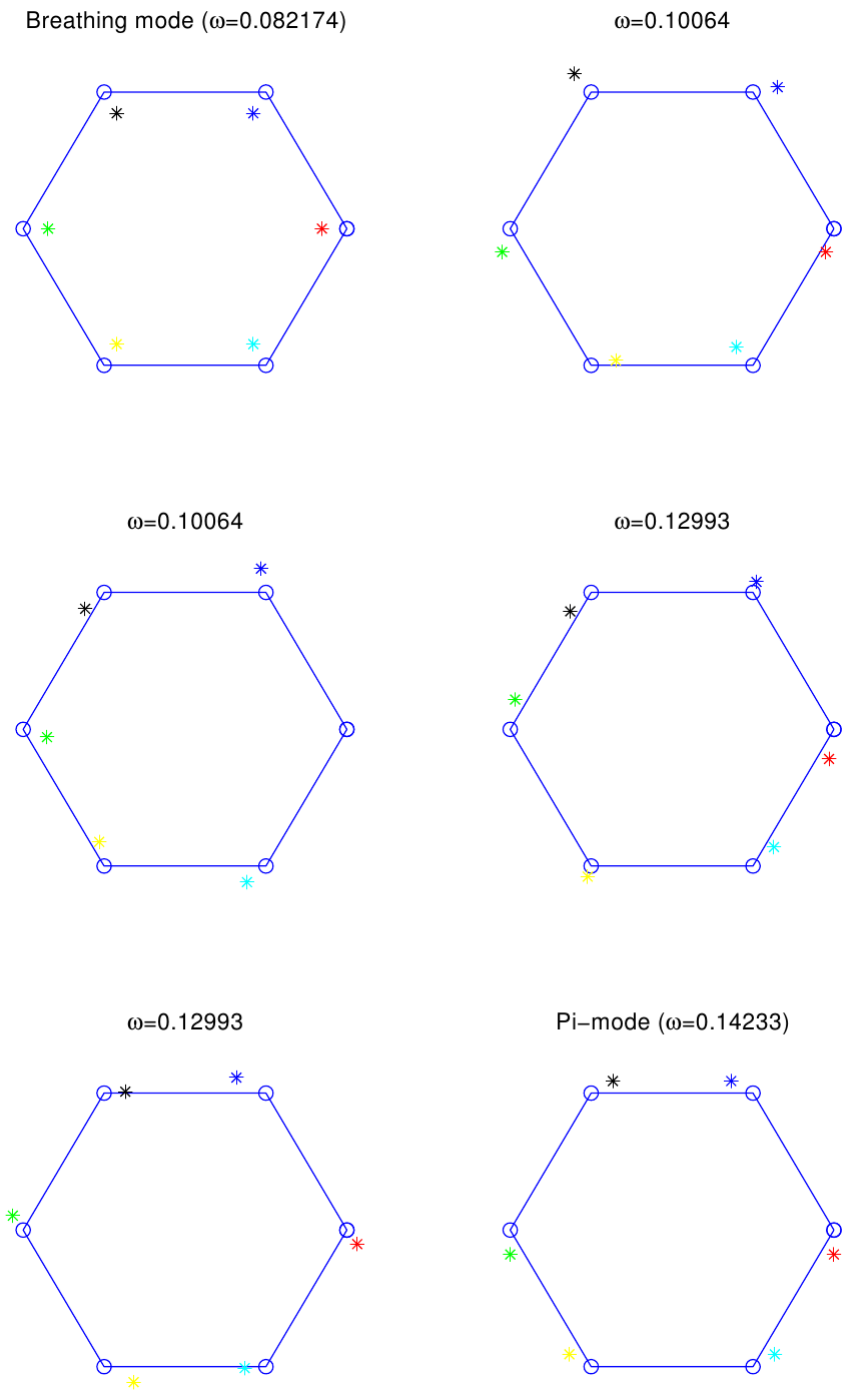

Figure 3.2: The modes of free benzene

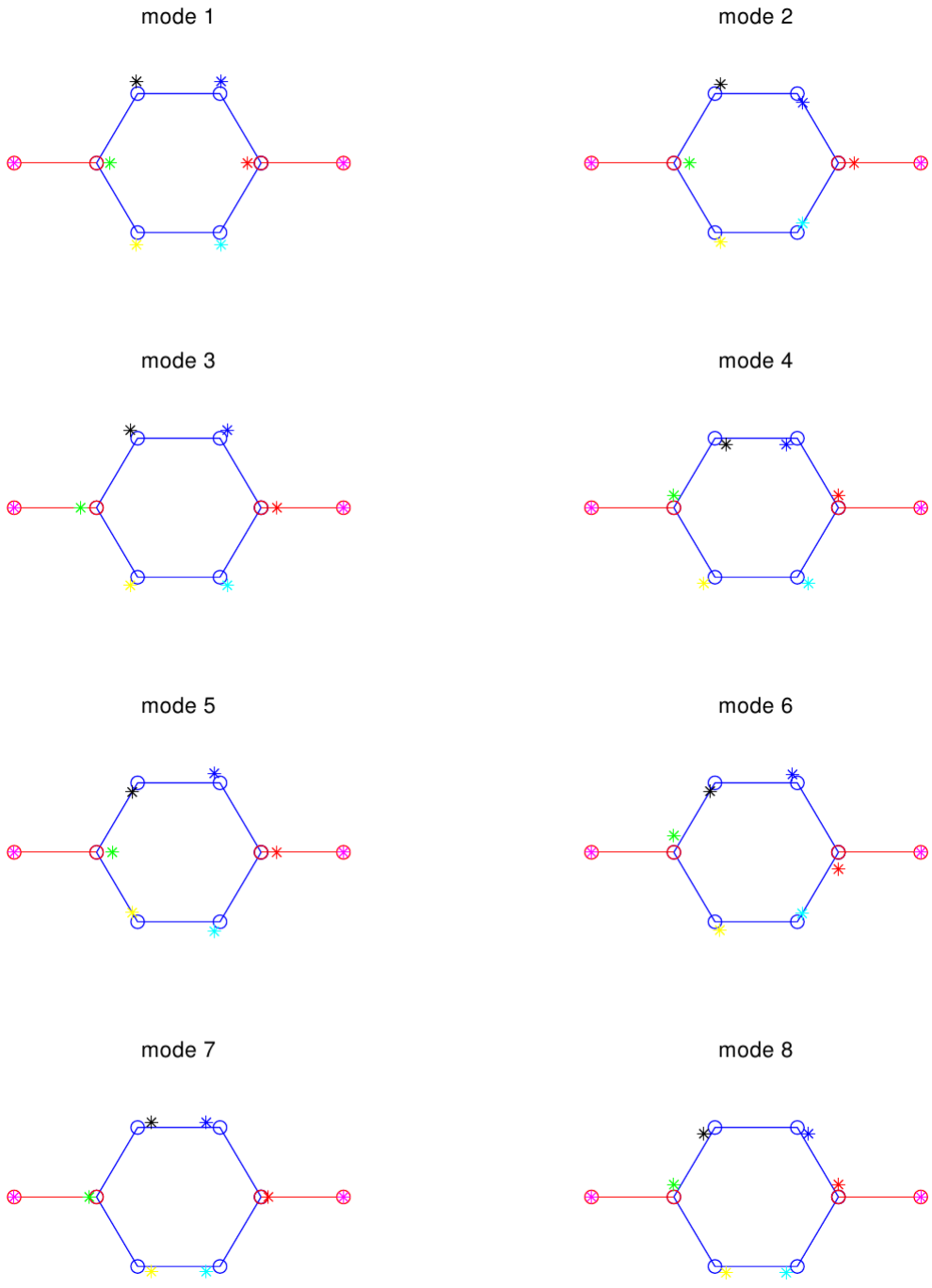

Figure 3.3: The modes for the para configuration. The equilibrium geometry is blue and the coloured stars indicate the changed positions of the atoms when the mode is excited.

Table 3.3: Properties of the modes for benzene in the para configuration. ω is the frequency/energy of the mode and the d_{ij} are the stretching amplitudes of a mode defined in eq.(1.83) and $\sum d$ indicates the sum over all of them. The labeling of sites starts at the right corner of the ring and continues counter-clockwise around the benzene, the left lead site is labeled as even and the right one as eight.

	mode 1	mode 2	mode 3	mode 4	mode 5
ω/eV	0.040502	0.044472	0.090541	0.100642	0.107365
d_{12}	-0.110823	-0.103553	0.363281	-0.353553	0.603553
d_{23}	-0.063072	$< 10^{-6}$	0.462191	-0.707107	$< 10^{-6}$
d_{34}	-0.110823	0.103553	0.363281	-0.353553	-0.603553
d_{45}	-0.110823	0.103553	0.363281	0.353553	-0.603553
d_{56}	-0.063072	$< 10^{-6}$	0.462191	0.707107	$< 10^{-6}$
d_{61}	-0.110823	-0.103553	0.363281	0.353553	0.603553
d_{47}	-0.431101	0.500000	-0.508793	$< 10^{-6}$	0.499999
d_{18}	-0.431101	-0.500000	-0.508793	$< 10^{-6}$	-0.499999
$\sum d$	-1.4316	0	1.3599	0	0

	mode 6	mode 7	mode 8		
ω/eV	0.129928	0.131043	0.142329		
d_{12}	-0.790569	-0.480360	0.707107		
d_{23}	$< 10^{-6}$	0.884535	-0.707107		
d_{34}	0.790569	-0.480360	0.707107		
d_{45}	-0.790569	-0.480360	-0.707107		
d_{56}	$< 10^{-6}$	0.884535	0.707107		
d_{61}	0.790569	-0.480360	-0.707107		
d_{47}	$< 10^{-6}$	0.235117	$< 10^{-6}$		
d_{18}	$< 10^{-6}$	0.235117	$< 10^{-6}$		
$\sum d$	0	0.3179	0		

3.2 Equilibrium effects of the electron phonon coupling in free benzene

Before we explore the nonequilibrium properties of a benzene ring attached to leads, it is useful to look at the equilibrium effects of the electron phonon coupling in order to interpret the nonequilibrium results. In this section we treat the isolated ring in equilibrium and therefore use the modes of free benzene, see tab.(3.2). In this context free means not connected to leads. For the sake of simplicity we consider spinnless fermions.

3.2.1 Model and solution

The hamiltonian of the SSH-model for the six site ring reads

$$\begin{aligned}\hat{H} = &\sum_{<ij>} t_{ij} c_i^\dagger c_j + \sum_i \varepsilon_i \hat{n}_i + \sum_i \frac{1}{2m_i}\hat{p}_i^2 + \sum_{<ij>} \frac{K_{ij}}{2}(|\hat{x}_i - \hat{x}_j| - r_{ij}^0)^2 \\ &+ \sum_{<ij>} \tilde{g}_{ij}(|\hat{x}_i - \hat{x}_j| - r_{ij}^0) c_i^\dagger c_j \end{aligned} \tag{3.1}$$

where for free benzene the nearest neighbor hoppings and onsite energies are given by $t_{ij} = -t = -2.5[eV]$ and $\varepsilon_i = \varepsilon = -1.5[eV]$ [3], M_i and K_{ij} are taken from table(3.1) and the electron phonon coupling constants $\tilde{g}_{ij} = \tilde{g} = 2.8[eV\mathring{A}^{-1}]$ [17]. After second quantisation of the vibronic degrees of freedom, see sec.(1.2) and sec.(1.3), and tracing out a single mode, we obtain

$$\begin{aligned}\hat{H} = &- t \sum_{<ij>} c_i^\dagger c_j + \varepsilon \sum_i \hat{n}_i + \hbar\omega_\mu (b_\mu^\dagger b_\mu + \frac{1}{2}) \\ &+ \sum_{<ij>} \underbrace{\tilde{g}\sqrt{\frac{\hbar}{2m\omega_\mu}} d_{ij}^\mu}_{:=g_{ij}} c_i^\dagger c_j (b_\mu^\dagger + b_\mu) \end{aligned} \tag{3.2}$$

with the d_{ij}^μ defined in eq.(1.83) and their values for a particular mode are shown in table(3.2). To transform the representaion of the problem to a more natural basis we apply the Lang-Firsov transformation, as discussed in sec.(1.4), leading to

$$\begin{aligned}\hat{\tilde{H}} = &- t \sum_{<ij>} d_i^\dagger d_j e^{\frac{1}{\omega_\mu}(\lambda_i - \lambda_j)(b^\dagger - b)} + \varepsilon \sum_i \hat{n}_i \\ &+ \omega_\mu (b^\dagger b + \frac{1}{2}) - \frac{1}{\omega_\mu}\left(\sum_i \lambda_i \hat{n}_i\right)^2 \end{aligned} \tag{3.3}$$

where λ_i are the eigenvalues of the matrix $G_{ij} := g_{ij}$.
As mentioned above we examine the electronic properties of free benzene with e-ph interactions by looking at the electronic DOS. To make the model numerically solvable we introduce a phonon cutoff which is increased until convergence in the desired quantity (here the DOS with a cutoff $n_{max} \approx 10$) is reached. To

obtain the DOS we first solve the many body hamiltonian eq.(3.3) for its eigensystem by an exact diagonalization technique [1] and calculate the single particle greensfunction by using the Lehman representaion, eq.(2.11). The DOS is then given by the well known formula

$$\rho(E) = -\frac{1}{\pi} tr(\Im(g_{ij}^{ret})) \tag{3.4}$$

A special case is the highly symmetric breathing mode which allows an analytical solution of the greensfunction due to a common set of eigenvectors of the hopping matrix $T_{ij} := t_{ij}$ and the coupling matrix G as demonstrated in [17]. Note that the Lang-Firsov transformation is optional in the sense that the same results are obtained without it but it requires a phonon cutoff approximately twice as big.

Beyond SSH model

As mentioned in sec.(1.2.3) the linear SSH model breaks down at some critical e-ph coupling. To treat strong e-ph coupling one has in general to model e-ph coupling by what we called the Beyond SSH model, with the Hamiltonian

$$H = -\sum_{i \neq j} t_{ij}^0 e^{-\sum_\mu \alpha_{ij}^\mu (b_\mu^\dagger + b_\mu)} c_i^\dagger c_j + \sum_i \epsilon_i^0 n_i + \hbar\omega_\mu (b_\mu^\dagger b_\mu + \frac{1}{2})$$

where $\alpha_{ij}^\mu = \sqrt{\frac{\hbar}{2m\omega_\mu}} \frac{g_{ij}^\mu}{t_{ij}^0}$, see eq.(1.58). Which is the natural extension of the linear e-ph coupling. When treating this many body Hamiltonian by numerical means one chooses a phonon cutoff N_p. Since we can not apply the Lang-Firsov transformation N_p may be large. The phonon matrix element appearing in the calculation is, see eq.(1.162), of the form

$$\langle n|e^{\gamma(a^\dagger + a)}|m\rangle = e^{\frac{\gamma^2}{2}} \sqrt{n!m!}\gamma^{n+m} \sum_{l=0}^{min(n,m)} \frac{\gamma^{-2l}}{l!(n-l)!(m-l)!} \tag{3.5}$$

For a phonon cutoff $N_p = 40$, which is the typical value for our parameters, there are 1600 (or about half if you use its symmetry) of them. This leads to a considerable amount of non zero matrix elements in the many body Hamiltonian leading to an significant increase of the numerical effort. However, the matrix $\langle n|e^{\gamma(a^\dagger + a)}|m\rangle$ is sparse by itself (it has only significant entries in the first few diagonals). Therefore, one can reduce the numerical effort drastically by introducing a limit, $eps = 10^{-12}$ in our calculations, and only respect matrix elements that are big enough.

3.2.2 Results and discussion

We show results for the breathing mode, the Pi-mode and the second highest energy mode (which is 2 fold degenerate) of free benzene in fig.(3.6)-(3.4). The other degenerate mode (the second lowest in energy) leads to the same DOS as the Pi-mode and is therefore not shown. For all plots of the DOS we set the

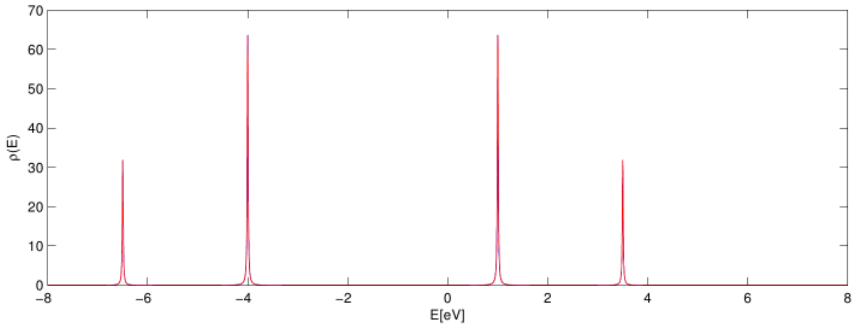

Figure 3.4: The DOS for the Pi-mode of free benzene in red and the non interacting case in blue. The curves are exactly on top of each other.

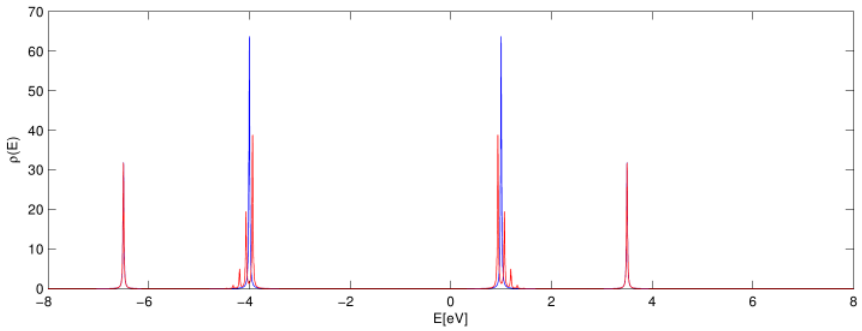

Figure 3.5: The DOS for the second highest energy mode of free benzene in red and the non interacting case in blue.

small imaginary quantity $0^+ = 0.01$ which yields broadened peaks instead of delta functions. The non interacting benzene has an electronic energy spectrum of $\varepsilon_k = (-6.5, -4, -4, 1, 1, 3.5)[eV]$. For a chemical potential of $\mu = 0$, the groundstate is at half filling and adding an electron leads to excitations at $E = (3.5, 1, 1)[eV]$ and removing one to hole like ones at $e = (-4, -4, -6.5)[eV]$ which correspond to the peaks of the non interacting DOS in fig.(3.4)-(3.6). The fact that the states responsible for the peaks at $E = (-4, 1)$ are degenerate is responsible for those peaks being twice as high as the ones originating from nondegenerate states. The system with and without interaction is electron hole symmetric but everything is shifted by the onsite energy of $\varepsilon = -1.5$.
Looking at the Pi-mode, fig.(3.4), we see that the phonons have no effect on the DOS. For the mode in fig.(3.5) one recognises that the degenerate peaks at $E = (-4, 1)[eV]$ split into multiple peaks (being smaller since the total spectral weight needs to be conserved) but the position in energy is unchanged, while the non degenerate states remain completely uneffected. A new effect appears when looking at the breathing mode, fig.(3.6), where all peaks split up and additionally the group of peaks replacing the non interacting ones are centered around different energies than the original ones. Therefore, we observe two effects namely splitting of peaks and shifting of peaks.

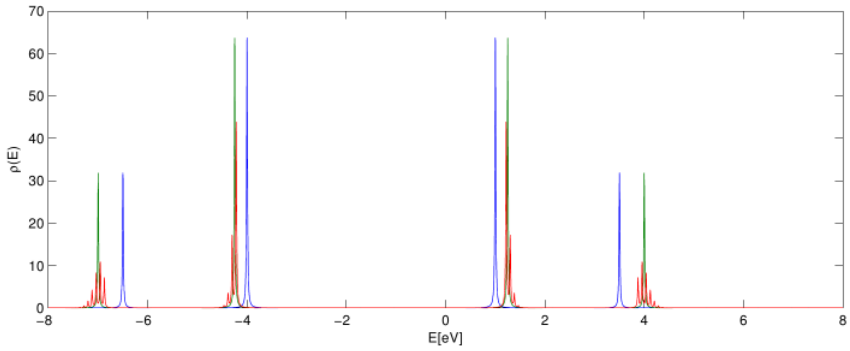

Figure 3.6: The DOS for the Breathing mode of free benzene in red, the non interacting case in blue and with frozen phonon approximation in green.

3.2.3 Shifting of peaks

First, we discuss the origin of peaks shifting position which for free benzene happens only for the breathing mode. When we go back to table(3.2), containing the stretching amplitudes d_{ij}, we realise that the breathing mode is the only mode where these amplitudes do not add up to zero. To see the connection between the two facts (peak shifting and non zero sum of stretching amplitudes) we look back to what d_{ij} is. It's defining equation is, see eq.(1.83)

$$\hat{\Delta}_{ij} = d_{ij}^{\mu}\hat{\eta}_{\mu} \tag{3.6}$$

where $\hat{\Delta}_{ij} = (|\hat{x}_i - \hat{x}_j| - r_{ij}^0)$ is the difference in bondlenght from equilibrium and $\hat{\eta}_{\mu} = \sqrt{\frac{\hbar}{2\omega_{\mu}}}(b_{\mu}^{\dagger} + b_{\mu})$, see eq.(1.34), is the position operator of the harmonic oszillator describing the mode μ. For the breathing mode $d_{ij} = d$ is bond independent and we can drop the subscripts ij. So d relates the amplitude of the quantum mechanical oszillator to the change in bondlenght. As mentioned previously the fact that they do not add up to zero means there is a net change in bondlenght when the mode is excited. Let us take a look at the expectation value of the change in bond lenght

$$\langle\hat{\Delta}\rangle = d\langle\hat{\eta}_{\mu}\rangle = \sqrt{\frac{\hbar}{2\omega_{\mu}}}d\langle b_{\mu}^{\dagger} + b_{\mu}\rangle \tag{3.7}$$

For an ordinary (uncoupled) oszillator this expectation value is zero, but in our case the oszillator is coupled to the electrons and thus the expectation value has to be taken with respect to the groundstate of the compound system where the groundstate has the generic form

$$|\psi_0\rangle = \sum_{e,n}\alpha_{en}|e\rangle_{el}|n\rangle_{ph} \tag{3.8}$$

The role of the electrons becomes more obviouse after the Lang-Firsov transformation where with eq.(1.119) and $\hat{T}_e = \sum_i \lambda_i \hat{n}_i$ eq.(3.7) becomes

$$\langle\hat{\Delta}\rangle = \sqrt{\frac{\hbar}{2\omega_{\mu}}}d\langle b_{\mu}^{\dagger} + b_{\mu} - \frac{2}{\hbar\omega_{\mu}}\hat{T}_e\rangle = \frac{x_{\mu}d}{\sqrt{2}}\langle b_{\mu}^{\dagger} + b_{\mu} - \frac{2}{\hbar\omega_{\mu}}\hat{T}_e\rangle \tag{3.9}$$

Calculating this expectation value in the interacting groundstate one gets $\langle\hat{\Delta}\rangle = -0.088889[\mathring{A}]$. This is to be compared to the equilibrium bondlenght of $r_0 = 1.39[\mathring{A}]$ which proves that the linear SSH model is applicable in this case as the deviations from equilibrium remain small. The non zero value of $\langle\hat{\Delta}\rangle$ means that the molecule has changed its geometry, which for the highly symmetric breathing mode leads to a contraction of every bond by the same amount. Due to the e-ph coupling this change in the geometry translates into a mean change of the hopping amplitude $\langle\Delta t\rangle = \tilde{g}\langle\hat{\Delta}\rangle = -0.2489[eV]$, which is again small compared to the $t = 2.5[eV]$ of non-interacting benzene. In this section non-interacting benzene means benzen without e-ph interaction. Replacing $\hat{\Delta}$ by its mean value one can make an approximate (non-interacting) model, which we want to call frozen phonon approximation, with renormalized hopping obtained by replacing the e-ph coupling by

$$H_{e-ph} \approx \sum_{<ij>} \tilde{g}_{ij}\langle\hat{\Delta}_{ij}\rangle c_i^\dagger c_j \tag{3.10}$$

The green DOS in fig.(3.6) shows the result obtained by applying the frozen phonon approximation to the breathing mode. By comparing with the interacting DOS (red curve) one can see that the position of the peaks matches well to the interacting case. From that we draw the conclusion that the shifting of the peaks in the DOS is due to the geometry change of the molecule induced by the e-ph interaction. Note that the frozen phonon approximation does not make the overall calculation more economic since one has to obtain the mean difference in bondlenght $\langle\hat{\Delta}\rangle$ from the interacting calculation beforehand. However, as will be shown in sec.(3.2.5) one can deduce the interacting value for $\langle\hat{\Delta}\rangle$ from a non-interacting calculation in the regime where where the linear SSH model is still applicable

3.2.4 Splitting of peaks

Contrary to the shifting of the peaks which can be understood as the consequence of the geometry change the effect of peak splitting is a real many-body effect, meaning that it does not occur in any non-interacting calculation. It corresponce to the fact that an electron can excite a phonon by loosing the required amount of energy $E_{ph} = \hbar\omega_\mu$ and therefore every non-interacting peak can (in principle) split into multiple peaks with their spacing given by exactly the phhonon energy. By examining the DOS in fig.(3.6)-(3.4) we see that it depends on the mode and peak in question wether it splits or not. The Pi-mode for example, fig(3.4), shows no peak splitting at all for an e-ph coupling of $\tilde{g} = 2.8[eV\mathring{A}^{-1}]$. If one goes to higher electron phonon coupling also the peaks of the Pi-mode split as demonstrated in fig.(3.7). Due to the high e-ph coupling, $\tilde{g} = 6[eV\mathring{A}^{-1}]$, used in fig.(3.7) it is computed from the beyond SSH model, see sec.(1.2.3). The DOS of the Pi-mode for high e-ph coupling looks like as if the peaks are shifted as well as splitted. This shift, however, is not due to a geometry change, which is still neglectible ($\langle\hat{\Delta}\rangle < 10^{-10}[\mathring{A}]$), but has a different origin. Although there is no prove for the following, we suspect the peaks appear to be shifted as a consequence of the poisson distribution of

the phonon matrixelement shown in fig.(2.1). Fig.(2.1) demonstrates that the phonon matrixelement which determines the weight of the poles of the greensfunction, and therefore the height of the peaks in the DOS, gets broader and shifts to larger n as the coupling is increased. This shift to larger n translates to a shift $\Delta E = n\hbar\omega_\mu$ of the peaks with weight to higher energies. The corresponding $\gamma = \frac{\lambda_i - \lambda_j}{\omega_\mu} \approx 1.7 - 3.4$, with λ from eq.(3.3), lead to $n \approx 5 - 10$ which translates to an energy shift $\Delta E \approx 0.7 - 1.4[eV]$ in good agreement with fig.(3.7). The latter suspicion can not be proven since the Lang-Firsov transformation can not by applied to the non-linear beyond SSH model. Although this argument was basically the same as in the explanation of the Franck-Condon effect, see sec.(2.2.3), the situation here is different since the shift of the harmonic oscillator remains zero even for an additional electron. Therefore, this behavior can not be ascribed to the Franck-Condon effect which argues with shifted oscillators. Because the peaks grow continuously with increasing coupling constant (not shown) we conclude that for small coupling all the weight is concentrated at the zeroth peak rendering the side peaks suppressed and not visible. This suppression is traceable by examining the system with first order perturbation theory in the e-ph coupling as is outlined in the following.

Argumentation of phonon peak suppression

The complete calculation is a little subtle and so instead of presenting the treatment with pertubation theory in detail we will illustrate the effect by following a qualitative argumentation. As a starting point we transform the hamiltonian, eq.(3.2), to k-space where the electronic part is diagonal. This amounts to transforming from c_i to d_k orbitals by $c_i = \frac{1}{\sqrt{6}} \sum_k e^{-ikx_i} d_k$ where $k \in \frac{n\pi}{3}$ for $n = 0, 1...5$. The hamiltonian then reads

$$\begin{aligned} \hat{H} =& \hat{H}_0 + \hat{H}_1 = \sum_k \underbrace{(\varepsilon - 2tcos(k))}_{\varepsilon_k} d_k^\dagger d_k + \hbar\omega_\mu (b_\mu^\dagger b_\mu + \frac{1}{2}) \\ &+ \tilde{g}(b_\mu^\dagger + b_\mu) \sum_{kk'} (\underbrace{U\tilde{D}U^\dagger}_{:=D})_{kk'} d_k^\dagger d_{k'} \end{aligned} \tag{3.11}$$

where $\tilde{D}$ is defined by

$$\tilde{D}_{ij} := \sqrt{\frac{\hbar}{2m\omega_\mu}} d_{ij} \text{ and } U_{ki} := \frac{1}{\sqrt{6}} e^{-ikx_i} d_k \tag{3.12}$$

The groundstate of the unperturbed hamiltonian is given by

$$|\psi_0\rangle^{(o)} = \prod_{k \leq k_f} d_k^\dagger |0\rangle_e \otimes |0\rangle_{ph} := |111000\rangle_e |0\rangle_{ph} \tag{3.13}$$

It is altered due to the e-ph coupling up to first order according to

$$|\psi_0\rangle = |\psi_0\rangle^{(o)} + \sum_{i,n=\{1\}} \frac{e\langle\, i|\, {}_{ph}\langle\, n|\hat{H}_1|0\rangle_{ph}|111000\rangle_e}{E_0^{(o)} - \hbar\omega_\mu - E_i^{(o)}} |i\rangle_e |n\rangle_{ph} \tag{3.14}$$

where i labels the different electronic states while n represents the nth excited harmonic oscillator state. The phononic part of the above matrixelement is proportional to $\delta_{n,1}$ since the perturbation is proportinal to $(b_\mu^\dagger + b_\mu)$ and can thus only mediate between states with $\Delta n = \pm 1$. Note that as a consequence of the same fact all first order energy corrections $E_n^{(o)} = \langle \psi_n^{(o)} | \hat{H}_1 | \psi_n^{(o)} \rangle$ are zero. From eq.(3.14) it is clear that the main contribution to the perturbation expansion comes from states where $E_0^{(o)} - E_i^{(o)} = 0$ because for all other possibilities the denominator would contain an electronic energy difference ΔE_e which are at least one order of magnitude larger than the phonon energy $\hbar\omega_\mu$ leading to surpressed states. The DOS is derived from the Greensfunction, eq.(2.11), using eq.(3.4) and the well known mathematical idintity

$$\lim_{\eta \to 0^+} \frac{1}{x \pm i\eta} = PV\frac{1}{x} \mp i\pi\delta(x) \tag{3.15}$$

as

$$\rho(E) = \sum_{k,n} |\langle \psi_0 | d_k | \psi_n \rangle|^2 \delta(E - (E_0 - E_n)) + |\langle \psi_0 | d_k^\dagger | \psi_n \rangle|^2 \delta(E + (E_0 - E_n)) \tag{3.16}$$

The above mentioned effect of suppression gets squared in the DOS which is why we consider only states whith $E_0^{(o)} - E_i^{(o)} = 0$ in the perturbation expansions. For the unperturbed system there are three excitations, corresponding to the three possibilities of adding an electron to the groundstate, at energies $\Delta E_n^{(o)} := E_0^{(o)} - E_n^{(o)}$. Due to the perturbation we expect, as explained above, that peaks arise at energies $E = \Delta E^{(o)} + n\hbar\omega_\mu$. For concreteness we want to consider the matrixelement $\langle \psi_0 | d_6 | \psi_n \rangle$ which for the unperturbed case is responsible for the peak at $E = 3.5[eV]$ with $|\psi_n^{(o)}\rangle = |111001\rangle_e |0\rangle_{ph}$. The excited state $|\psi_n^{(o)}\rangle$ that leads to the desired energy difference $\Delta E^{(o)} = 3.5 + \hbar\omega_\mu$ is $|\psi^{(o)}\rangle = |111001\rangle_e |1\rangle_{ph}$. The state $|\psi^{(o)}\rangle = |111001\rangle_e |0\rangle_{ph}$ is not a valid candidate since there is no energy correction up to first order. In analogy to eq.(3.14) we write up to first order

$$|\psi\rangle = |111001\rangle_e |1\rangle_{ph} + \sum_{i,n=\{0,2\}} \frac{{}_e\langle i|\, {}_{ph}\langle n | \hat{H}_1 | 1 \rangle_{ph} | 111001 \rangle_e}{E_\psi^{(o)} - \hbar\omega_\mu - E_i^{(o)}} |i\rangle_e |n\rangle_{ph} \tag{3.17}$$

From eq.(3.14) and eq.(3.17) wee see that the matrixelement $\langle \psi_0 | d_6 | \psi_n \rangle$ has contributions from:

- The zeroth order of the excited state $|\psi\rangle$ with the first order correction of the groundstate when i in eq.(3.14) corresonds to the state $|111000\rangle$. The resulting overlap is

$$Q_1 = \langle 111000 | \langle 1 | \hat{H}_1 | 0 \rangle | 111000 \rangle \tag{3.18}$$

- The zeroth order of the groundstate with the first order correction of the excited state when $n = 0$ and $|i\rangle = |111001\rangle$ in eq.(3.17). The resulting overlap is

$$Q_2 = \langle 111001 | \langle 0 | \hat{H}_1 | 1 \rangle | 111001 \rangle \tag{3.19}$$

Table 3.4: The diagonal elements of the matrix D defined in eq.(3.11) without the prefactor $\sqrt{\frac{\hbar}{2m\omega_\mu}}$.

	D_{11}	D_{22}	D_{33}	D_{44}	D_{55}	D_{66}
Breathing mode	-0.8165	-0.4082	-0.4082	0.4082	0.4082	0.8165
First degenerate mode	0	0	0	0	0	0
Second degenerate mode	0	-0.7906	0.7906	0.4716	-0.4716	0
Pi-mode	0	0	0	0	0	0

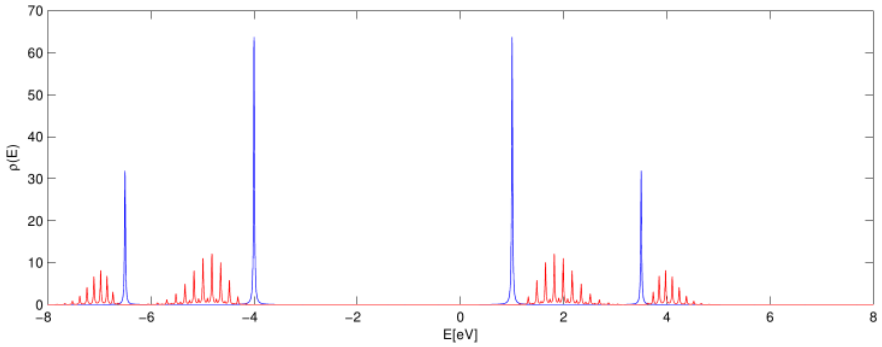

Figure 3.7: The DOS for the Pi-mode with an e-ph coupling of $\tilde{g} = 6[eV\mathring{A}^{-1}]$ in red and the non-interacting case as reference in blue. Due to the high e-ph coupling this result is obtained by application of the beyond SSH model

The matrixelements, Q_1 and Q_2, are diagonal in the electronic states (meaning the electronic bra and ket vector correspond to the same state). Thus, for one of the matrixelements to be non zero the matrix D, which is different for every mode, has to contain non zero diagonal elements. For the matrixelements in eq.(3.18) and eq.(3.19) the contributing entries of the matrix D would be the elements D_{11}, D_{22}, D_{33} and D_{66}. If we would have used $d_{4/5}$ instead of d_6 in the derivation above the important elements of D would still be the first three diagonal elements plus the 4th or 5th depending on what annihilation operator we chose. Table.(3.4) shows the diagonal elements for the four (two are degenerate leading to the same physics) different modes. For the breathing mode, where all peaks are split, the matrix D is diagonal with all diagonal elements being non zero leading to a splitting of every peak. In the case of the Pi-mode and the first degenerate mode the diagonal elements of the corresponding D-matrix are all zero resulting in no peak splitting at all. The behaviour of the second degenerate mode lies in between the two extreme above as only the degenerate peaks split. This is clear by recognising that the first three entries of the D-diagonal add up to zero and the 6th entry is identically zero leading to no splitting of the non-degenerate peak while the sum of the first three plus the 4th or the 5th diagonal entry is non zero giving rise to the peak splitting of the degenerate peak.

3.2.5 The optimized geometry approximation

In sec.(3.2.4) we learned that the effect of peak shifting in the DOS can be interpreted by a geometry change of the molecule. Owing to that, we were able to predict the correct (interacting) positions of the peaks by means of a non-interacting calculation which only required the mean change in bondlenghts $\langle\hat{\Delta}_{ij}\rangle$, obtained from an interacting one, as inputs. When the molecule adopts a different geometry the electronic hoppings get modified which can lead to a lower electronic energy. On the other hand any change in geometry comes at the price of potential energy between the ions. This tradeoff has an energy minimum leading to an optimal geometry. We start with the mean field approximation (Born-Oppenheimer approximation) to the hamiltonian eq.(3.1)

$$\begin{aligned}
&= \sum_{<ij>} (t_{ij} + \tilde{g}_{ij}\Delta_{ij}) c_i^\dagger c_j + \sum_i \varepsilon_i \hat{n}_i + \sum_{<ij>} \frac{K_{ij}}{2}\Delta_{ij}^2 \\
&= \sum_{<ij>} (t_{ij} + \tilde{g}_{ij} \sum_\mu d_{ij}^\mu \eta_\mu) c_i^\dagger c_j + \sum_i \varepsilon_i \hat{n}_i + \sum_{<ij>} \frac{K_{ij}}{2} \left(\sum_\mu d_{ij}^\mu \eta_\mu \right)^2
\end{aligned} \tag{3.20}$$

First, we will consider the effect of a single mode and simplify to

$$\begin{aligned}
\hat{H} =& \hat{H}(\eta_\mu) = \sum_{<ij>} (t_{ij} + \tilde{g}_{ij} d_{ij}^\mu \eta_\mu) c_i^\dagger c_j + \sum_i \varepsilon_i \hat{n}_i + \sum_{<ij>} \frac{K_{ij}}{2} \left(d_{ij}^\mu \eta_\mu \right)^2 \\
=& \sum_{ij} h_{ij}(\eta_\mu) c_i^\dagger c_j + \sum_{ij} v_{ij}(\eta_\mu) = \hat{H}_{el}(\eta_\mu) + V_{Ion}(\eta_\mu)
\end{aligned} \tag{3.21}$$

with $h_{ij}(\eta_\mu) := \delta_{<ij>}(t_{ij} + \tilde{g}_{ij} d_{ij}^\mu \eta_\mu) + \delta_{ij}\varepsilon_i$ and $v_{ij}(\eta_\mu) := \delta_{<ij>} \frac{K_{ij}}{2} \left(d_{ij}^\mu \eta_\mu \right)^2$. This leaves us with a hamilton operator of non-interacting electrons $\hat{H}_{el}(\eta_\mu)$ describing them for a given ion geometry and a classical potential $V_{Ion}(\eta_\mu)$. The optimal value of η_μ is then determined by the variational principle of minimal energy

$$\begin{aligned}
E(\eta_\mu) =& \langle \hat{H}(\eta_\mu) \rangle_0 = \langle \psi_0 | \hat{H}_{el}(\eta_\mu) + V_{Ion}(\eta_\mu) | \psi_0 \rangle \\
=& \min_{\eta_\mu} \left(E_0(\eta_\mu) + V_{Ion}(\eta_\mu) \right)
\end{aligned} \tag{3.22}$$

with the electronic groundstate energy

$$E_0(\eta_\mu) = \min \left(\sum_i \lambda_i(\eta_\mu) \right) \tag{3.23}$$

where $\lambda_i(\eta_\mu)$ are the eigenvalues of the matrix built from $h_{ij}(\eta_\mu)$ and $\min(\sum_i \lambda_i(\eta_\mu))$ indicates the minimal value possible by summing up any combination of the $\lambda_i(\eta_\mu)$. Fig.(3.8) shows the function $E(\eta_\mu)$ for the different modes. The shift of the harmonic potential in the case of the breathing mode is exactly the shift treated in the Lang-Firsov transformation and the different curvatures are of course due to the different energies of the modes (higher energy $\Rightarrow$ steeper potential). In principle the minimization procedure can be done analytically

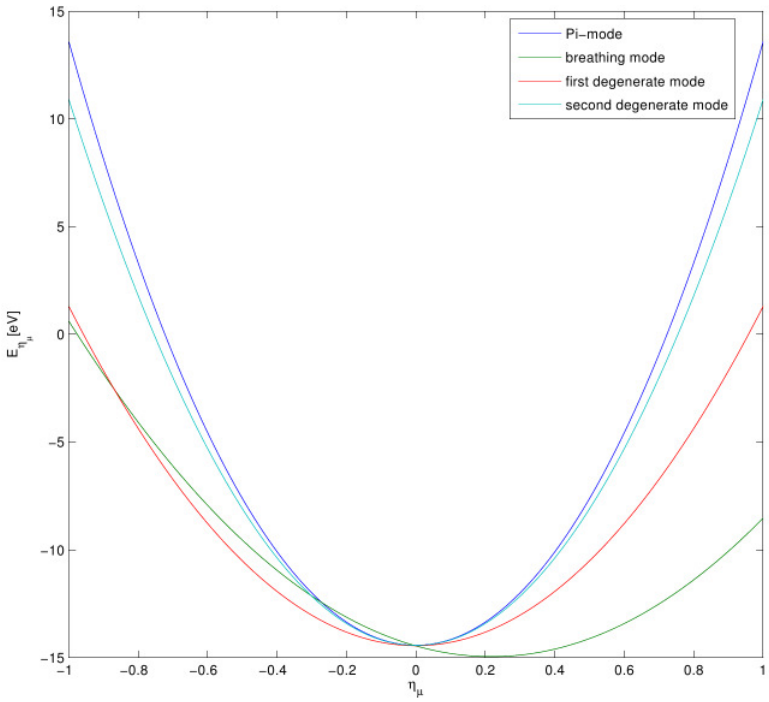

Figure 3.8: The energy function $E(\eta_\mu)$ for the different modes of free benzene. The same parameters as for fig.(3.4)-(3.7)

by using calculus but it requires the differentiation of eigenvalues $\lambda_i(\eta_\mu)$ with respect to a parameter η_μ in the corresponding matrix $h_{ij}(\eta_\mu)$ which can be troublesome especially in the case of degeneracy. Conveniently the evaluation of eq.(3.22) for a given η_μ is computationally quick (the biggest part is diagonalizing a six by six matrix) allowing a numerical solution of the minimization problem eq.(3.22). The geometry obtained from this approximation shows very good agreement, $\Delta_{int} - \Delta_{opt} < 10^{-5}[\mathring{A}]$, with the one calculated from the interacting hamiltonian throughout the parameter regime where the linear SSH model is applicable (see sec.(1.2.2)). To gain further insight in what property of the modes, translating to a property of the d^μ_{ij}, determines whether a geometry change can lead to a lower energy we continue analytically. Eq.(3.21) together with the Hellman-Feynman theorem, yields

$$\begin{aligned}\frac{\mathrm{d}E(\eta_\mu)}{\mathrm{d}\eta_\mu} =& \langle\psi_0(\eta_\mu)|\frac{\partial\hat{H}(\eta_\mu)}{\partial(\eta_\mu)}|\psi_0(\eta_\mu)\rangle \\ =& \langle\psi_0(\eta_\mu)|\sum_{ij}\tilde{g}_{ij}d^\mu_{ij}c^\dagger_i c_j + \sum_{<ij>}k_{ij}(d^\mu_{ij})^2\eta_\mu|\psi_0(\eta_\mu)\rangle \\ =& \langle\psi_0(\eta_\mu)|\mathbf{c}^\dagger G\mathbf{c}|\psi_0(\eta_\mu)\rangle + \sum_{<ij>}k_{ij}(d^\mu_{ij})^2\eta_\mu \end{aligned} \tag{3.24}$$

To evaluate the expectation value we transform from $\mathbf{c}$ to $\mathbf{d}$ operators by the definition $\mathbf{c} = U(\eta_\mu)\mathbf{d}$ where the transformation matrix $U(\eta_\mu)$ diagonalizes h_{ij} in eq.(3.21). With the corresponding groundstate (fermi sea) $|\psi_0\rangle = \prod_{k\leq k_f} d^\dagger_k|0\rangle$

we obtain

$$\begin{aligned}\langle\psi_0(\eta_\mu)|\mathbf{c}^\dagger G\mathbf{c}|\psi_0(\eta_\mu)\rangle =&\langle\psi_0(\eta_\mu)|\mathbf{d}^\dagger U^\dagger(\eta_\mu)GU(\eta_\mu)\mathbf{d}|\psi_0(\eta_\mu)\rangle\\ =&\langle 0|\left(\prod_{k\leq k_f} d_k\right)\sum_{k'k''}(U^\dagger_{\eta_\mu}GU_{\eta_\mu}))_{k'k''}d^\dagger_{k'}d_{k''}\left(\prod_{k\leq k_f} d^\dagger_k\right)|0\rangle\\ =&\sum_{k=1}^{k_f}(U^\dagger_{\eta_\mu}GU_{\eta_\mu}))_{kk}=\sum_{k=1}^{k_f}\mathbf{u}_k^\top G\mathbf{u}_k \end{aligned} \tag{3.25}$$

where $\mathbf{u}_k$ are the eigenvectors of h_{ij}. Plugging this result back into eq.(3.24)and demanding that the derivative vanishes furnishes the equation

$$\frac{\mathrm{d}E(\eta_\mu)}{\mathrm{d}\eta_\mu}=\sum_{k=1}^{k_f}\mathbf{u}_k^\top(\eta_\mu)G\mathbf{u}_k(\eta_\mu)+\eta_\mu\sum_{<ij>}k_{ij}(d^\mu_{ij})^2\stackrel{!}{=}0 \tag{3.26}$$

For modes with no net difference in bondlenght the follwowing rule applies. What is gained in energy by enhanced hopping is lost again on an equivalent bond which has its hopping surpressed. Due to this symmetry the system cannot lower (or increase for that matter) its electronic energy by a geometry change according to such a mode. In these cases the first part in eq.(3.26) is zero by symmetry and since $\sum_{<ij>}k_{ij}(d^\mu_{ij})^2>0$ the only solution is $\eta_\mu=0$ meaning no geometry change. For $\eta_\mu=0$ the electronic part of the hamiltonian remains unaltered and the diagonal elements of $(U^\dagger_{\eta_\mu=0}GU_{\eta_\mu=0}))_{kk}$ coinside with the ones shown in tab.(3.4) which are either exactly zero or (the first three) add up to zero for modes with $\eta^{min}_\mu=0$. Note that $\sum_{k=1}^{k_f}(U^\dagger_{\eta_\mu=0}GU_{\eta_\mu=0}))_{kk}=0$ is only a neccesary condition for $\eta^{min}_\mu=0$ since the reverse argument, concluding $\eta_\mu=0$ from the fact that the matrixelements are zero is not generally true. An example that violates this argumentation is when $\tilde{g}_{ij}$ is non isotropic or more specefic when the e-ph coupling constants do not reflect the symmetry of the purely ionic problem.
The generalization to treat any number of modes is straight forward by keeping the sum $\sum_\mu$ from eq.(3.20) to eq.(3.21) leading to an energy function $E=E(\eta_1,\ldots,\eta_n)=E(\boldsymbol{\eta})$ with the objects h_{ij} and v_{ij} in eq.(3.22) changed into

$$\begin{aligned}h_{ij}(\boldsymbol{\eta}):=&\delta_{<ij>}(t_{ij}+\tilde{g}_{ij}\sum_\mu d^\mu_{ij}\eta_\mu)+\delta_{ij}\varepsilon_i\\ v_{ij}(\boldsymbol{\eta}):=&\delta_{<ij>}\frac{K_{ij}}{2}\left(\sum_\mu d^\mu_{ij}\eta_\mu\right)^2=\delta_{<ij>}\frac{K_{ij}}{2}\sum_{\mu\nu}d^\mu_{ij}d^\nu_{ij}\eta_\mu\eta_\nu\end{aligned} \tag{3.27}$$

Solving the minimization problem for the case of multiple modes shows the same agreement with interacting values as the limitation to one mode. In this approximation it is also visible why the contribution to the geometry change from a particular mode, is in very good approximation, independent of how much modes one includes in the calculation meaning that the optimal values η^{min}_μ are practically independent. From eq.(3.27) we see that after differentiation the mixing between the η_μ can only come from the ion potential as the

electronic part is linear in the differentiation variables. By differentiating v_{ij} from eq.(3.27) with respect to η_ν, yields

$$\frac{\partial}{\partial\eta_\nu}v_{ij} = \delta_{<ij>}\frac{K_{ij}}{2}\frac{\partial}{\partial\eta_\nu}\left(\sum_\mu d_{ij}^\mu\eta_\mu\right)^2 = \delta_{<ij>}K_{ij}\sum_\mu d_{ij}^\mu\eta_\mu d_{ij}^\nu \tag{3.28}$$

By summing over ij we get the contribution which contains the mixing of modes

$$\frac{\partial}{\partial\eta_\nu}\sum_{ij}v_{ij} = \sum_\mu\eta_\mu\sum_{<ij>}K_{ij}d_{ij}^\mu d_{ij}^\nu \tag{3.29}$$

For free benzene $K_{ij} = K$ and it simplifies to

$$\frac{\partial}{\partial\eta_\nu}\sum_{ij}v_{ij} = K\sum_\mu\eta_\mu\sum_{<ij>}d_{ij}^\mu d_{ij}^\nu = K\delta_{\mu\nu}\eta_\mu\sum_{<ij>}(d_{ij}^\mu)^2 \tag{3.30}$$

The property

$$\sum_{<ij>}K_{ij}d_{ij}^\mu d_{ij}^\nu \sim \delta_{\mu\nu} \tag{3.31}$$

is exact for the modes of free benzene. One might think that this orthogonality relation is a consequence of the modes being orthonormal, $\boldsymbol{\xi}_\mu^\top\boldsymbol{\xi}_\nu = 0$. To see that even for free benzene this argumentation is not true we collect the contributions from each bond $< ij >$, there are six for free benzene, in eq.(3.30) and form a vector $\mathbf{D}_\mu$ defined by

$$(\mathbf{D}_\mu)_{<ij>} := d_{ij}^\mu = \mathbf{e}_{ij}^\top S_{ij}\boldsymbol{\xi}_\mu \Leftrightarrow \mathbf{D}_\mu = ES\boldsymbol{\xi}_\mu \tag{3.32}$$

with

$$E := \begin{pmatrix} \mathbf{e}_{12}^\top & & & \\ & \mathbf{e}_{23}^\top & & 0 \\ & & \ddots & \\ & 0 & & \\ & & & \mathbf{e}_{61}^\top \end{pmatrix} \text{ and } S := (S_{12}, S_{23}, \ldots, S_{61})^\top \tag{3.33}$$

This allows us to rewrite eq.(3.31) in terms of a scalar product as

$$\sum_{<ij>}K_{ij}d_{ij}^\mu d_{ij}^\nu = K\mathbf{D}_\mu^\top\mathbf{D}_\nu = K\boldsymbol{\xi}_\mu^\top\underbrace{S^\top E^\top ES}_{\neq\sim\mathbb{1}}\boldsymbol{\xi}_\nu \tag{3.34}$$

Since the matrix $S^\top E^\top ES$ is not proportional to the identity the orthonormality of the modes is not a sufficient condition for eq.(3.31) to be true but it may well be a neccesary condition. The fact that it is exact for the modes of free benzene is due to the high symmetry of the problem. For the symmetric para configuration it holds to an approximation of $\sum_{<ij>}K_{ij}d_{ij}^\mu d_{ij}^\nu < 10^{-6}[eV\mathring{A}^{-2}]$ for $\mu \neq \nu$ and it fails for the ortho and meta configurations. Thus, for this symmetric cases the minimization conditions for the different η_μ are independent from each other. Of course when performing a calculation with multiple modes one can exclude modes with $\eta_\mu^{min} = 0$, which are the majority, beforehand.

Optimized geometry in the Beyond SSH model

It is straight forward to apply the optimized geometry calculation to the Beyond SSH model. The difference to the optimized geometry in the linear SSH model is in the case of multiple modes. There, the exponential leads to direct cross terms for the modes in the hamiltonian which are of higher orders in g. This means that the optimal values of η_μ are not independent anymore in a calculation with multiple modes and strong coupling. If only the e-ph coupling g is increased, and all the other parameters entering the Hamiltonian are kept constant, even the Beyond SSH model breaks down for some critical value of g (for example $g > 6[eV\mathring{A}]$ for the Pi-mode). The reason is not that the hopping becomes positive, as it was the case for the linear SSH model, because this is taken care of by the exponential. To find the answer one has to consider the optimized geometry argument from above. For a high enough coupling constant the electronic contribution to the Hamiltonian has a higher negative curvature, viewed as a function of η_{mu}, than the ionic potential meaning that increasing η_{mu} always decreases the energy. This would make the system unstable since the total energy would then be a negatively unbound function for $\eta_\mu \longrightarrow \infty$. Note that this is confirmed by the many body calculation as the groundstate energy diverges to minus infinity as N_p is increased. This of course just means that one would have to increase the ionic spring constant k when going to very strong coupling, which is only natural since a big spring constant usually corresponds to a strong e-ph coupling.

3.3 Non-equilibrium steady state current through a molecular ring structure with e-ph coupling

We present results for the steady state current, obtained by ssCPT, as a function of bias voltage of benzene with e-ph SSH-type interaction. Unless stated differently the parameters for benzene are the same as in sec.(3.2) and the leads are characterised by $t_{leads} = 12[eV], \varepsilon_{l,r} = 0[eV], v_{l,r} = 0.4[eV]$ and the e-ph coupling to the leads is $g_{leads} = 0.5[eV\mathring{A}^{-1}]$. For the evaluation of the current we use $0^+ = 10^{-12}$. The value of g_{leads} is chosen lower since we assume a weaker coupling to leads, for the electronic hopping v and e-ph coupling, compared to the values in benzene. We do so to stay, for intermediate e-ph coupling, in the parameter regime of the linear SSH model, see sec.(1.2.2). Also, the current is very sensible to $v_{r,l}$ since it enters squared in the lead induced hybridisation, $\Gamma = \frac{v^2}{t_{leads}}$, and defines the longest timescale in the system which can lead to highly suppressed or enhanced currents, depending on the mode, compared to the non-interacting case. For results with stronger e-ph coupling g_{leads} is chosen such that the ratio $\frac{g_{benz} := g}{g_{leads}} = const.$.
From the Meir-Wingreen formula [22] we know that the current through an interacting electron region is qualitatively given by integrating the DOS of the central region from $[\varepsilon_l - \frac{\Phi}{2}, \varepsilon_r + \frac{\Phi}{2}] = [-\frac{\Phi}{2}, +\frac{\Phi}{2}]$ which is often referred to as the fermi window. This suggests to expect steps in the current voltage characteristics when $\frac{\Phi}{2} = E_{peak}$ where E_{peak} is some energy for which there is a peak in the DOS. Thus, if there are peaks in the DOS split by the phonon energy $\hbar\omega_\mu$ we anticipate steps in the I/V curves spaced by $2\hbar\omega_\mu$. From sec.(3.2) we know that the effects of the linear SSH interaction on the DOS is shifting and splitting of the non-interacting excitations. If the electronic DOS remains unaffected by the e-ph coupling, which is true for the majority of the modes, we would expect the steady state current to be close to the non-interacting case. Unless stated differently all results shown in this section are obtained by using the Lang-Firsov transformation.

3.3.1 Investigations of convergence and consistency

We check the convergence of our method in the cluster sizes N_c and phonon-cutoff N_p.

Convergence of CPT with increased N_c

We demonstrate the convergence of the CPT approximation with increasing N_c for intermediate coupling $g = 2.8[eV\mathring{A}^{-1}]$. Fig(3.9) shows currents of three different modes for cluster sizes $N_c = 6, 8$. The minimal central cluster can be chosen with six sites because the considered modes do not alter the hopping to the leads $d_{benz,lead} = d_{47} = d_{81} = 0$. Note that the data in picture two and three of fig.(3.9) is not yet converged in the phonon cut off. However, the convergence in N_p does not influence the CPT convergence in N_c since different N_p define particular physical models.

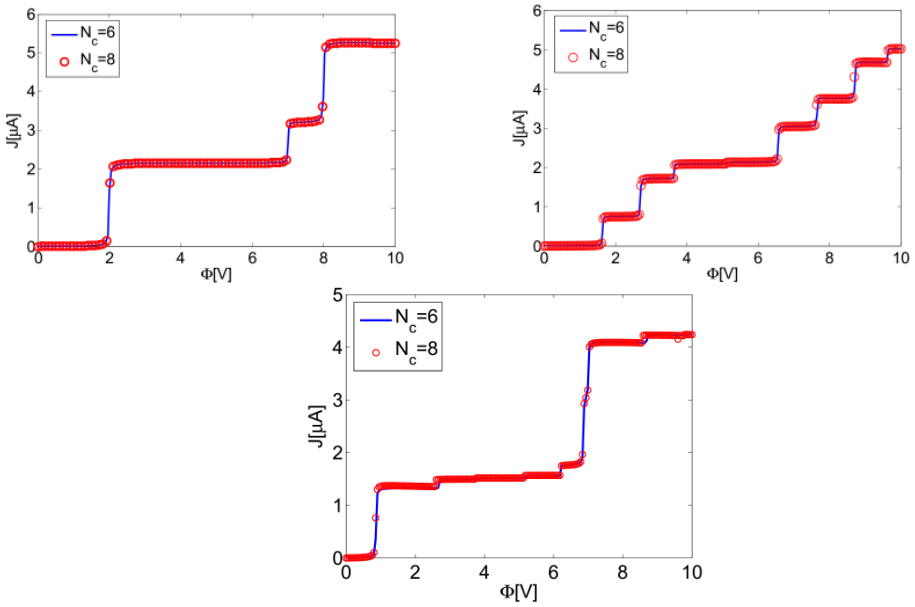

Figure 3.9: Convergence of CPT with increased N_c. From left to right and top to bottom the pictures correspond to mode 4, mode 6 and the Pi-mode (mode 8). For all three pictures a phonon cutoff $N_p = 5$ was used. Note that the currents for mode 6 and 8 here are not converged in the phonon cut off.

Convergence in the phonon cut off

An important parameter for all observables obtained from a numerical calculation involving phonons is the phonon cut off N_p, the highest excited phonon state one allows the ionic system to be in. In calculations for bulk materials the needed N_p is often times too high to treat numerically. For our model and parameters the needed cut off depends on the observable, mode and method of solution (with or without Lang-Firsov transformation) in question and is within the range of $N_p = 10 - 40$. For the linear SSH and Holstein model a very good estimate for the needed N_p can be obtained from the matrix element in fig.(2.1) as the n corresponding to the peak of the poisson distribution. Fig.(3.10) and fig.(3.11) demonstrate the convergence of the current with increasing N_p for mode 6 and 8, respectively. In both cases we see a rather confuse convergence pattern for a small cutt off's. Fig.(3.12) shows the same results when considering the breathing mode of free benzene. For the latter the convergence in N_p shows a simpler pattern which may be due to the fact that for the breathing mode of free benzene the hamiltonian is diagonal after the LF-transformation. We also see our suspicion confirmed that modes with no effect on the electronic DOS lie on top of the non-interacting curve, see fig.(3.11). For mode 6, where there is no geometry change but the degenerate peaks in the DOS are split, we see that it follows the non-interacting case but the steps which originate from the degenerate peaks in the DOS consist of smaller steps with twice the phonon energy.

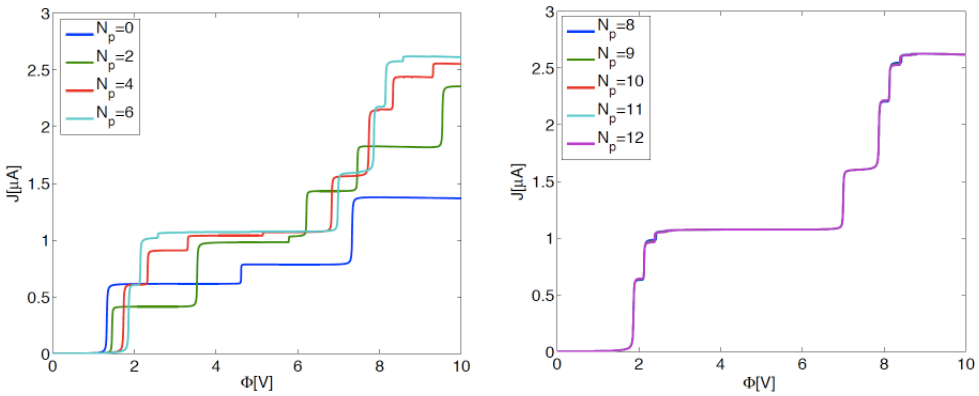

Figure 3.10: The current altered by mode 6 with $N_c = 6$ for different phonon cut offs N_p

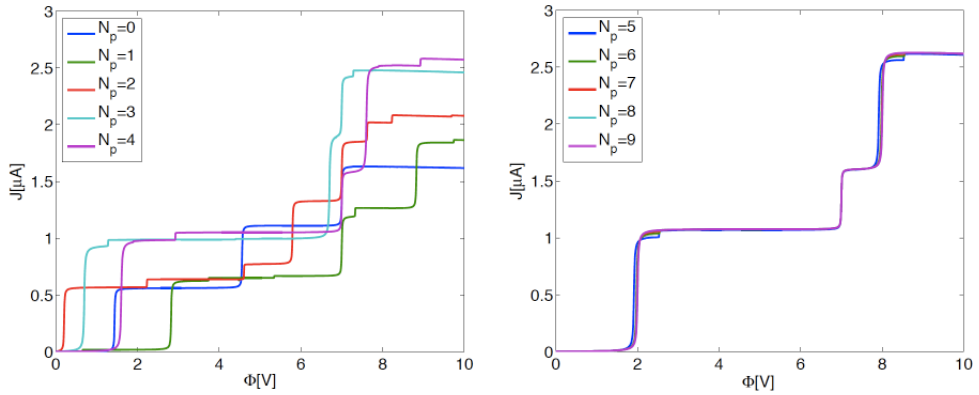

Figure 3.11: The current altered by the Pi-mode (mode 8) with $N_c = 6$ for different phonon cut offs N_p

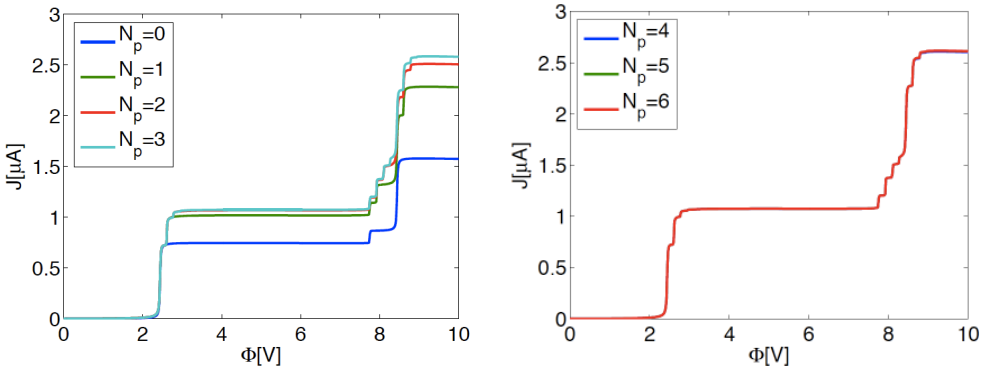

Figure 3.12: The current altered by the breathing mode of free benzene with $N_c = 6$ for different phonon cut offs N_p

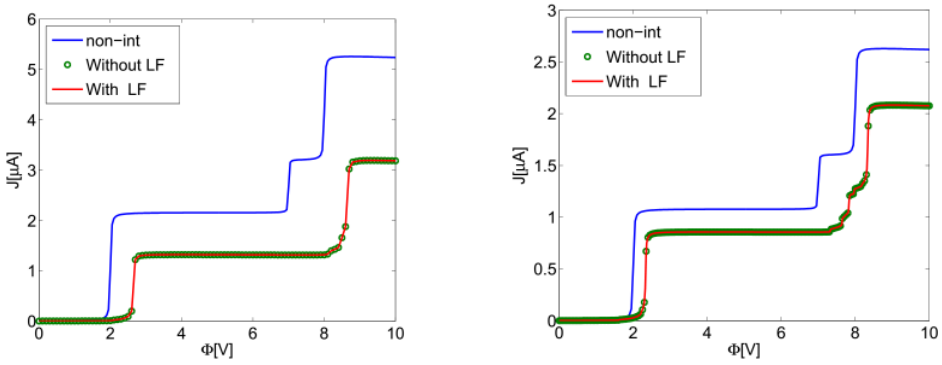

Figure 3.13: Comparison of the current for mode 3 obtained with and without the Lang-Firsov transformation. Left with spin and right spinless. Phonon cut offs: $N_p = 20$ with LF-transformation and $N_p = 40$ without it. $N_c = 8$

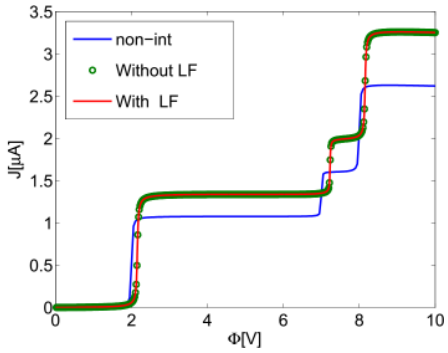

Figure 3.14: The same as fig.(3.13) but only the spinless case and mode 1. Phonon cut off's: $N_p = 25$ with LF-transformation and $N_p = 40$ without it. $N_c = 8$

Lang-Firsov vs. no Lang-Firsov transformation

As mentioned in sec.(3.2) applying the Lang-Firsov transformation is an optional step in the method of solution. This allows us to check our results for consistency by comparing results obtained with and without the Lang-Firsov transformation. Fig.(3.13) and fig.(3.14) show a direct comparison of the two equivalent methods. The approach without the LF-transformation requires, for our system, a phonon cutoff N_p about twice as high compared to the one with LF-transformation. This leads to increased numerical effort especially when respecting spin.

3.3.2 Frozen phonon approximation and optimized geometry

In sec.(3.2) we introduced what we call the frozen phonon approximation and were able to predict the correct position of the shifted peaks in the DOS for modes which give rise to a geometry change. Due to the fact that in the parameter regime of the linear SSH model the optimized geometry calculation

yields the same geometry change than a calculation with interaction, the frozen phonon approximation is equivalent to performing the whole calculation with optimized geometry which does not require the solution of a many body hamiltonian. The shifting of peaks in the DOS translates to a shifting of the steps in the I/V curves. Fig.(3.15) compares results with interaction to data obtained by the frozen phonon approximation with and without spin. As expected the position of the big steps, corresponding to the electronic excitations, are very well reproduced by the frozen phonon approximation while the smaller steps, originating from electrons exciting phonons which is only possible in a calculation with interaction, are not recovered by the frozen phonon approximation. Note that the curve with spin in fig.(3.15) does not show distinguished smaller steps because the voltage grid, $\Delta\Phi = 0.1[V]$ is too coarse to resolve steps with twice the phonon energy $2\hbar\omega_\mu = 1.72[eV]$ well. Besides the position of the big steps beeing reproduced very well the amplitude of them is also in excellent agreement. We see that the frozen phonon approximation does work better for the calculation without spin. This may be caused by the phonon induced (negative U-term see sec.(1.4.4)) e-e interactions between the two spin channels. In both cases, with and without spin, the current is suppressed in comparison with the non-interacting curve. Since this is recovered by the frozen phonon approximation we can ascribe it to an effect of the geometry change. In fact it is easily explained by how the coupling to the leads v is changed due to the new equilibrium geometry. For mode 3 (altered breathing mode) all the sites of the benzene move closer together leading to a larger distance to the leads and therefore a decreased coupling $v_{l,r}$. As mentioned above the current responds very sensible to this change which results in the current suppression observed in fig.(3.15). The same argument is responsible for the enhanced current in fig.(3.14). This effect is stronger for the model with spin since the geometry change is bigger. This can be understood by recalling the argument of the optimized geometry approximation, see sec.(3.2.5). In short, the equilibrium geometry was determined by the trade off between gaining energy by changing the electronic hopping and loosing energy due to the ionic potential. Due to spin the effect of lowering the electronic energy, through moving the atoms closer together, gets doubled while the contribution from the ion potential remains unaffected leading to an extremer geometry change at the overall energy minimum.

Taking two modes into account

We investigate wether the optimized geometry/frozen phonon approximation does work similarly well for multiple modes. From sec.(3.2.5) we know that, for the symmetric para configuration and free benzene, the geometry change of the modes is just the sum of the contribution from each mode under consideration. Because this was due to the fact that terms that mix the modes in the hamiltonian are very small we expect good agreement between the optimized geometry approximation and the calculation with interaction. In sec.(1.4.5) we proved that the Lang-Firsov transformation can not be applied to the SSH model respecting multiple modes at once. Thus, the results for two modes at a

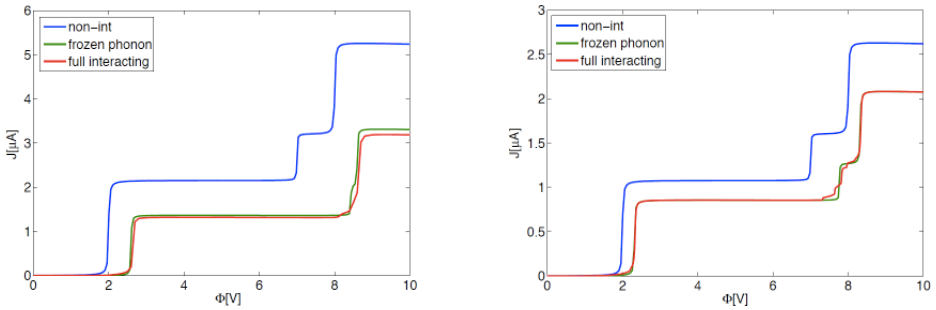

Figure 3.15: Comparison of a calculation with interaction to the frozen phonon approximation for mode 3 (altered breathing mode) with (left) and without (right) spin. $N_P = 15$, $N_c = 8$.

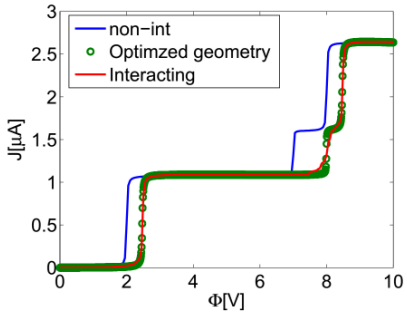

Figure 3.16: Optimized geometry approximation vs. calculation with interaction for modes 1 and 3 without Lang-Firsov transformation $N_c = 8$, $N_p = 40$.

time are obtained without the Lang-Firsov-transformation. Due to the higher phonon cutoff's and the bigger Hilbert space we can only present results without spin. Fig.(3.16) shows the current when considering mode 1 and 3 at the same time and comparing it to the optimized geometry calculation. Again, the optimized geometry approximation is capable of reproducing the interacting case very well.

3.3.3 Strong coupling regime and the beyond SSH model

To examine the effects of strong e-ph coupling we apply the beyond SSH model, see sec.(1.2.3), to the benzene system. Due to the higher phonon cutoff needed for stronger couplings, and because the Lang-Firsov transformation can not be applied, we again present only results for spinless fermions.

Convergence of CPT

In analog to sec.(3.3.1) we present some results for different cluster sizes of the central region. First, in fig(3.17) and fig.(3.18), we check the intermediate e-ph coupling studied above. We see that for the cases without steps (all modes except mode 3 and mode 6) the $N_c = 8$ and $N_c = 10$ curves match exactly. For

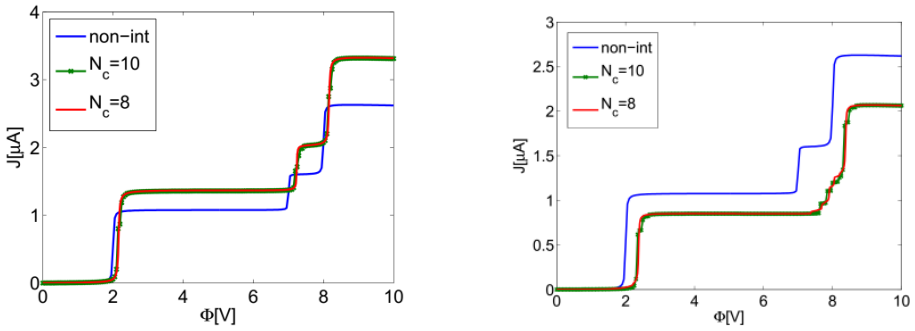

Figure 3.17: Currents for different cluster sizes of the central region obtained from the beyond SSH model for mode 1 (left) and mode 3 (right) without spin. $N_p = 40$, $g = 2.8[eV\mathring{A}^{-1}]$

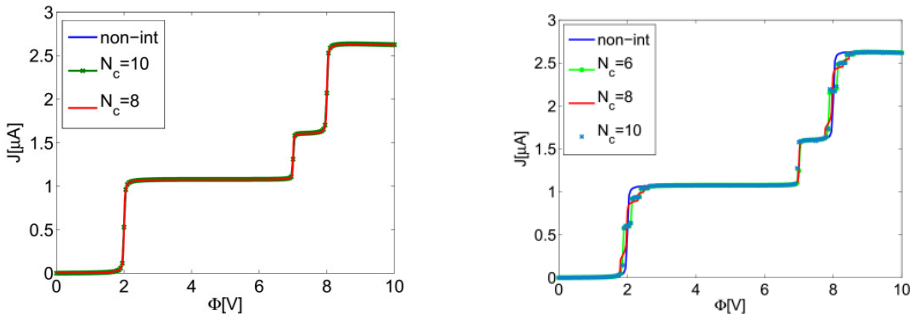

Figure 3.18: The same as fig.(3.17) for mode 2 and 6.

the other modes the steps of the $N_c = 8$ and $N_c = 10$ curves do not match but the overall results are similar. From the example of mode 6 in fig.(3.18) we see that the steps of $N_c = 10$ match with the ones from $N_c = 6$. This suggests that as for of the Anderson-Holstein model, see sec.(2.2) fig.(2.5), different N_c lie alternately on two close but different curves converging very slowly into each other. Fig.(3.19) shows the I/V curves of different cluster sizes for the Pi-mode in the strong coupling regime. We see the same effect as in fig.(3.18), namely that the data of $N_c = 6$ and $N_c = 10$ match very well.

Comparison of beyond SSH and linear SSH for intermideate e-ph coupling

We ckeck the beyond SSH model against the linear SSH model for the intermideate e-ph coupling of $g = 2.8[eV\mathring{A}^{-1}]$ used above. In fig.(3.20) and fig.(3.21) we see good agreement of the two models for this parameter regime. The deviations for mode 1 and mode 3 are due to minor corrections to the geometry when applying the beyond SSH model which are magnified by the fact that this two modes alter the hopping to leads.

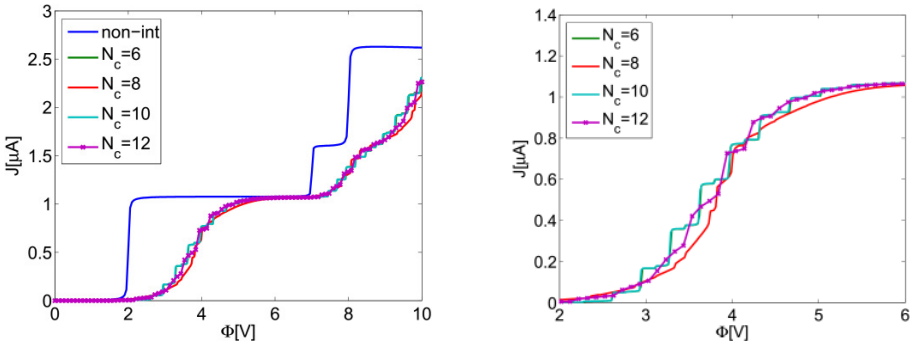

Figure 3.19: The same as fig.(3.17) but for the Pi-mode and strong e-ph coupling. Right, a zoomed in version of the left graph.$g = 6[eV\mathring{A}^{-1}]$,$N_p = 40$

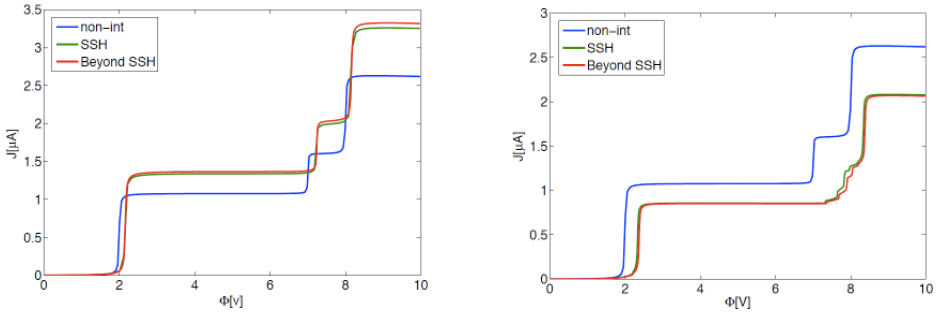

Figure 3.20: Comparison of results obtained from the beyond SSH model to the linear SSH model for mode 1 (left) and mode 3 (right). $N_c = 8$, $N_p = 40$

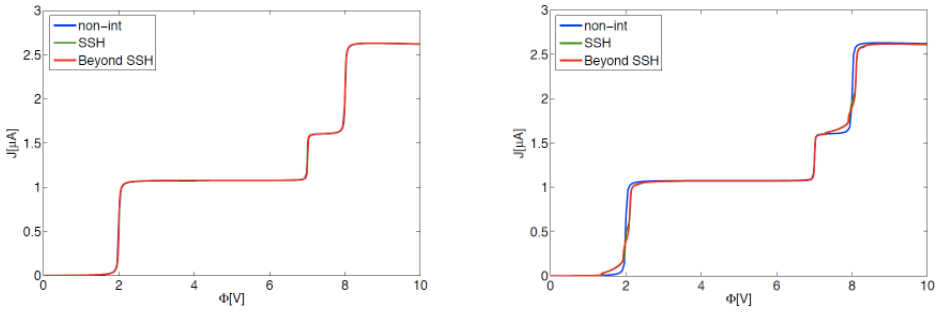

Figure 3.21: The same as fig.(3.20) but for modes 4 (left) and 7 (right).

Breakdown of the Optimized geometry/Frozen phonon approxiamtion for strong coupling

The Beyond SSH model allows us to find out when the optimized geometry approximation breaks down indicating that the current for stronger e-ph coupling can not be understood in a non-interacting picture and many-body effects take over. We investigate boundaries for the optimized geometry approximation for the altered breathing mode (mode 3), which shows a geometry change even for intermediate e-ph coupling, and the Pi-mode (mode 8) which does not. Fig.(3.22) demonstrates that for the altered breathing mode the optimized geometry approximation does fit very well untill $g = 4[eV\mathring{A}^{-1}]$ where it deviates a little from the interacting data and breaks down for higher e-ph coupling. From fig.(3.23), which shows the same for the Pi-mode, we can conclude that the optimized geometry approximation breaks down between $g = 5-6[eV\mathring{A}^{-1}]$. Interestingly, the optimized geometry calculation for the contacted benzene, in contrast to the treatment of free benzene, yields a geometry change, of about $|\Delta_{ij}| = 0.18[\mathring{A}]$ for $g = 6[eV\mathring{A}^{-1}]$, which is the reason why the corresponding curve in fig.(3.23) is altered with respect to the non-interacting one. However, this geometry change is not confirmed by the calculation with interaction which predicts an unaltered geometry. Thus, the suppression of the current, in fig.(3.23), at low bias for high g does not originate from a changed geometry. In fig.(3.7) the corresponding DOS is shown and we see that the spectral weight has been shifted to higher phonon excitations leading to the energetically displaced states. As explained in sec.(3.2.4) this may be similar to the Franck-Condon effect but can not be explained in terms of shifted harmonic oscillators. For weaker e-ph coupling, $g < 5[eV\mathring{A}^{-1}]$ the curves are exactly on top of the non-interacting case and are therefore not shown. Note that the values where the optimized geometry approximation tends to fail are in the same parameter regime where the linear SSH model breaks down.

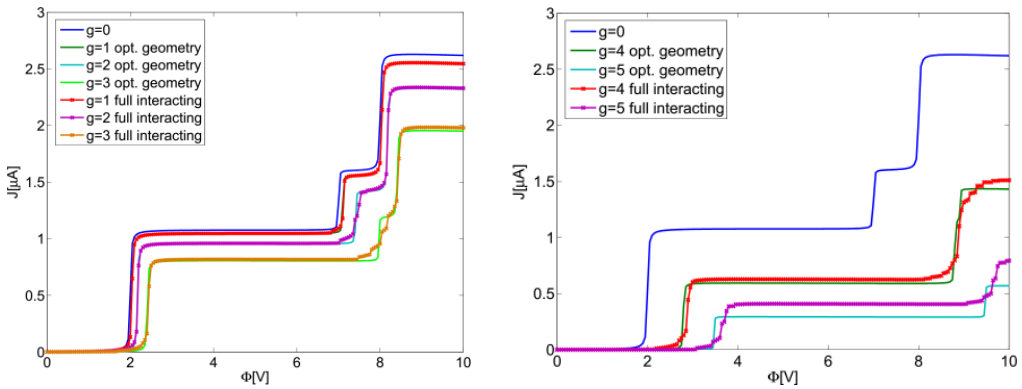

Figure 3.22: Comparison of the calculation with interaction and the optimized geometry approximation for different e-ph couplings. Mode 3 $N_c = 8$, $N_p = 40$

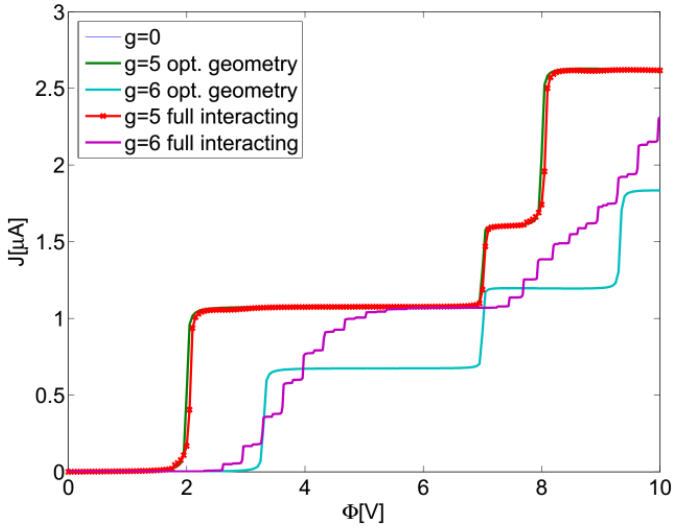

Figure 3.23: The same as fig.(3.22) except for mode 8. $N_c = 6$, $N_p = 40$

Chapter 4

Summary, conclusion and outlook

We have investigated the effects of the SSH type e-ph interaction on the transport properties of a molecular ring connected to leads by means of NEGF obtained by steady state CPT. For our parameters the CPT approximation does in most cases converge with increasing size of the central region within the realm of still numerically treatable (Exact Diagonalisation) central clusters. If not converged the data for different N_c seems to alternate between two solutions, see fig.(3.19).

4.1 Anderson-Holstein model

Tests of the NEGF steady state CPT approach on the widely studied Anderson-Holstein model, see sec.(2.1), show good agreement with results from the literature in the parameter regime where the coupling to the leads is small compared to the temperature $\Gamma << kT$. An inherent advantage of the method is that it can be applied up to strong e-ph coupling as the current formalism does inlcude the many-body effects of the correlated region non perturbatively [18]. Therefore, we are able to reproduce the Franck-Condon blockade for strong e-ph coupling which is an important mechanism in such systems.

4.2 SSH model for a contacted molecular ring

To study the effects of the SSH-type e-ph interaction on a molecular transistor we applied the SSH model, in linear and non-linear approximation, to a molecular ring, modeled as benzene, out of equilibrium. The vibronic eigenmodes of the compound system, benzene connected to one-dimensional leads, where calculated from a classical model of masses and springs, see sec.(3.1). From weak to strong e-ph coupling the current voltage chracteristics of the studied system can be qualitively predicted from the electronic DOS of the correlated molecular ring in agreement with the Meier-wingreen formula [22]. The results in sec.(3.3) confirm the need to include at least one site of the leads into the correlated central region since the current is very sensible to a change in

the molecule lead coupling (electronic hopping) which enters quadratically in the molecule lead hybridisation. When the molecule adopts a new geometry this coupling gets enhanced, suppressed or unmodified and leads to a likewise behaviour of the current.

4.2.1 Linear SSH model for intermediate e-ph coupling

Throughout the parameter regime of the linear SSH model, which we call intermediate e-ph coupling, we are able to interpret the DOS and hence the steady state current in terms of geometry changes and excitation of phonons through electrons, see sec.(3.2). In the parameter regime where the approximation of the linear SSH model is valid the change of the equilibrium geometry leads to changed electronic hoppings which results in energetically shifted electronic excitations explaining the different offsets occuring in the I/V curves. In sec.(3.2.5), we showed that this geometry change can be obtained from a calculation with non-interaction as the tradeoff between lowering the electronic energy due to the changed hoppings but loosing some of the effect to the ion potential. As does the linear SSH model, the optimized geometry approxiamtion breaks down for strong e-ph coupling. In the case of considering multiple modes at a time the geometry change is to a good approxiamtion the sum of the different contributions. The current obtained from the non-interacting optimized geometry calculation does agree very well with the interacting one, see sec.(3.3.2), and differs only by little steps, corresponding to electrons exciting a phonon, being absent which is to be expected from a calculation without e-ph coupling. For the para configuration there are only two out of eight modes which show these steps since for the majority of the modes the corresponding peaks in the DOS are suppressed for intermediate e-ph coupling as is exemplified in sec.(3.2.4). The validity of the optimized geometry approximation for intermediate coupling does imply that the widely used LDA-NEGF approach, given that it uses a geometry optimization, is justified in this regime as well. The only difference to the calculation with interaction would be the small steps which may be smeared out in experiments depending on the lead coupling, tempertaure and relaxation channels for the phonons.

4.2.2 Non-linear beyond SSH model

The linear SSH model of the e-ph coupling breaks down for the contacted benzene due to the weak hopping to the leads which can even get positive for modes where this hopping gets suppressed when exciting it. To study the system at stronger e-ph coupling we therefore extend the linear approximation to its exponential generalisation introduced in sec.(1.2.3). Unlike in the realm of the linear SSH model the optimized geometry and thus likewise also the LDA-NEGF approach breaks down and is not a viable approximation to the interacting case anymore. We observe a current suppression at low bias similar to the Franck-Condon blockade in the Anderson-Holstein model at high e-ph coupling. Both effects are traceable by looking at the corresponding electronic DOS of the central region. For the Holstein interaction the Franck-Condon blockade can

be understood in terms of shifted harmonic oscillators, see sec.(2.1.2), while in the SSH model this argumentation fails since the suppression is observed in cases where there is no shift of the oscillator for any excited state of the compound system (electrons and phonons).

4.3 Outlook

The goal of course would be to model specific experiments to get better insight into the mechanisms important to describe these systems accurately. To do so the presented method can be fed by parameters obtained by ab initio calculations. Other important mechanisms to inlcude into the model would be relaxation channels. When the molecule is contacted on a substrate one may include Holstein type of modes into the central region to take into account the coupling to the substrate as a relaxtion mechanism. Coupling to modes of the leads can in most cases be neglected as relaxation channels since they typically have a lot higher energy than the vibrations of the molecule and therefore will not get excited. However, the specific form of the relaxation channel incorporated into the model is rather unimportant as most of them have the same effect of smearing/broadening the peaks in the electronic DOS. The current CPT approach is well suited to treat systems with small coupling to the leads which is a realistic assumption depending on the molecule, the material of the leads and whether or not anchoring groups are used to trap the molecule between the leads which could lead to stronger molecule lead coupling.

Bibliography

[1] Z. Bai and R. W. Freund. *SIAM J. Sci. Comput.*, 23:542, 2001.

[2] J. Bardeen, L. N. Cooper, and J. R. Schrieffer. *Phys. Rev.*, 108:1175–1204, 1957.

[3] W. Barford. *Electronic and Optical Properties of Conjugated Polymers*. Oxford University Press, 2005.

[4] A. L. Botelho, Y. Shin, M. Li, L. Jiang, and X. Lin. *J. Phys.: Condens. Matter*, 23, 2011.

[5] S. Braig and K. Flensberg. *Phys. Rev. B*, 68, 2003.

[6] M. Büttiker. *Phys. Rev. B*, 38, 1988.

[7] A. N. Pasupathy et al. *Nano letters*, 5(2), 2005.

[8] H. Park et al. *Nature*, 407(6800), 2000.

[9] O. Delaire et al. *Nature Materials*, 10(8), 2011.

[10] T. Frederiksen, M. Paulsson, M. Brand byge, and A. P. Jauho. *Phys. Rev. B*, 75, 2007.

[11] M. Galperin, A. Nitzan, and M. Ratner. *Phys. Rev. B*, 73:045314, 2006.

[12] M. Galperin, A. Nitzan, and M. Ratner. *J. Phys.: Condens. Matter*, 19, 2007.

[13] M. Galperin, A. Nitzan, M. Ratner, and A. Troisi. *Science*, 319, 2008.

[14] R. Hützen, S. Weiss, M. Thorwart, and R. Egger. *Phys. Rev. B*, 85, 2012.

[15] M. Čížek, M. Thoss, and W. Domcke. *Phys. Rev. B*, 70:125406, 2004.

[16] M. Kiguchi, O. Tal, S. Wohlthat, F. Pauly, M. Krieger, D. Djukic, J. C. Cuevas, and J. M. van Ruitenbeek. *Phys. Rev. Lett.*, 101, 2008.

[17] M. Knap, E. Arrigoni, and W. von der Linden. *Phys. Rev. B*, 88, 2013.

[18] M. Knap, W. von der Linden, and E. Arrigoni. *Phys. Rev. B*, 84, 2011.

[19] J. Koch and F. von Oppen. *Phys. Rev. Lett.*, 94, 2005.

[20] J. Koch, F. von Oppen, and A. V. Andreev. *Phys. Rev. B*, 74, 2006.

[21] T. Koch, J. Loos, A. Alvermann, and H. Fehske. *Phys. Rev. B*, 84, 2011.

[22] Y. Meir and N. S. Wingreen. *Phys. Rev. Lett.*, 68, 1992.

[23] A. J. Millis. *Phil. Trans. R. Soc. Lond. A*, 356(1742):1473–1480, 1998.

[24] M. Nuss, M. Ganahl, H. G. Evertz, E. Arrigoni, and W. von der Linden. *Phys. Rev. B*, 88, 2013.

[25] M. Nuss, C. Heil, M. Ganahl, M. Knap, H. G. Evertz, E. Arrigoni, and W. von der Linden. *Phys. Rev. B*, 86, 2012.

[26] X. H. Qiu, G.V. Nazin, and W. Ho. *Phys. Rev. Lett.*, 92:206102, 2004.

[27] M. Ratner. *Nature Nanotechnology*, (8):378–381, 2013.

[28] J. Ren, J. X. Zhu, J. E. Gubernatis, C. Wang, and B. Li. *Phys. Rev. B*, 85:155443, 2012.

[29] D. A. Ryndyk, M. Hartung, and G. Cuniberti. *Phys. Rev. B*, 73:045420, 2006.

[30] H. Song, Y. Kim, Y. H. Jang, H. Jeong, M. Reed, and T. Lee. *Nature*, 462(7276), 2009.

[31] B. C. Stipe, M. A. Rezaei, and W. Ho. *Science*, 280(5370), 1998.

[32] O. Tal, M. Krieger, B. Leerink, and J. M. van Ruitenbeek. *Phys. Rev. Lett.*, 100, 2008.

[33] J. van der Molen et al. *Nature Nanotechnology*, (8):385–389, 2013.

[34] N. B. Zhitenev, H. Meng, and Z. Bao. *Phys. Rev. Lett.*, 88, 2002.